

AN ABSTRACT OF THE DISSERTATION OF

Andrew R. Sabalowsky for the degree of Doctor of Philosophy in Civil Engineering presented on December 11, 2008.

Title: Electron Donor and Chlorinated Ethene Effects on Activity and Community Composition in Anaerobic Reductively Dechlorinating Consortia.

Abstract approved: _____
Lewis Semprini

This research focused on anaerobic transformation of trichloroethene (TCE), a groundwater contaminant. The mixed anaerobic Evanite culture (EV) was studied to determine community behavior and composition responses to different electron donors and chloroethene electron acceptors. The potential toxicity from high concentrations of TCE and its daughter product *cis*-1,2-dichloroethene (cDCE) was also evaluated.

Electron donor and acceptor studies were performed in three continuous flow stirred tank reactors (CFSTRs) operated with 12.5 day cell retention times. Each reactor received either TCE or vinyl chloride (VC) and a soluble electron donor at twice the stoichiometric hydrogen formation potential to dechlorinate the influent TCE or VC completely to ethylene (ETH). The EV inoculum for the CFSTRs contained the critical dehalogenating organisms, *Dehalococcoides* spp., as well as three reductive dehalogenase genes found only in *Dehalococcoides* and commonly referred to as the *pceA*, *tceA*, and *vcrA* genes. CFSTR assessments consisted of: continual chloroethene and organic acid monitoring; periodic batch rate measurements of TCE, cDCE and VC dechlorination under non-limiting conditions; and quantitative polymerase chain reaction (qPCR) analyses of the aforementioned reductase genes plus the *Dehalococcoides* 16S rRNA and universal *Bacteria* 16S rRNA genes.

Formate was a better electron donor for TCE dechlorination in terms of completeness and longevity of dechlorination, and in maintaining *Dehalococcoides* populations. In the VC-fed reactor, formate could not sustain dechlorination, but supported an unknown TCE to cDCE dechlorinating population. The lactate-fed CFSTR produced a *Dehalococcoides* community dominated by the *tceA* gene, while the two formate-fed systems were generally dominated by the *vcrA* gene. *Dehalococcoides* 16S

rRNA gene quantities correlated well with cDCE and VC batch-measured dechlorination rates. cDCE and VC maximum dechlorination rates could be predicted by qPCR *Dehalococcoides* 16S rRNA gene measurements.

High chloroethene concentration toxicity effects were studied using batch-fed reactors, a CFSTR and a recirculating packed column reactor. In all reactor types TCE dechlorination activity was lost as cDCE concentrations reached 9 to 12 mM. A toxicity model, based on cDCE and TCE concentrations directly increasing the endogenous decay coefficients of the cultures, fit the temporal concentration responses observed in all reactors, with slightly different toxicity constants.

©Copyright by Andrew R. Sabalowsky
December 11, 2008
All Rights Reserved

Electron Donor and Chlorinated Ethene Effects on Activity and Community Composition
in Anaerobic Reductively Dechlorinating Consortia

by
Andrew R. Sabalowsky

A DISSERTATION

submitted to

Oregon State University

in partial fulfillment of
the requirements for the
degree of

Doctor of Philosophy

Presented December 11, 2008
Commencement June 2009

Doctor of Philosophy dissertation of Andrew R. Sabalowsky presented December 11, 2008.

APPROVED:

Major Professor, representing Civil Engineering

Head of the School of Civil and Construction Engineering

Dean of the Graduate School

I understand that my dissertation will become part of the permanent collection of Oregon State University libraries. My signature below authorizes release of my dissertation to any reader upon request.

Andrew R. Sabalowsky, Author

ACKNOWLEDGEMENTS

I would like to express deep gratitude to the members of my advising committee, Drs. Peter Bottomley, Mark Dolan, Lewis Semprini, and Brian Wood. Each one has provided a great deal of patience, motivation, and insight regarding my research or otherwise through the ups and downs that have come with the territory. Special thanks to my advisor, Lewis Semprini for the countless hours, opportunities, input, and perspective he supplied.

Many thanks also to Dr. Mohammad Azizian, especially for his technical expertise and ability to keep our equipment serving their intended purposes. I am also very grateful to Drs. Alfred Spormann and Sebastian Behrens for their expertise, training, facilities, and collaborations in the molecular characterization of the cultures used in this study. I greatly appreciate the time spent with colleagues in both scientific and non-scientific capacities. For fear of leaving anyone out of that long list, I would just like to thank you all. I wish each of you great happiness and success in your paths, whether you have led or followed me.

My success and survival is owed principally to my wife, Skye, and son, Oliver. They have been in infinite wealth of joy, motivation, and nourishment, both physically and mentally, through this entire process that began in April of 2002. Thanks also to the rest of my family and friends for understanding my excitement or angst, even if they might not understand my research.

TABLE OF CONTENTS

	<u>Page</u>
1. Introduction.....	1
2. Evaluating formate versus lactate as electron donors for dechlorinating TCE-saturated media by mixed anaerobic consortia in short retention time continuous culture reactors.....	13
3. Gene quantification tracks electron donor and acceptor effects on multiple <i>Dehalococcoides</i> strains in mixed community chemostats and predicts cDCE and VC dechlorination rate potential.....	45
4. Trichloroethene and <i>cis</i> -1,2-dichloroethene concentration-dependent toxicity model fits activity loss in batch-fed, continuous flow, and attached growth anaerobic cultures.....	86
5. Summary and Engineering Significance.....	119
6. Bibliography.....	124
7. Appendix A: Supporting information for Chapter 2.....	133
8. Appendix B: Supporting information for Chapter 3.....	140
9. Appendix C: Supporting information for Chapter 4.....	143

LIST OF FIGURES

<u>Figure</u>	<u>Page</u>
1.1 Pathway for reductive dehalogenation of TCE completely to ETH.....	12
2.1 Continuous reactor effluent monitoring data.....	38
2.2 Continuous reactor electron balances.....	40
2.3 Culture specific dechlorination rates under non-limiting conditions in batch assays.....	41
2.4 CAH monitoring compared to theoretical non-reactive washout.....	43
2.5 Endpoint hydrogen consumption during all CAH batch assays after 10 hours of incubation.....	44
3.1 Effluent CAH and organic acids monitoring.....	78
3.2 Total <i>Bacteria</i> and <i>Dehalococcoides</i> 16S rRNA gene quantities.....	79
3.3 Reductase genes quantities.....	80
3.4 <i>Dehalococcoides</i> and total <i>Bacteria</i> populations compared to dechlorination rates.....	81
3.5 Reductase gene presence compared to dechlorination activity.....	82
3.6 Predicted dechlorination rates based upon DNA quantification compared to measured dechlorination rates from reactor harvested cells....	85
4.1 CFSTR schematic diagram.....	111
4.2 RPC schematic diagram.....	113
4.3 Difference in cDCE accumulation in TCE batch-fed reactors for the PM and EV cultures.....	115
4.4 Modeled cDCE accumulation in batch-fed reactors.....	116
4.5 CAH monitoring data for the CFSTR with fitted cDCE and TCE concentration-dependent toxicity model and previously proposed Haldane inhibition model.....	117
4.6 CAH monitoring data for the RPC with fitted cDCE and TCE concentration-dependent toxicity model.....	118

LIST OF TABLES

<u>Table</u>	<u>Page</u>
2.1 Relevant electron donating and electron consuming reactions and energetics.....	39
2.2 Maximum utilization rates (k_{\max}) for EV culture previously reported versus current study.....	42
3.1 CFSTR influent electron donor/acceptor conditions.....	77
3.2 Comparability of dechlorination rates normalized to <i>Dehalococcoides</i> 16S rRNA gene copies.....	83
3.3 Dechlorination rates and gene quantity correlations.....	84
4.1 CFSTR pumping conditions.....	112
4.2 Model kinetic parameters for batch, CFSTR, and RPC simulations.....	114

LIST OF APPENDIX FIGURES

<u>Figure</u>	<u>Page</u>
A1 Influent TCE concentrations for both continuously fed suspended growth reactors.....	135
A2 Schematic diagram of continuous culture reactors.....	136
A3 Formate-fed effluent CAH monitoring with theoretical ETH concentrations.....	138
B1 Reductase gene profiles of the Evanite culture and pure <i>Dehalococcoides</i> strains.....	141
C1 CFSTR acids monitoring data (a), and (b) measured influent TCE, modeled influent TCE concentrations, and modeled biomass (X).....	144
C2 Best fit models for CFSTR data with TCE Haldane inhibition plus either cDCE toxicity alone (black lines), or both cDCE and TCE toxicity (gray lines).....	145
C3 RPC acids monitoring data (a), and (b) measured influent TCE, modeled influent TCE concentrations, and modeled biomass (X).....	146

LIST OF APPENDIX TABLES

<u>Table</u>	<u>Page</u>
A1 Tabulated pH values for all three CFSTRs reported in this study.....	134
A2 Electron equivalent assumptions for electron balance.....	139

Chapter 1

Introduction

Trichloroethylene (TCE) is a common solvent that has been used extensively in the past by the military, automotive, dry-cleaning, and computer industries. Improper disposal, accidental releases, and the density of TCE exceeding that of water has resulted in numerous groundwater contamination sites throughout the United States and elsewhere. TCE and the lesser-chlorinated aliphatic hydrocarbons (CAHs), such as *cis*-1,2-dichloroethene (cDCE) and vinyl chloride (VC) are contaminants of environmental concern because they are known to be toxic and/or carcinogenic (Ensley, 1991; McCarty, 1997; Kielhorn et al., 2000; Moran et al., 2007). Anaerobic reductive dechlorination, or dehalogenation, is the biological process by which TCE is generally sequentially dechlorinated to cDCE, VC and ethylene (ETH). This is a well-documented process for remediating TCE and other chlorinated aliphatic hydrocarbons (CAHs), desirable for its simplicity in implementation, success in completely dechlorinating CAHs to non-toxic ETH, and the abundance of organisms capable of reductive dechlorination (Aulenta et al., 2006). Complete reductive dechlorination to ETH can often be achieved with little more than the addition of electron donor(s) in the presence of halorespiring organisms or consortia (Aulenta et al., 2006). Though reductive dechlorination has been implemented and studied extensively, many factors that influence microbial community performance and composition remain unexamined.

Reductive dehalogenation

Reductive dehalogenation, or halorespiration, is the process by which organisms gain energy for growth by reducing halogenated organic compounds, such as TCE (McCarty, 1997). Reductive dehalogenation requires the presence of a halogenated organic compound as the electron acceptor, an electron donor, and a relevant enzyme such as those typically referred to as dehalogenases or reductases. TCE dehalogenation, or dechlorination, generally proceeds as depicted in Figure 1.1, where 2 electrons are

required for each dechlorination step from TCE to cDCE, cDCE to VC, and VC to ETH. The sources electrons can be from organic compounds, or dihydrogen (H_2), to be discussed below, though the source of hydrogen and electrons is represented as H_2 in Figure 1.1. Note that dehalogenation of TCE and its daughter products is an acid producing process, in addition to chloride releasing.

Reductively dehalogenating organisms

Numerous organisms have been found capable of CAH reductive dechlorination, and both mixed and pure culture studies have been devoted to characterizing their performance. Of the total number of organisms known to perform anaerobic reductive dehalogenation, the majority are capable only of reductive dechlorination of tetrachloroethene (PCE) and TCE to cDCE, including *Desulfitobacterium spp.*, *Dehalospirillum multivorans*, *Desulfomonile tiedjei*, *Desulfuromonas spp.*, *Dehalobacter restrictus*, (Holliger et al., 1999) *Sulfurospirillum spp.*, (Luijten et al., 2003) and *Geobacter lovleyi* (Sung et al., 2006a). *Dehalococcoides spp.* are of particular interest, however, because they are the only organisms known to reductively dechlorinate PCE and lesser chlorinated CAHs to vinyl chloride (VC), and completely to ethylene (ETH) (Cupples, 2008). To date, six strains of *Dehalococcoides* with differing dechlorination capabilities have been described (as summarized in Cupples, 2008), five of which can dechlorinate chloroethenes to ETH, and only three of which have been shown to obtain energy for growth from dechlorination of VC to ETH (Adrian et al., 2000; Maymó-Gatell et al., 1997; He et al., 2003; He et al., 2005; Sung et al., 2006b, Müller et al., 2004).

For *Dehalococcoides spp.*, the only organisms known to dechlorinate cDCE and VC to ETH (Cupples, 2008), only acetate and H_2 have been shown to serve as electron donors, and only H_2 has been shown to serve as an electron donor for cDCE and VC dechlorination (Cupples et al., 2003; Lee et al., 2007). Therefore, a mixed anaerobic consortium is required to achieve complete reductive dechlorination to ETH with fermenting organic electron donors, including at least one relevant *Dehalococcoides spp.*

Dehalogenating enzymes

Among the known *Dehalococcoides* spp., various dehalogenase (or reductase) genes associated with production of reductive dehalogenase enzymes have been discovered. While 18 putative dehalogenase genes have been identified within the *Dehalococcoides ethenogenes* strain 195 genome (Sechadri et al., 2005; Reagard et al., 2005), and up to 32 in the CBDB1 strain (Kube et al., 2005), only four genes have been identified and associated with formation of an enzyme relevant to CAH dechlorination (as summarized in Cupples, 2008). Specifically, the reductase genes commonly referred to as *pceA*, *tceA*, *vcrA*, and *bvcA* are associated with the production of enzymes capable CAH dechlorination. The known CAH dechlorination reactions associated with each reductase gene are as follows: PCE to TCE dechlorination (*pceA*), TCE to cDCE and cDCE to VC dechlorination (*tceA*), cDCE to VC and VC to ETH dechlorination (*vcrA*), and VC to ETH dechlorination (*bvcA*).

Studies have investigated single time-point shifts in reductases under batch enrichment of different CAH electron acceptors (Ritalahti et al., 2006; Holmes et al., 2006; Waller et al., 2005), but to date no studies have investigated enrichment with different CAHs in continuous flow systems, or over multiple time points to observe how population gene profiles respond temporally. Numerous studies have investigated performance of reductively dechlorinating cultures enriched with different electron donors, but these studies have been in the absence of molecular genetic characterization, and predominantly in batch-fed enrichments (Heimann et al., 2007; Fennell et al., 1997; Freeborn et al., 2005; He et al., 2002; Yang and McCarty, 1998). There is thus a need to evaluate how performance and community composition changes temporally with continuous reactor operation that permits direct electron donor and CAH comparisons.

Organic electron donors

Numerous organic compounds have been shown to function as electron donors for reductive dechlorination either directly, or as fermentable sources of hydrogen (H₂) (Fennell et al., 1997; Holliger et al., 1999; Heimann et al. 2007). The use of soluble organic substrates is attractive because of the ease of delivery *in situ*, versus

complications associated with delivering gaseous H_2 into the subsurface aquifer. While lactate is a common organic substrate utilized in laboratory and field applications for reductive dechlorination (Adamson et al., 2003; Ellis et al., 2000; Aulenta et al., 2007; Rahm et al., 2006a; Lendvay et al., 2003), many soluble organic electron donors have been successfully utilized for CAH dechlorination in batch-fed laboratory studies to varying degrees, including: butyrate (Aulenta et al., 2007; Freeborn et al., 2005; Panagiotakis et al., 2007; Fennell and Gossett, 1998), benzoate (Lee et al., 2007; Yang and McCarty, 1998), propionate (Heimann et al., 2007; Freeborn et al., 2005; Yang and McCarty, 1998; Fennell and Gossett, 1998), acetate (Lee et al., 2007; Yang and McCarty, 1998), pyruvate (Zheng et al., 2001), glucose (Lee et al., 2004), ethanol (Fennell and Gossett, 1998), methanol (Freeborn et al., 2005; Panagiotakis et al., 2007), and formate (Lee et al., 2007; Carr et al., 2000)

Issues to consider when using organic substrates for the purposes of reductive dechlorination are the rates of fermentation, electron donor use and efficiency, and the degree and rate of dechlorination that can be achieved with any given substrate. Batch experiments have shown slow-fermenting substrates such as propionate or butyrate, and fast-fermenting substrates such as lactate, formate or ethanol can all serve as valid electron donors for dechlorination given enough time and substrate (Fennell et al., 1997; Aulenta et al., 2006; Aulenta et al., 2007; Heimann et al., 2006; Lee et al., 2007). Since dechlorinating bacteria are often associated with maintaining low hydrogen thresholds, slow-fermenting substrates have the potential to support dehalogenation while virtually excluding other processes that require higher hydrogen thresholds, such as acetogenesis or methanogenesis (Löffler et al., 1999; Yang and McCarty, 1998; Luijten et al., 2004).

However, because H_2 is the only electron donor shown to be used for cDCE and VC dechlorination (Lee et al., 2007; Cupples et al., 2003; Zheng et al., 2001), relevant organisms and contact time must be established to ensure H_2 is released when and where needed in flowthrough systems, such as a contaminated site with groundwater flow or a continuous flow suspended growth reactor. Even when performance is similar in batch systems with different fast-fermenting substrates (Lee et al., 2004) understanding how

populations change in response to different electron donors, or how such electron donors compare in flowthrough systems is lacking. While batch tests have been successful in illustrating the rates of hydrogen release and what organic electron donors are utilizable for dechlorination, they do not indicate how dechlorination performance and electron donor usage will occur in a continuous feed system, where substrate addition can be maintained in a slow and uniform fashion and the selective pressure of microbial (cell) washout can be exerted. Continuously fed packed column or reactor studies have been performed, but such systems are not amenable to repeated cell harvesting over time to thoroughly inspect culture performance and composition (Azizian et al., 2008; Behrens et al., 2008; Adamson et al., 2003). Continuously fed suspended growth reactors have also been studied for CAH dechlorination, but to date none have specifically assessed temporal shifts in culture genetic composition and dechlorination activities (Yang and McCarty, 1998; Adamson et al., 2004; Carr et al., 2000)

Dehalogenating performance and genetic correlations

One goal common to remediation practitioners is the ability to predict remediation performance and timeframes for cleanup. Understanding what communities are present and relevant to the dechlorination process can be an important tool for predictions. Recent work has shown that the 16S rRNA genes of the various *Dehalococcoides* strains are too similar to distinguish between different strains, or to allow inference of what functional genes are present within a *Dehalococcoides*-containing community (Duhamel et al., 2004; He et al., 2005; Sung et al., 2006b; Daprato et al., 2007). Different functional genes, however, such as reductive dehalogenase genes have been successfully quantified in *Dehalococcoides*-containing communities to monitor the dominance of different strains, but to date functional gene presence has not been correlated with dechlorination rates (Holmes et al., 2006; Ritalahti et al., 2006; Lee et al., 2008; Lee et al., 2006). Gene expression has been identified as an indicator of dehalogenation activity and can correlate with dechlorination over a narrow range of concentrations and rates. However, a correlation between gene expression and dechlorination activity over a broad

range has yet to be found (Fung et al., 2007; Rahm and Richardson, 2008a; Rahm and Richardson, 2008b; Lee et al., 2006).

Multiple dehalogenase gene quantification has been used to describe multiple *Dehalococcoides* populations in field sites (Lee et al., 2008) and different batch-fed mixed cultures enriched from separate sites (Daprato et al., 2007). Few studies to date have analyzed shifts, however, in multiple *Dehalococcoides* populations within a mixed community fed different CAH electron acceptors, and these have been restricted to endpoint analyses in enriched batch systems (Holmes et al., 2006; Ritalahti et al., 2006; Sung et al., 2006b). The effects of different electron donors on batch dechlorination performance has been previously evaluated, but generally in the absence of community genetic analyses (Lee et al., 2007; Heimann et al., 2007; Yang and McCarty, 1998), though one known study has investigated community genetic composition changes with differing electron donors (Freeborn et al., 2005).

Studies are currently needed of a single mixed community receiving different electron donors and acceptors over time periods where population shifts can occur. Studies in continuous flowthrough systems are also needed to determine how such operational differences affect the dehalogenation community profiles and performance. Because only the *vcrA* and *bvcA* genes have been associated with VC dechlorination to ETH, and only H₂ has been shown to serve as a valid electron donor for cDCE and VC dechlorination, it is important to gain a greater understanding of what conditions and soluble electron donors can promote activity in the presence of these dehalogenase systems.

Separation or co-occurrence of dechlorination steps

The co-occurrence of multiple CAHs has been observed in field sites (Rahm et al., 2006a; Lendvay et al., 2003; Major et al., 2002). The testing of cultures in a way that allows the simultaneous presence of multiple CAHs and dechlorination steps is therefore of interest to gain insight into community response under conditions that can be observed in field sites. Continuously fed suspended growth reactors represent an approach that maintains a community where multiple dechlorination steps can occur simultaneously

without spatial or temporal separation (Zheng et al., 2001), thereby supplying a relatively simple means to select culture conditions and allow repeated temporal assessment.

A separation of CAHs and dechlorination steps can also occur in field sites, as well as temporally in batch-fed reactors, indicating the relevance of the variety of methods used to elucidate reductive dechlorination. Sequential separation of dechlorination steps can result for a variety of reasons, such as energetic favorability of dechlorination of PCE and TCE (He et al., 2002), faster maximum utilization rates of the higher chlorinated compounds (Yu et al., 2005), lower hydrogen tension associated with the higher chlorinated compounds (Lu et al., 2001; Yang and McCarty 1998; Luijten et al., 2004), or greater number of organisms capable of reductively dechlorinating PCE and TCE (Holliger et al., 1999). Furthermore, the presence of multiple chlorinated compounds is known to competitively inhibit dechlorination of the other chlorinated compounds (Yu and Semprini, 2004; Yu et al., 2005; Cupples et al., 2004). Additionally, the different chemical properties of the CAHs result in greater sorption of higher-chlorinated CAHs and greater mobility of lesser-chlorinated CAHs, which contributes to spatial separation in the field (e.g., Ling and Rifai, 2007; Chapelle et al., 2005). The separation of dechlorination steps is an important phenomenon because it can often result in high cDCE concentrations (as summarized by Gerritse et al., 1995 and van Eekert and Schraa, 2001). Furthermore, TCE concentrations in the source zone of a site can potentially approach the solubility limit of approximately 8 mM, and high CAH concentrations can have negative effects on the dechlorination process.

High CAH inhibition or toxicity

Although reductive dechlorination is relatively simple in implementation, complications can arise due to CAH inhibition or toxicity to the organisms responsible for their dechlorination. Although organisms can perform reductive dechlorination for energetic gain, high concentrations of PCE, TCE and cDCE, on the order of 1 mM, have been shown to reduce the activity of reductively dechlorinating cultures (Yang and McCarty, 2000; Duhamel et al., 2002), and can potentially cause toxicity. Toxicity has been indicated with elevated decay coefficients for two reductively dechlorinating mixed

cultures in the presence of cDCE above 8 mM (Chu, 2004). With the high solubility limits of TCE (8 mM) and cDCE (53 mM), and the demonstration of enhanced dissolution of non-aqueous phase liquids (NAPLs) such as TCE or PCE (Cope and Hughes, 2001; Yang and McCarty, 2000; Adamson et al., 2004), it is possible to achieve zones with cDCE concentrations exceeding the molar solubility limit of TCE near a NAPL source zone.

cDCE concentrations ranging from 3 to 9 mM cDCE have been produced biogenically from PCE dechlorination and shown to have a toxic effect on dechlorinating cultures (Chu, 2004; Adamson et al., 2004). Competitive inhibition of higher chlorinated CAHs on the reductive dechlorination of lesser chlorinated CAHs has also been demonstrated (Yu et al., 2005; Cupples et al., 2004; Lee et al., 2004) and Haldane inhibition by high concentrations of CAHs reducing their own dechlorination rates has been proposed to simulate reductive dechlorination observations (Yu and Semprini, 2004). High CAH concentrations therefore produce complicated and negative interactions that are important to understand more fully.

Batch-fed, continuously-fed suspended, and attached modes of growth

There is an abundance of batch data for reductive dechlorination comparing different cultures (Daprato et al., 2007; Ritalahti et al., 2006; Löffler et al., 1999), different electron donors (Heimann et al., 2007; Fennell et al., 1997; Freeborn et al., 2005; He et al., 2002; Yang and McCarty, 1998), and effects of different CAHs (Ritalahti et al., 2006; Holmes et al., 2006; Waller et al., 2005). In batch fed systems, as concentrations of different electron donors and acceptors rise and fall over time, it is difficult to develop a stable population. There is the need to understand how communities respond and change in continuously fed systems, where relatively stable population can be maintained over time.

Only a few studies have been devoted to evaluating or comparing culture performance in continuous flow suspended growth systems (Drzyzga et al., 2001; Yang and McCarty, 1998; Zheng et al., 2001; Carr et al., 2000). These studies have investigated varying electron donor or acceptor concentrations, residence times, or

microbial activity to increase PCE dissolution. There is thus a need to improve our understanding of temporal changes in culture capabilities and composition as it pertains to the selective pressures of a continuously fed suspended growth culture where multiple simultaneous dechlorination steps and cell washout can occur.

It is additionally important to compare attached and suspended growth modes for reductive dehalogenating communities, to assess how populations of these different growth modes might differ. Planktonic and attached cells can both occur in the environment, and suspended growth batch experiments are common and relatively inexpensive to perform. There is therefore the need to understand how the multitude of batch growth experiments can be related to other conditions more representative of field sites. Comparisons between different growth modes (such as batch-fed, continuously fed, or attached growth) can be especially important regarding issues of inhibition or toxicity, where it has commonly been observed that chemostat cells exhibit increased resistance compared to batch-fed cells (Chang and Alvarez-Cohen, 1996; Qu, and Bhattacharya, 1997; Piringer and Bhattacharya, 1999), and attached growth cells have greater resistance than suspended cells (Harrison et al., 2007; Stewart and Costerton, 2001; Walters et al., 2003). Such comparisons can supply information valuable to designing treatment strategies or relating microcosms to field observations or predictions.

The Evanite reductively dechlorinating mixed culture

The Evanite (EV) mixed anaerobic culture was utilized for the majority of experiments in this work. It is a culture maintained in our laboratory and has been characterized extensively. The EV culture was enriched from groundwater collected at the TCE-contaminated Evanite site in Corvallis, Oregon and maintained for many years with additions of PCE, butanol and H_2 (Yu et al., 2005) in an enriched basal medium (Yang and McCarty, 1998). The EV culture has been shown to obtain energy for growth on dechlorination of PCE, TCE, cDCE, and VC, and the half-velocity coefficients and maximum utilization rates for all CAH dechlorination steps have been determined previously (Yu et al., 2005). Additionally competitive inhibition coefficients of the CAHs on dechlorination of other CAHs, and Haldane inhibition coefficients have been

successfully modeled for this culture (Yu et al., 2005; Yu and Semprini, 2004). The EV culture is also known to contain at least one *Dehalococcoides* sp. and the reductase genes, *pceA*, *tceA*, *vcrA*, and *bvcA* (Yu and Semprini, 2004; Behrens et al., 2008).

Dechlorination with this culture has been demonstrated with H₂, lactate, and tetrabutoxysilane (TBOS), which hydrolyses to form 1-butanol (Yu et al., 2005; Azizian et al., 2008; Yu and Semprini, 2002). The EV mixed culture is therefore suitable for investigating effects on performance and community molecular composition as affected by different electron donors or CAHs.

Thesis objectives:

1. Evaluate formate versus lactate effects on culture performance and capabilities in continuously fed stirred tank reactors (CFSTRs).

Formate and lactate are two soluble organic compounds associated with relatively fast rates of hydrogen release, by dehydrogenation for the former and fermentation for the latter. In Chapter 2, two separate CFSTRs were inoculated with the EV culture to compare reactor performance and temporal shifts in culture capabilities resulting from continuous operation with either formate or lactate as electron donors to reductively dechlorinate the TCE-saturated influent media. Batch kinetic assays were conducted approximately once every two weeks on effluent harvested cells from each reactor to measure maximum dechlorination rates for TCE, cDCE, and VC. CFSTRs have been successfully operated at retention times as short as 11 days to treat PCE to predominantly VC with some cDCE (Zheng et al., 2001), and faster dechlorination ultimately reduces time and costs of treatment. These CFSTRs were thus operated at short retention times (12.5 days) as part of the approach to satisfy the specific objectives of: 1) determining if a mixed anaerobic culture could sustain dechlorination of TCE-saturated medium in short retention time continuous culture reactors with soluble electron donors (formate or lactate); 2) comparing how lactate and formate affected longevity and completeness of dechlorination in the CFSTRs; and 3) evaluating how culture dechlorination potential, measured on effluent harvested cells in non-limiting batch kinetic tests, shifted temporally as a function of electron donors supplied in continuous cultures.

2. Use gene quantification to predict dechlorination rates and track electron donor and acceptor effects on community composition

Recent developments in quantitative polymerase chain reaction (qPCR) analyses of reductase genes has allowed researchers to track multiple functional genes in field applications (Lee et al., 2008), and lab studies (Daprato et al., 2007; Holmes et al., 2006; Ritalahti et al., 2006; Sung et al., 2006b). However, this technique has yet to be reported with the focus of relating gene quantities to rates, monitoring temporal shifts in communities, or comparing electron donor effects on community composition. In Chapter 3 of this study, qPCR analysis was utilized to quantify the following genes: universal *Bacteria* 16S rRNA, *Dehalococcoides* spp. 16S rRNA, (*Dehalococcoides* spp.) *pceA*, *tceA*, *vcrA* and *bvcA*. These quantifications were compared with periodic batch kinetic tests of TCE, cDCE and VC maximum dechlorination rates on cells harvest from CFSTRs fed either, TCE and lactate, TCE and formate, or VC and formate. The aforementioned reactor operations and analyses were performed to address the following specific objectives: 1) determine how different electron donors and CAHs affect temporal shifts in the dehalogenating community composition and performance within continuously fed reactors; and 2) determine if maximum dechlorination rates can be predicted from qPCR analysis of gene presence.

3. Evaluate CAH toxicity in different growth modes and cultures

Inhibition and toxicity of high concentrations of CAHs has long been documented in studies of reductive dehalogenation (Yang and McCarty, 2000; Duhamel et al., 2002; Chu, 2004; Adamson et al., 2004; Yu and Semprini, 2004). In Chapter 4, batch-fed reactors, a CFSTR and a recirculating packed column reactor were operated to accumulate cDCE from TCE dechlorination. The objectives were first to determine the effects of high CAH concentrations (e.g. ~10 mM cDCE) on dechlorinating cultures in different growth modes (batch-fed suspended, continuously fed suspended, and attached), and second to develop a model to describe high CAH toxic effects on the temporal responses observed in these three systems.

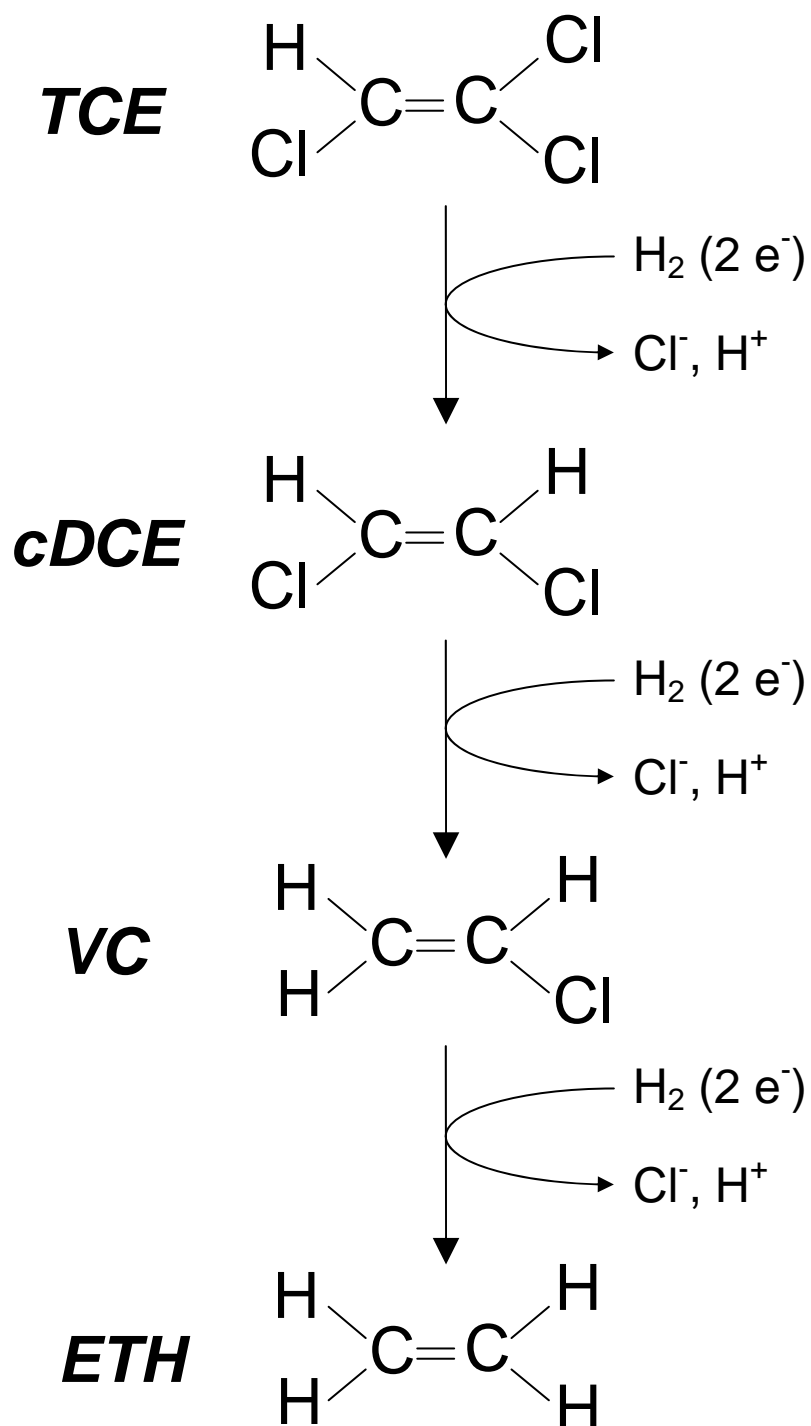


Figure 1.1. Pathway for reductive dehalogenation of TCE completely to ETH.

Chapter 2

Evaluating formate versus lactate as electron donors for dechlorinating TCE-saturated media by mixed anaerobic consortia in short retention time continuous culture reactors.

ABSTRACT

Two continuous culture reactors were started from the same mixed anaerobic reductively dechlorinating (Evanite, or EV) consortium. They were operated 125 to 295 days with a 12.5 day retention time to treat a trichloroethene (TCE)-saturated influent (~7.5 mM). The reactors were fed either lactate or formate at 2 times the stoichiometric electron requirement, based on the H₂ production potential, for complete dechlorination of TCE to ethene (ETH). The lactate-fed reactor initially dechlorinated TCE to ~85% vinyl chloride (VC) and ~15% ethene prior to *cis*-1,2-dichloroethene (cDCE) accumulation at 44 days, and TCE accumulation after 72 days. The formate-fed reactor dechlorinated TCE to approximately 66% ETH and 33% VC for 204 days prior to the initial accumulation of cDCE, with TCE accumulation after 227 days. Maximum chlorinated aliphatic hydrocarbon (CAH) utilization rates for TCE, cDCE, and VC, as well as hydrogen consumption patterns, were determined by frequent batch assays with cells harvested from the reactors. Batch assays mimicked chemostat performance, and demonstrated substantial differences in the metabolic status of the chemostat microbial communities that could not be assessed by reactor monitoring alone. During similar reactor dechlorination performance, batch assays revealed substantial differences in maximum dechlorination rates and H₂ consumption patterns. During peak performance, maximum dechlorination rates for TCE, cDCE, and VC were 70.1, 20.5, and 5.1 μmoles/mg protein/day in the lactate-fed reactor, and 105, 29.8, and 11.2 μmoles/mg protein/day in the formate-fed system, indicating greater enrichment of dechlorinating biomass in the formate system. Excess hydrogen consumption was prevalent in batch incubations of the formate-fed culture, but not in the lactate-fed culture, due to increased homoacetogenic activity in the formate system. Continuous reactor operation revealed formate was a more effective electron donor for reductive dechlorination compared to lactate, and that lactate fermentation to acetate and propionate could not support the dechlorinating population under the conditions tested. Formate supported dechlorination for up to 200 days, or 16 reactor volumes. The reactor eventually failed, which coincided with loss of measurable dechlorination in batch assays as well.

INTRODUCTION

Chlorinated ethenes such as trichloroethylene (TCE) and its daughter products are groundwater contaminants of environmental concern due to their ubiquity, toxicity and/or carcinogenicity (Ensley, 1991; McCarty, 1997; Kielhorn et al., 2000; Moran et al., 2007). Anaerobic reductive dechlorination is a well documented phenomenon for remediation of TCE and other chlorinated aliphatic hydrocarbons (CAHs) (Aulenta et al., 2006). This is an attractive process because TCE (and other CAHs) can be completely dechlorinated by adding the appropriate electron donor(s) in the presence of halorespiring organisms or consortia. Numerous organic compounds have been shown to function as electron donors for reductive dechlorination either directly or as fermentable sources of hydrogen (H_2) (Fennell et al., 1997; Holliger et al., 1999; Heimann et al. 2007). The use of soluble organic substrates is attractive because of the ease of delivery *in situ*, versus complications associated with delivering gaseous H_2 into the subsurface.

For *Dehalococcoides* spp., the only organisms known to dechlorinate cDCE and VC to ETH (Cupples, 2008) only acetate and H_2 have been shown to serve as electron donors, and only H_2 has been shown to serve as an electron donor for cDCE and VC dechlorination (Lee et al., 2007; Cupples et al., 2003). Therefore, a mixed anaerobic consortium is required to achieve complete reductive dechlorination to ETH with fermenting organic electron donors.

Issues to consider when using organic substrates for the purposes of reductive dechlorination are the rates of fermentation, electron donor use and efficiency, and the degree and rate of dechlorination that can be achieved with any given substrate. Batch experiments suggest slow-fermenting substrates such as propionate or butyrate, and fast-fermenting substrates such as lactate, formate or ethanol can all serve as valid electron donors for dechlorination given enough time and substrate in a closed system (Fennell et al., 1997; Aulenta et al., 2006; Aulenta et al., 2007; Heimann et al., 2006; Lee et al., 2007). While batch tests have been successful in illustrating what organic electron donors are utilizable for dechlorination and the rate of hydrogen release, they do not indicate how dechlorination performance and electron donor usage will occur in a

continuous feed system, where substrate release can be maintained in a slow and uniform fashion and the selective pressure of microbial (cell) washout can be exerted.

Whether in batch systems or in attached growth systems, there is generally a separation of dechlorination steps, be it temporally in the former, or spatially in the latter. This sequential dechlorination is due to a variety of reasons, such as energetic favorability of dechlorination of PCE and TCE (He et al., 2002), faster maximum utilization rates of the higher chlorinated compounds (Yu et al., 2005), lower hydrogen tension associated with the higher chlorinated compounds (Lu et al., 2001; Yang and McCarty 1998; Luijten et al., 2004), and greater number of organisms capable of reductively dechlorinating PCE and TCE (Holliger et al., 1999). Furthermore, the presence of higher chlorinated compounds is known to competitively inhibit dechlorination of the lesser chlorinated compounds (Yu and Semprini, 2004, Yu et al., 2005).

Performing dechlorination in a continuous flow suspended growth system permits examination of a system where all steps are potentially occurring simultaneously. Though much is known about anaerobic reductive dechlorination, only a few studies have been devoted to evaluating or comparing culture performance in continuous flow suspended growth systems (Drzyzga et al., 2001; Yang and McCarty, 1998; Zheng et al., 2001; Carr et al., 2000). There is thus a need to improve our understanding of dechlorination as it pertains to the selective pressures of a continuous culture and the treatability of high input CAH concentrations, such as solubility limit concentrations of TCE that might be seen in or near a TCE source zone.

The objectives of this study were to 1) determine if a mixed anaerobic culture could sustain dechlorination of TCE-saturated medium in short retention time continuous culture reactors with soluble electron donors; 2) compare how lactate as a fermentable substrate and formate, a more direct soluble hydrogen supply, affected longevity and completeness of dechlorination; and 3) evaluate how culture dechlorination potential shifted as a function of electron donor supplied and time of operation, as determined by frequent batch kinetic tests on harvested cells under non-limiting conditions. To satisfy

these objectives, a mixed anaerobic (“Evanite”, or EV) consortium was inoculated into two continuous culture reactors fed either lactate or formate at twice the stoichiometric requirement (based on hydrogen production potential) to completely dechlorinate 7.5 mM TCE to ETH. The consortium is able to dechlorinate PCE completely to ETH, obtain growth from each dechlorination step, and is confirmed to contain at least one *Dehalococcoides*-like organism (Yu and Semprini, 2004, Yu et al., 2005; Behrens et al., 2008). Additionally, rates for each dechlorination step were periodically measured with cells harvested from the continuous reactors under optimized batch conditions. Batch assays coupled with reactor effluent monitoring data tracked metabolic capabilities and differences of the cultures in the continuous flow reactors. This approach proved useful in deducing dominant reductase systems present and whether reactor performance was limited by electron donors or dechlorinating biomass during operation.

MATERIALS AND METHODS

Chemicals: CAHs and ETH for reactor feed stocks, kinetic tests, and analytical standards were: TCE (99.9%), and cDCE (97%) (Acros Organics, Pittsburgh, PA), VC (99.5%) and ETH (99.5%), (Aldrich Chemical, Milwaukee, WI). Hydrogen gas (99%), and 10%CO₂/90%N₂ mixed gas for kinetic rate tests and media sparging were supplied by Airco, Inc., Albany, OR. Lactate for reactor feed was supplied as 60% sodium lactate syrup, Baker grade (Mallinckrodt Baker, Inc., Phillipsburg, NJ, Lot #A49585). Sodium formate for reactor feed and analytic standards was 99+% reagent grade (Sigma-Aldrich, Inc., St. Louis, MO). Sodium acetate (NaC₂H₃O₂•3H₂O) for reactor feed and analytic standards was 100.5% analytic reagent grade (Mallinckrodt Baker, Inc., Phillipsburg, NJ). Sodium propionate (99%) and sodium L-lactate (99%) were used for analytic standards (Sigma-Aldrich, Inc., St. Louis, MO).

Analytics: Chlorinated ethenes and ethene were quantified with a HP-6890 gas chromatogram (GC), equipped with a flame ionization detector (FID) and 30 m x 0.53 mm GS-Q column (J&W Scientific, Folsom, CA). Helium was used as the carrier gas at 15 mL/min. The GC oven was operated at an initial temperature of 150°C for 2 min, heated at 45°C/min to a final temperature of 220°C, and held at 220°C for 0.7 min, for a sample run time of 4.26 min. The detection limits for TCE, cDCE, VC, and ETH were 0.9, 2.3, 0.5, and 0.04 µM aqueous concentrations, respectively. Hydrogen gas was analyzed on a HP5890 GC with thermal conductivity detector (TCD) and Carbonex 1000 column (15 ft x 1/8 in, Supelco, Bellefonte, PA), with argon as the carrier gas at a flow rate of 15 mL/min. and isothermal heating at 220°C. The hydrogen detection limit was 43 nM (aqueous concentration). Gaseous and aqueous concentrations, and total mass for CAHs, ETH, and hydrogen were determined based upon published Henry's Law constants (Gossett, 1987; Perry et al., 1997; Young, 1981) and the relationships of $H_{cc} = C_g/C_l$, $M_{total} = C_g V_g + C_l V_l$. Lactate, formate, propionate and acetate, were analyzed by high pressure liquid chromatography (HPLC) on a Dionex-500 HPLC. Separation was achieved on a Prevail Organic Acid 5u column (250 mm x 4.6 mm I.D., (Alltech, Deerfield, IL), and an ultraviolet lamp (UV) detector at 210 nm wavelength was used for

signal quantification. The mobile phase was 25.0 mM KH_2PO_4 and 17.3 mM H_3PO_4 in ultrapure deionized water effluent. The detection limits for lactate, propionate, acetate, and formate were 50, 120, 60, and 110 μM , respectively. pH was monitored approximately once per week from each reactor, harvesting 1 mL of effluent and analyzing with a VWR® sympHony® meter model SB70P (VWR International, West Chester, PA).

Protein Measurements: The total protein concentration was determined with the Pierce Micro BCA™ Protein Assay Reagent Kit (Pierce, Rockford, IL). Samples were pretreated with the Compat-Able™ Protein Assay Preparation Reagent Set (Pierce, Rockford, IL) per manufacturer's instructions. Measurements were made on a HP 8453 UV/VIS spectrophotometer on the visible lamp and quantified at 562 nm. The protein detection limit was 0.5 mg/L.

Media preparation: A modified basal growth medium stock was prepared as previously described using reagent grade salts (Yang and McCarty, 1998; Yu et al., 2005). The basal medium for each reactor was augmented with additional Na_2S (anhydrous) to a final concentration of 0.45 mM. Na_2CO_3 (0-220 mg anhydrous) per 250 mL batch of reactor feed was supplied as needed for additional pH buffering capacity to counteract acidification from dechlorination. Na_2CO_3 concentrations were adjusted, based upon weekly effluent pH measurements to maintain reactor target pH values between 6.5 and 7.5. The lactate-fed reactor pH was 6.7 ± 0.4 , and the formate-fed reactor pH was 7.1 ± 0.3 (see Appendix Table A1). Each 250 mL batch of prepared reactor feed was also augmented with 0.5 mL of N_2 -purged neat TCE and either Na-lactate syrup (60%) to a target concentration of 27 mM, or Na-formate (anhydrous) plus Na-acetate· $3\text{H}_2\text{O}$ to target concentrations of 54 mM and 2.5 mM respectively. Acetate as carbon for growth was added with formate feed, but at concentrations low enough (10% of formate on a carbon-basis, 5% molar basis) to ensure formate served as the principle electron donor. Media were prepared in 250 mL (nominal volume) GL-45 bottles (Kimax) fitted with three-hole teflon caps (Kontes Glass Co., Vineland, NJ), outfitted with a plug, an inlet connected with 1/16" PEEK tubing and valve (for N_2 pressurizing), and an outlet with 1/8" PEEK tubing to transfer the media into a 100 mL Hamilton gas-tight feed syringe

(Leno, NV). After TCE addition, media was stirred for approximately 30 minutes, and settled for approximately 30 minutes to obtain a reactor feed with TCE at its solubility limit (~7.5mM). The bottle was then pressurized with anaerobic N₂ gas, and media was extracted with the 100 mL reactor feed syringe. Actual reactor influent TCE concentrations are supplied in Figure A1.

Continuous flow reactor design and operation: A schematic diagram of the reactors is shown in supplemental Figure A2. Each continuous growth reactor was constructed using a GL-45 250 mL (nominal) Kimax bottle fitted with a three-hole Teflon cap (Kontes Glass Co., Vineland, NJ). The holes were ¼-28 thread and accommodated PEEK tubing, fittings, and valves (Upchurch Scientific, Oak Harbor, WA). The reactor inlet was created by extending 1/8” PEEK tubing to the bottom of the bottle. The outlet was 1/16” tubing inserted flush with the Teflon cap. This resulted in a 303 mL reactor with zero headspace. The influent line was fitted with a three-way T-valve to permit influent sampling, while the effluent tubing was fitted with a two-way valve for effluent sampling. Each reactor was continuously stirred with a 1.5” Teflon stir bar and an IKA Ultra-Flat Lab Disc stir plate (IKA-Works Inc, Wilmington, NC), with corrugated cardboard between reactor and stir plate to insulate against heating. The continuous growth reactors were operated at 21°C (± 1.4°C std dev). The influent of each reactor was connected to a Hamilton 100 mL gastight syringe that was driven by an Orion M361 syringe pump (Thermo Electron Corp., Beverly, MA). The pumps delivered a very constant flow of 24 mL/day resulting in a mean cell residence time of 12.5 days.

The EV inoculum for the chemostats was harvested from a fill-and-draw batch fed mother reactor that was previously enriched on TCE with butanol and excess H₂. The EV culture dechlorination kinetics, reductase gene composition, and relative amounts of *Dehalococcoides* have been characterized previously (Behrens et al. 2008; Yu et al., 2005). The chemostat inoculum was created by harvesting 500 mL of the EV liquid mother culture and adding it to 500 mL of basal medium. The mixture was shaken and poured into each reactor flush with the top and capped. These activities were performed inside an anaerobic glove box with 5% H₂, 95% N₂ atmosphere (Coy Laboratory

Products, Inc., Grass Lake, MI). The reactors were removed from the glove box and connected to influent and effluent lines as shown in Figure A2. The influent lines were flushed with their respective media and continuous pumping was initiated. The 100 mL influent syringes were filled approximately every three days, as described above. The reactor influent lines were flushed with each refill to maintain anaerobic conditions. Resazurin was present as a redox indicator and neither system was ever oxidized according to the colorimetric reaction.

To assess culture performance, both continuous flow reactor influents and effluents were monitored every three to four days for CAHs plus ETH, dissolved hydrogen and organic acids concentrations. The samples were collected by pushing 1.5 mL of feed into the reactor and extracting the influent or effluent with a disposable 3.0 mL syringe from the appropriate valve. A headspace sample was created by injecting 1.0 mL of sample into a 2.0 mL crimp-top glass vial. The vial was vortexed for 1 minute at 21°C ($\pm 1.4^\circ\text{C}$ std dev), and 100 μL of gas headspace was immediately removed (Hamilton gastight syringe, Leno, NV) and injected into the GC-FID injection port. A second headspace sample was also extracted (100 μL) and injected into the GC-TCD for hydrogen quantification. The liquid contents of the vial were transferred to a 1.5 mL Eppendorf tube, and frozen for subsequent organic acids analyses.

Batch Kinetic Assays: Batch kinetic tests were conducted on effluent cells approximately every 14 days. The tests were performed in duplicate on 24-hour composite effluent cell samples for TCE, cDCE, and VC separately to quantify maximum dechlorination rates and extents of hydrogen utilization. The batch assays consisted of two phases: first, a 10-hr incubation, followed by a dechlorination rate measurement over a period of one to three hours. Details of the batch kinetic methods are supplied in the supplemental data section, Appendix A. Concentrations during the 10-hour incubation ranged from 50 μM to 800 μM for TCE, 100 to 1100 μM for cDCE, and 600 to 1200 μM for VC, to ensure maximum rates without substrate inhibition (Yu and Semprini, 2004; Yu et al., 2005). Headspace hydrogen was maintained above 5% for the incubation and rate measurements. After the 10-hr incubation step, headspace hydrogen, CAH and ETH

concentrations were analyzed. Batch reactors were then sparged, reaugmented with the CAH of interest, and CAH product formation was measured five times within three hours to obtain a rate from a linear regression through the product formation data. At the end of the kinetic assays, 1 mL of solution was extracted for acids analysis and 0.1 mL of solution for protein analysis.

RESULTS AND DISCUSSION

Chemostat effluent monitoring. Effluent concentrations for both reactors are presented in Figures 2.1a through 2.1f. Initial responses follow classic chemostat theory with a buildup of CAHs from near-zero initial concentrations, and transition from original organic acid concentrations present in the inocula. As shown in Figure 2.1a, the lactate-fed chemostat maintained fairly consistent dechlorination performance for approximately 44 days (3.6 hydraulic residence times (HRTs)), as predominantly VC and ETH accumulated in the reactor. TCE was dechlorinated to approximately 15% ETH and 85% VC, with trace cDCE and TCE ($<20\ \mu\text{M}$ and $<50\mu\text{M}$ respectively). Rather than complete simultaneous failure, a sequential loss of each dechlorination step was observed. First VC dechlorination began to gradually decline on day 12, as indicated by the decrease in ETH in Figure 2.1a, followed by a decline in cDCE dechlorination (day 44) with rapid declines in VC and the buildup of cDCE. TCE dechlorination began to decline on day 72, as seen by the buildup of TCE, and total loss of dechlorination occurred by day 103 as cDCE rapidly declined and TCE accumulation increased.

Organic acid concentrations for the lactate-fed reactor are presented in Figure 2.1b. Initial conditions for the reactor consisted of 7.9 mM acetate, with no detectable propionate or lactate. Acetate and propionate formation from lactate were observed immediately, with increases in acetate and propionate, but no detectable lactate. Lactate was fermented to propionate and acetate until day 69, after which time lactate began to appear in the effluent and increase over time (Figure 2.1b). Prior to day 19, lactate was fermented to approximately 66% acetate, and 33% propionate. This ratio is the inverse of acetate and propionate proportions in Reaction 2 of Table 2.1, suggesting a combination of fermentation Reactions 1 through 3 were possible. A shift in fermentation was observed between day 19 and 96, with stable concentrations of propionate as acetate concentrations declined, accompanied by two instances of rapid decrease on days 58 and 81.

The protein data presented in Figure 2.1c shows an increase in biomass to day 16 followed by a decline to the end of the experiment. The maximum protein concentration

measured at day 16, followed by a decline agrees with the most complete dechlorination to VC and ETH occurring up to day 12 followed by sequential losses in dechlorination steps (Figure 2.1a), as well as the rapid buildup in propionate and acetate to day 19, followed by decreased observable fermentation (Figure 2.1b). A theoretical non-reactive washout curve plotted with the protein data shows that some cell growth was occurring during the gradual biomass loss. The gradual loss of biomass, versus a pure flushing, agrees with the observed gradual and sequential loss in activities.

The formate-fed chemostat exhibited greater completeness of dechlorination and longevity of performance, as shown in Figure 2.1d. In general, the formate-fed system treated TCE to approximately 66% ETH and 33% VC, with cDCE and TCE effluent concentrations generally below 20 μM and 70 μM , respectively. Although periodic fluctuations were observed in effluent CAHs, the formate-fed reactor continued to dechlorinate TCE to approximately 33% VC and 66% ETH for 195 days (15 HRTs). After day 195, sequential loss of each dechlorination step was observed, with losses of VC, cDCE, and TCE dechlorination on days 195, 204, and 227, respectively.

The average effluent VC concentration during the first 185 days of operation was approximately 2.5 mM, with the remaining TCE being converted almost entirely to ETH. Production of ETH in excess of its solubility limit did produce some complications with analysis, however. The aqueous concentrations of ETH were generally measured to be 2 mM. The theoretical solubility for ETH in distilled water, based on the Henry's coefficient at 20°C is 0.5 mM (Perry et al., 1997). Approximately 5 mL of headspace developed in the formate-fed reactor, which was likely due to production of ETH in excess of its solubility limit. Gas bubbles were frequently observed in the effluent sampling, which likely caused the ETH concentration measurements above the 2 mM solubility limit. Gas bubbles were also in the effluent collection vial (see Figure A2 for schematic diagram), which resulted in mass balances of less than 100%. Theoretical ETH concentrations based upon a CAH-addition mass balance are shown in supporting data Figure A3.

In the formate fed reactor, effluent acetate concentrations were consistently above acetate-carbon supplied in the influent from reactor startup to day 54 (Figure 2.1e), indicating homoacetogenesis was occurring. Approximately 20% of the formate carbon was converted to acetate, based on electron donor balances. After day 54, intermittent acetogenesis was observed to day 150, as can be seen in periodic effluent acetate concentration exceeding influent concentrations (Figure 2.1e). From day 156 to the end of the experiment (day 295), generally half (1.2 mmol/L) of the influent acetate was consumed. Formate was not detectable in the reactor effluent until day 195, when an increase to 15 mM was observed, which was below the supplied $39.5 \text{ mM} \pm 9.0 \text{ mM}$. Hydrogen was detected in the effluent during formate appearance, but no higher than aqueous concentrations of $258 \text{ } \mu\text{M}$, which is insufficient to account for the 24.5 mM difference in effluent and influent formate. Hydrogen was generally detectable in the effluent above $1 \text{ } \mu\text{M}_{\text{aq}}$ (data not shown) from startup to day 81, and rarely detectable from day 85 to 195. After day 195, concurrent with effluent formate increases, effluent hydrogen concentrations were typically between 14 and $250 \text{ } \mu\text{M}_{\text{aq}}$. Initial excess hydrogen agreed with observed acetogenesis and our knowledge of hydrogen thresholds, as did the period of undetectable hydrogen and lack of observed acetogenesis (Aulenta et al., 2006; Yang and McCarty, 1998; Löffler et al., 1999). Excess hydrogen after day 195 corresponded to observed formate dehydrogenation coupled with declining dechlorination and acetogenic activity.

Protein data in the formate fed reactor, along with a theoretical non-reactive flushing curve, are displayed in Figure 2.1f. As with the lactate fed reactor, protein concentrations reflected reactor performance, with an increase in cells from startup to day 16, stable biomass from day 16 to day 193, and declining biomass from day 193 to 295. The relatively high levels of protein between days 193 and 295 (Figure 2.1f) exceeded the pure theoretical flushing of biomass, indicating observed acetate consumption may have been utilized for cell synthesis. Similar to the lactate-fed reactor, the protein data shows growth occurred during CAH transformation failure.

Periodic fluctuations of TCE, cDCE, and VC concentrations appeared in the effluent of the formate-fed system, though not in the lactate-fed system (Figures 2.1a and 2.1d). The rapid H₂ release associated with formate (Lee et al., 2007) added in excess and producing relatively high reactor concentrations potentially resulted in competition for hydrogen utilization in non-dechlorinating processes such as observed acetogenesis. Thus, although completeness of dechlorination and longevity of performance was inferior in the lactate-fed system, lactate did appear to foster a community less prone to short-term disturbances in performance.

Electron Flow and Balance. A cumulative electron balance for both reactors is shown in Figures 2.2a and 2.2b. Biomass electron equivalents were estimated by assuming 1 mg of protein equates to 2 mg of biomass, with a biomass stoichiometry of C₅H₇O₂N and 20 electron equivalents per mole of biomass (Lee et al., 2004). The protein distributions used for these estimations are shown in Figures 2.1c and 2.1f. Electron equivalent assumptions for the major organic compounds and dechlorination processes measured are summarized in supplemental Table A2.

In the lactate-fed reactor, a majority of electrons left the system as acetate and propionate. As can be seen in Figures 2.1b and 2.2a, a large amount of lactate fermented to propionate, which built up in the reactor, rather than ferment to acetate. Equation 3 of Table 2.1 indicates each mole of propionate represents potentially 3 moles of H₂, if fermented to acetate. Expecting that two moles of H₂ would be released per mole of lactate added, the influent lactate concentration was set to 25 mM. With effluent propionate concentrations typically around 10 mM, and 3 moles of H₂ theoretically associated with propionate, only approximately 40% of expected H₂ moles were likely released through fermentation. As a result, a relatively small percentage of electrons added as lactate were available for cDCE and VC dechlorination, known to require H₂ as the direct electron donor (Cupples et al., 2003; Lee et al., 2007). During the first 60 days of operation, approximately 35% of the electron equivalents left the system as acetate, 25% as propionate, 9% as biomass, and 6% were used for dechlorination (Figure 2.2a). The remaining percentage of electron equivalents could not be accounted for.

The organic acid mass balance in the lactate fed reactor declined significantly after day 85, which was also associated with the appearance of interfering and unidentified compounds during HPLC analysis. Similar unidentified peaks were not observed in influent samples, analytic standards, or effluent samples from the formate-fed reactor, indicating alternate products were present in the failing lactate-fed reactor. Alternative organic products such as butyrate, succinate, glutamate, trehalose, malate or other simple organics are possible unidentified products (Deborde and Boyaval, 2000; Schulman and Valentino, 1975). Some gases were observed to bubble out of the effluent, which could have contained hydrogen gas or CO₂ that also could have affected the total mass balance. Methane production was not observed.

The presence of H₂, as was detected in the lactate-fed reactor up to day 58, is known to favor fermentation of lactate to propionate and acetate (Reaction 2, Table 2.1) versus fermentation of lactate directly to acetate and H₂ (Reaction 1, Table 2.1) (Aulenta et al., 2007). Furthermore, the presence of acetate at approximately 10 mM has been shown to inhibit the rate of propionate fermentation (initial concentration 12 mM) by approximately 50% (Fukazaki et al., 1990). Batch fermentation of propionate has been shown to extend beyond 70 days in a TCE dechlorinating mixed culture (Heimann et al., 2007). Thus, despite conditions being energetically favorable for fermentation of propionate to acetate and H₂, (see $\Delta G'$ calculations supplied in Table 2.1), the reaction kinetics are not necessarily favorable, especially in a 12.5 day retention time continuous flow reactor. With lactate fermentation proceeding by Reaction 2 (Table 2.1) to a significant degree, as observed (Figure 2.1b), H₂ availability for dechlorination was substantially reduced from the amount possible if lactate and propionate were fermented to acetate and H₂ only.

While only 6% of the electron equivalents added as lactate were accounted by reductive dechlorination, a substantial amount of theoretical electrons released from fermentation of lactate to propionate and acetate were devoted to dechlorination. When the CAH electron equivalents reduced are compared to the difference in lactate electron equivalents added minus organic electron equivalents leaving the reactor as acetate and

propionate, rather than simply comparing to the total electron equivalents supplied as lactate, 19 to 33% were generally associated with reductive dechlorination between startup and day 89. After day 89, however, less than 10% of electron equivalents released from lactate were utilized for dechlorination, indicating inefficient electron usage with respect to dechlorination despite subtracting electrons associated with acetate and propionate.

Formate was removed below the 110 μM detection limit, presumably by dehydrogenation to H_2 , until failure beginning at day 195 (Figure 2.1e). From startup to day 150, 35 to 45% of electron equivalents added as formate were directed to reductive dechlorination, another 25 to 35% of electrons left the system as effluent biomass, and 15 to 35% were associated with homoacetogenesis (see Figures 2.2b and 2.1e). Unaccounted electron equivalents in the formate fed system amounted to only 5% by day 204 and increased to 22% by day 295, which might be associated with escaping gases, such as CO_2 and H_2 . Generally, there was a factor of six times greater electron equivalents added directed toward reductive dechlorination in the formate-fed reactor, compared to the lactate-fed reactor (35% compared to 6%). Even when subtracting the electrons of propionate and acetate in the effluent, the formate-fed reactor achieved a much greater percent of electron flow directed toward dechlorination than the lactate-fed reactor.

Batch Rate Kinetic Tests. Periodic batch kinetic assays were conducted with cells harvested from the reactors to determine how dechlorination rates changed with time. The rates are presented in Figures 2.3a and 2.3b. The dechlorination rates reflected the temporal performance of both lactate- and formate-fed reactors with increasing batch rates corresponding to enhanced reactor performance, and declines in rates timed with diminished performance. The rates were also very constant during stable operation. Additionally, when both reactors failed with sequential increases in VC, cDCE, and TCE effluent concentrations (Figures 2.1a and 2.1d), batch measured rates for each CAH declined substantially in series as well, with rates falling by two orders of magnitude in

similar time frames to reactor failure, starting first with VC dechlorination, followed by cDCE and TCE dechlorination (Figures 2.3a and 2.3b).

The stability of performance in the formate-fed reactor is reflected in the batch rate measurements. Consistent removal of approximately 99% of the 7.5 mM influent TCE to below 70 μM (detection limit 0.9 μM) from startup to day 231 (Figure 2.1d) was reflected in measured rates consistently being above 20 $\mu\text{moles/day/mg protein}$ (Figure 2.3b). Though TCE removal in the formate-fed reactor was stable and 99% complete during the first 231 days of operation, the rate tests were constant only between days 50 and 191. cDCE and VC dechlorination rates were semi-steady during the same time frame (Figure 2.3b), but not truly stable. Significant differences in cDCE and VC rates over time, whereas TCE rate measurement differences were not significant (Figure 2.3b), indicating true changes in culture cDCE and VC dechlorination capabilities over time.

Short term CAH concentration fluctuations observed in the formate-fed reactor were closely mirrored by changes in the batch kinetic rate measurements (Figures 2.1d and 2.3b). For instance, when VC and cDCE effluent concentrations rose in the chemostat between days 25 and 45 (Figure 2.1d), the corresponding batch rate declined (Figure 2.3b). Conversely, when the formate-fed reactor VC and cDCE concentrations declined between days 45 and 80, batch rates increased. As VC and cDCE increased in the effluent from days 81 to 112, batch rates declined. Reactor removal of VC and cDCE also improved between days 112 and 141, and batch dechlorination rates for VC and cDCE increased. These data illustrate how batch-measured kinetic rates indicate cell activity and capabilities of the continuously grown culture, and help explain the transient concentration behavior in the reactor. The batch kinetic tests closely reflect the transient conditions in the continuous reactor.

The batch rate tests also demonstrated shifts in proportions of dechlorination activity. For instance, rates normalized to protein concentration should remain constant if the microbial composition of the mixed community were to remain steady. The protein-normalized batch rates did not remain constant, however, indicating the proportion of the dechlorinating biomass with respect to total biomass changed over time. The rate batch

assays also indicated changes in dechlorinating sub-populations in the formate-fed system. Between days 50 and 168, batch rate tests for cDCE and VC dechlorination showed a steady increase in maximum rates normalized to protein content, while TCE dechlorination rates remained constant (Figure 2.3b). Thus, a subpopulation of cDCE and VC dechlorinators were likely increasing over time, while a TCE dechlorinating population was not. Such community dynamics are not apparent from flowthrough reactor monitoring alone.

Shifts in batch measured rates showed not only differences in each reactor over time, but also differences between the two reactor communities. Comparing protein-normalized rates between the lactate and formate fed systems (Figures 2.3a and 2.3b) shows similar maximum rates were achieved when both chemostats were effectively degrading the CAH of interest, though the formate-fed system was able to maintain higher rates. This was likely due to longer-term stability of performance in the formate-fed system, with greater opportunity for growth of the dechlorinating population within the total community. The maximum observed batch-measured rates for both reactors are summarized in Table 2.2. Both sets of rates compare well with previously reported rates for the EV culture, also presented in Table 2.2. These data indicate that *Dehalococcoides* were enriched during peak performance, especially in the formate-fed system. It is interesting to note that rates from this work compare closely with previous characterization of the EV culture. Our cultures were grown with TCE and either formate or lactate as sole electron donors in continuous flow reactors, while the previous rates were determined with a community grown on PCE, butanol and hydrogen in sequential batch fed reactors (Yu et al., 2005).

Batch kinetic assays also highlighted differences between the two reactors that suggest different dechlorinating enzymes could have been dominant in the separate systems. For instance, in the lactate fed system, rate tests demonstrated the VC-dechlorinating ability declined between days 2 and 32, while cDCE dechlorination ability increased over the same time period (Figure 2.3a). In the formate-fed system, VC and cDCE dechlorination rates closely mirrored each other from days 1 to 197, with

sequential loss in batch measured rates from days 197 to 291 (Figure 2.3b). A Pearson correlation test was performed, comparing VC with cDCE normalized dechlorination rates. The Pearson correlation coefficients for the lactate and formate-fed systems were 0.11 and 0.72, respectively. Thus, there was a poor correlation between VC and cDCE dechlorination rates in the lactate fed system, and a stronger correlation in the formate-fed system. The *vcrA* gene product is known to dechlorinate both cDCE and VC to ETH (Müller et al., 2004; Sung et al., 2006b). Thus, the formate fed system likely allowed a *vcrA*-type enzyme system to dominate these dechlorination steps, while the lactate-fed system did not. The *vcrA* gene has been detected in the EV culture (Behrens et al., 2008), and molecular analyses of these reactors support these rate observations (Chapter 3)

The batch dechlorination rates confirmed CAH flushing observations in the reactors as well. Portions of reactor CAH effluent monitoring are displayed again in Figures 2.4a through 2.4f, with theoretical non-reactive washout curves added. Batch rate data was elevated when CAHs left the reactor slower than theoretical non-reactive flushing, and batch measured rates were low when reactor CAH data more closely matched theoretical non-reactive flushing. Theoretical curves assumed a reactor volume of 303 mL and constant flow of 24 mL/day. A decline in the CAH of interest by at least 15% between two consecutive time points was selected as the initial time of theoretical flushing. Initial flushing of ETH, VC, and cDCE were assumed to be on days 12, 58, and 103, respectively in the lactate-fed reactor (Figures 2.4a, 2.4b and 2.4c), and on days 199, 208 and 231, respectively in the formate-fed reactor (Figures 2.4d, 2.4e and 2.4f). These time frames highlight the gradual loss of dechlorination activity in the lactate-fed reactor over 91 days, while a rapid succession occurred in the formate-fed reactor over a span of 32 days.

As can be seen in Figures 2.4a through 2.4c, ETH and VC were not flushed as quickly as calculated theoretical flushing, while cDCE closely follows a theoretical non-reactive flushing for the lactate-fed reactor. This indicates low levels of VC and cDCE dechlorination were still occurring beyond days 12 and 49, respectively, while TCE dechlorination ceased almost completely on day 103. Batch measured rates for VC

dechlorination on days 17 and 32 were within the same order of magnitude as the initial VC dechlorination rate, supporting minor VC dechlorination during ETH flushing from days 12 to 50 (Figure 2.3a). Similarly, the VC flushing in the effluent from days 58 to 125 (Figure 2.4b) were accompanied by cDCE batch dechlorination rate measurements of 5.5 down to 0.14 $\mu\text{moles/day/mg protein}$ from days 52 to 93 (Figure 2.3a), again indicating dechlorination activity was present when non-reactive flushing would require zero activity. TCE dechlorination rate of 0.06 $\mu\text{moles/day/mg protein}$ measured on day 114, compared to the initial rate of 25.2 $\mu\text{moles/day/mg protein}$ (Figure 2.3a), which is consistent with the observed non-reactive flushing of cDCE (Figure 2.4c).

In the formate-fed reactor, ETH, VC, and cDCE flushing all matched theoretical non-reactive washout curves (Figure 2.4d through 2.4f). This indicates that flushing of ETH, VC, and cDCE on days 199, 208, and 231 coincided with virtually complete loss of VC, cDCE, and TCE dechlorination activity. Flushing of ETH between days 200 and 250 in the reactor (Figure 2.4d) corresponded to VC dechlorination rates in batch tests of less than 0.08 $\mu\text{moles/day/mg protein}$ on days 226 and 256 (Figure 2.3b). Flushing of VC from days 208 onward (Figure 2.4e) corresponded to cDCE batch rates of 1.66 $\mu\text{moles/day/mg protein}$ on day 214, and no detectable activity in batch on day 254. cDCE flushing observed from day 231 onward (Figure 2.4f) related to TCE batch dechlorination rates between 1.2 and 0.3 $\mu\text{moles/day/mg protein}$ on days 240, 252, and 291 (Figure 2.3b), compared to a maximum rate of 29.8 $\mu\text{moles/day/mg protein}$.

Batch Hydrogen Consumption. In addition to maximum dechlorination rates, the hydrogen consumption during 10 hours of batch incubation was measured. Endpoint analysis of the hydrogen required for observed dechlorination, and total hydrogen consumption measured are presented in Figures 2.5a and 2.5b. In batch assays with excess hydrogen present, the formate-fed system demonstrated the presence of organisms capable of utilizing H_2 for non-dechlorinating activity, while the lactate-fed system generally only used H_2 in stoichiometric amounts required for dechlorination. Given excess electron donor supply and measurable hydrogen, as well as faster hydrogen release associated with formate dehydrogenation compared to lactate fermentation (Lee et

al., 2007; Heimann et al., 2007) this observation is somewhat expected.

Homoacetogenesis was consistently observed and accounted for 20 to 30% of formate utilization (Figures 2.1e and 2.2b). Homoacetogenic activity has also been previously documented in the EV mixed culture (Pon et al., 2003). Hydrogen levels in the reactor were frequently above 1100 nM, which should sustain acetogenic organisms (Aulenta et al, 2006; Yang and McCarty, 1998; Löffler et al., 1999). Excess hydrogen consumption observed in the lactate-fed batch tests to day 29 (Figure 2.5a) coincided with hydrogen levels in the lactate-fed reactor frequently above 1100nM to day 58, with no detectable hydrogen from days 61 to 100 in the continuously fed lactate reactor.

Low levels of hydrogen production were measured in the formate-fed culture batch tests after day 214 (Figure 2.5b), which was likely the result of formate dehydrogenation. Note that formate and protein biomass was present in the chemostat after day 204 (Figures 2.1e and 2.1f). The ability of the formate-fed culture to consume excess hydrogen when available, the fact that formate can result in high rates of hydrogen release, and the fact that acetogenic activity was prevalent in the formate-fed reactor would suggest dechlorinators had constant competition for electron donors in the chemostat. This could have been a contributing factor in washout of dechlorinating organisms in the formate-fed chemostat, or possible consequence of operating with high loading in a short retention-time reactor.

Lactate has successfully been used as a fermenting electron donor to dechlorinate PCE and TCE to VC and ETH in batch incubation (Heimann et al., 2007; Fennell et al., 1997), and lactate has been used in short-term continuously stirred reactors to successfully dechlorinate PCE to cDCE (Drzyzga et al., 2001; Gerritse et al., 1999). Here, we have shown lactate could sustain dechlorination of TCE at saturation concentrations to approximately 15% ETH and 85% VC for over 50 days, with a relatively short retention time (12.5 days), and two times the stoichiometric H₂ production potential. Incomplete fermentation under the operating conditions tested likely caused the modest performance and duration. It is unknown whether propionate buildup was the result of *in situ* conditions favoring lactate fermentation to propionate

and acetate, rather than to acetate and hydrogen, or if perhaps propionate fermentation to acetate and hydrogen could not be maintained with the short retention time. Studies have compared the effects of differing electron donors on community performance and dechlorination in long- and short-term batch studies (Yang and McCarty, 1998; Drzyzga et al., 2001; Lee et al., 2007; Heimann et al., 2007). This, to our knowledge, is the first study comparing electron donor effects in reductively dechlorinating continuous flow suspended cultures.

Additionally, this study showed formate could successfully sustain dechlorination of TCE fed at saturation concentrations in continuous flow suspended cultures to approximately 30% VC and 70% ETH. Performance was sustained for nearly 200 days with a 12.5 day residence time and twice the stoichiometric H₂ production potential requirement. Previous work has shown the success of formate stimulating dechlorination of PCE to cDCE, VC, and ETH in batch incubation, but this appears to be the first study demonstrating its success long term in continuous suspended growth cultures (Lee et al., 2007).

To our knowledge comparisons have not been made on continuous reactors with periodic batch tests to track performance potential and shifts over time parallel to reactor monitoring. Studies have assessed endpoint culture performance or single analyses from steady-state operation (Lee et al., 2007; Cupples et al., 2003). The repeated periodic batch tests illustrated that steady reactor performance does not necessarily equate to steady community abilities. Single time point analyses from steady-state reactors cannot capture the total range of potential activity associated with a perceived reactor steady state. Field studies have compared DNA and RNA measurements with *in situ* performance, but relating molecular data specifically to observed field dechlorination rates has yet to be achieved (Lendvay et al., 2003; Rahm et al., 2006a; Lee et al., 2008). This study has demonstrated that simple batch kinetic tests, shown to reflect the continuous community, can potentially be used to reliably model and predict *in situ* dechlorination capabilities and rates.

The use of chemostat monitoring combined with batch kinetic assays illustrated how the microbial activities changed over time as a result of different soluble electron donors. Batch rate measurements were highly reproducible and reflected reactor performance, yet supplied more specific information on the range of capabilities during steady reactor performance. Batch rate tests supplied greater details than reactor monitoring regarding specific dechlorination rates and capabilities, hydrogen utilization, and changes in percent biomass devoted to dechlorination.

Though formate and lactate are both relatively fast fermenting organic substrates, here we have shown the selective pressure of a short retention time yields superior performance with formate. Reactor performance in this work has shown the importance of relevant fermenting capabilities, *in situ* conditions promoting different fermentation reactions, and contact and reaction time for fermentation. While slow fermentation of propionate has produced thorough dechlorination in long-term batch experiments (Heimann et al., 2007; Yang and McCarty, 1998), field application with groundwater flow or a recirculation strategy could result in poor hydrogen release in the zone of CAH contamination as propionate can migrate with groundwater. Propionate formation from lactate addition with incomplete dechlorination has been observed in laboratory attached growth systems, as well as field operations, indicating the possibility of insufficient H₂ release in the CAH contamination zone (Adamson et al., 2003; Azizian et al., 2008; Rahm et al., 2006a). Formate added in excess did result in homoacetogenesis, and may have led to hydrogen competition, but maintained fairly thorough dechlorination for approximately 200 days.

This work has also shown that two relatively fast-releasing hydrogen sources can produce two very different mixed communities and abilities to dechlorinate TCE. While both formate and lactate supplied at roughly twice the required H₂ to completely dechlorinate TCE to ETH produced nearly complete dechlorination at startup, both systems eventually lost dechlorination activity. The lactate-fed system failed first, likely from the washout of key fermenting organisms to produce sufficient hydrogen to maintain the dechlorinating population. It is not known why the formate-fed system lost

dechlorination activity, since reasonably stable performance was maintained for 200 days, or 16 hydraulic residence times. Hydrogen competition with acetogens, toxicity from possible TCE NAPL droplets, or bulk conditions affecting energetic favorability of reactions combined with the pressures of cell washout are possible explanations. Future molecular characterization and multi-population modeling of hydrogen competition may supply explanations of population dynamics to help account for system failures.

ACKNOWLEDGEMENTS

Funding for this research was provided by NSF Integrative Graduate Education and Research Traineeship Program (IGERT), U.S. EPA Western Region Hazardous Substance Center (Grant # R-828772), and National Institute of Environmental Health Sciences (Graduate Training Grant #1P42 ES10338). This article has not been reviewed by the above agencies and no endorsement should be inferred.

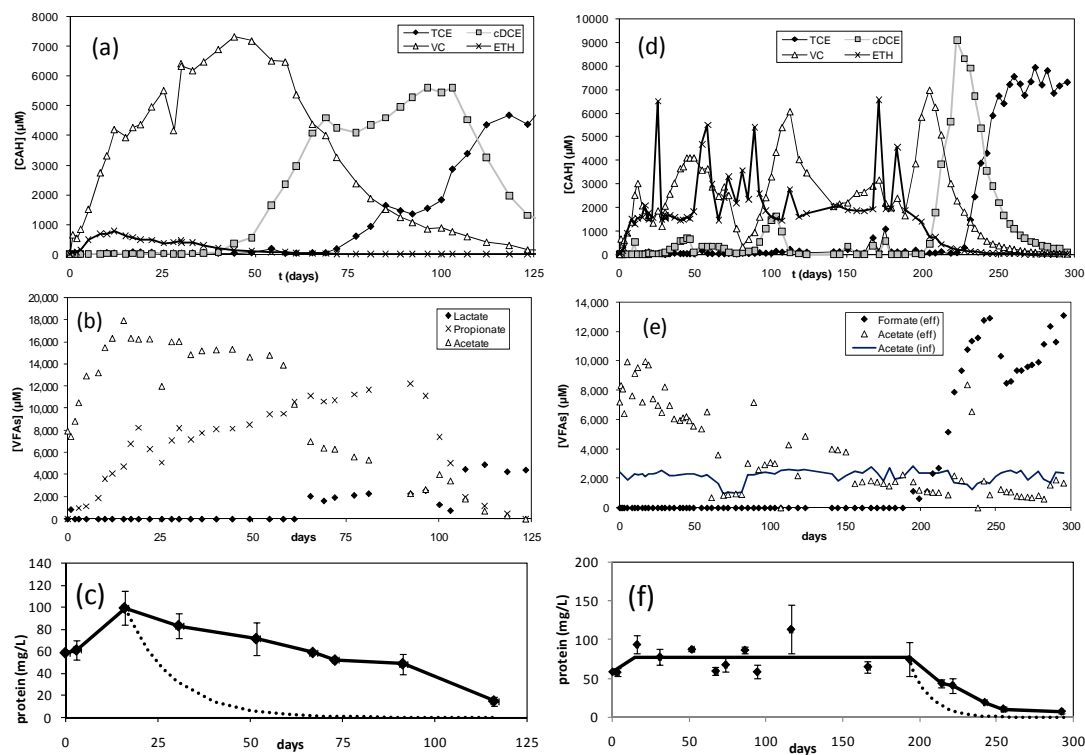


Figure 2.1. Continuous reactor effluent monitoring data. Data for the lactate fed reactor are a) CAHs, b) organic acids, and c) protein concentration. Data for the formate-fed reactor are d) CAHs, e) organic acids, and f) protein. CAHs and VFAs are singlet effluent sample analyses. Instrument error is $\pm 5\%$. Symbols for CAHs and VFAs are supplied in the legend for Figures a, b, d, and e. Protein concentrations are plotted as averages of 2 to 6 samples collected within one week. Horizontal and vertical error bars represent the standard deviation of sample times and protein measurements, respectively. The assumed protein distribution (solid lines) for electron balance and rate measurement normalization and theoretical non-reactive washout (dashed lines) are also plotted with the protein data.

Table 2.1. Relevant electron donating and electron consuming reactions and energetics.

	$\Delta G^{o'}$ (kJ/mol rxn) ^a	$\Delta G'$ (kJ/mol rxn) ^b	
H₂-producing reactions			
1) lactate + 2H ₂ O → acetate + HCO ₃ ⁻ + H ⁺ + 2H ₂	-3.96	-135.89	
2) lactate → 1/3 acetate + 2/3 propionate + 1/3 HCO ₃ ⁻ + 1/3 H ⁺	-54.95	-63.97	
3) propionate + 3H ₂ O → acetate + HCO ₃ ⁻ + H ⁺ + 3H ₂	76.48	-78.0726	
4) formate + H ₂ O → HCO ₃ ⁻ + H ₂	1.37	-34.35	
H₂-consuming reactions			
		lac-fed	for-fed
5) TCE + H ₂ → cDCE + Cl ⁻ + H ⁺	-170.74	-171.66	-170.97
6) cDCE + H ₂ → VC + Cl ⁻ + H ⁺	-141.28	-126.01	-127.28
7) VC + H ₂ → ETH + Cl ⁻ + H ⁺	-151.35	-155.94	-149.31
8) 1/2 HCO ₃ ⁻ + H ₂ + 1/4 H ⁺ → 1/4 acetate + H ₂ O	-26.14	56.84	46.17

^a Calculated from Gibbs free energies of formation under standard atmospheric conditions (25°C, concentrations of 1M, at pH 7.0) as supplied in Thauer et al., 1977; Weaste and Astle, 1980; and Dolfig and Janssen, 1994.

^b Calculations of free energies of reactions under typical extant conditions for each reactor. The following assumptions were used for both reactors: T=25 °C, pH 7.0, [HCO₃⁻] = 0.03 M, [H_{2,aq}] = 500 nM, [H₂O] = 55 M, [TCE] = 50 μM, [cDCE] = 20 μM. For the lactate-fed reactor, additional assumptions are: [VC] = 5.5 mM, [ETH] = 0.5 mM, [Cl⁻] = 17.3 mM, [lactate] = 0.5 mM, [propionate] = 7 mM, [acetate] = 15 mM. Additional assumptions for the formate-fed reactor are: [VC] = 2.5 mM, [ETH] = 2.5 mM, [Cl⁻] = 22.8 mM, [formate] = 0.5 mM, [acetate] = 5 mM.

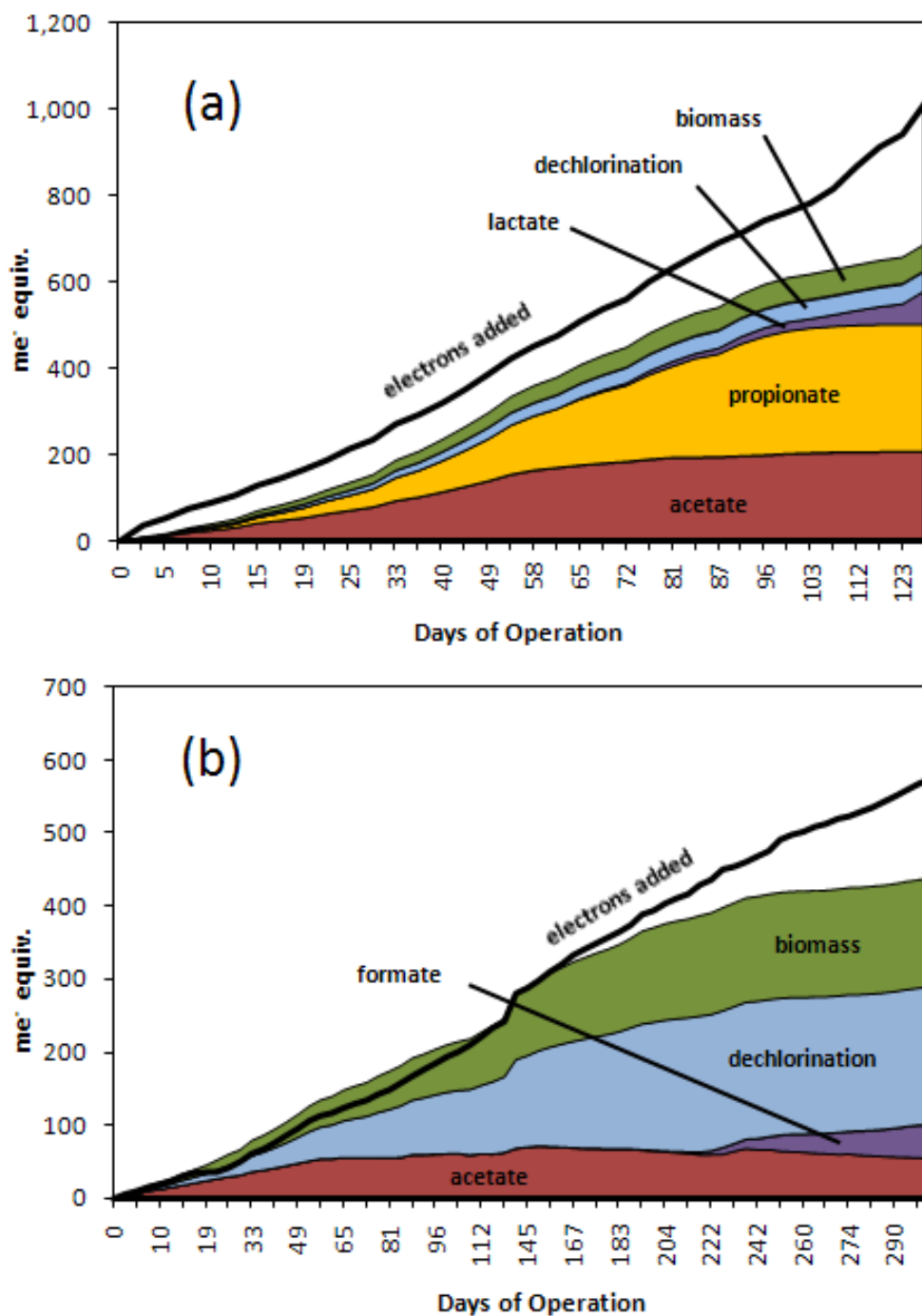


Figure 2.2. Continuous reactor electron balances. a) The lactate-fed reactor, and b) the formate-fed reactor. Bold line represents cumulative electrons added as either a) lactate, or b) formate. Shaded areas labeled as effluent electrons or dechlorination. Influent acetate has been excluded from 2(b) electron equivalents added to illustrate net homoacetogenesis or acetate consumption.

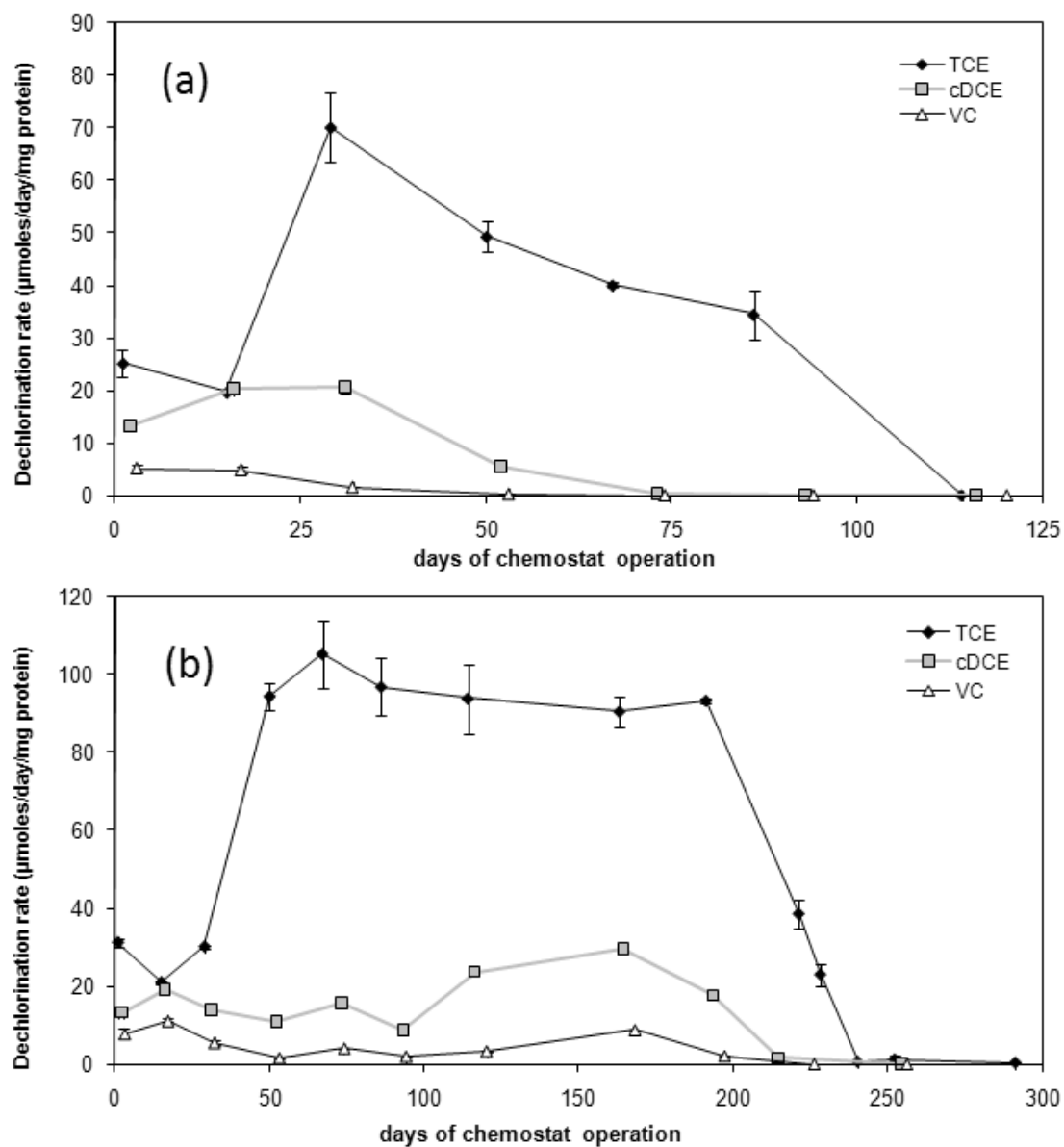


Figure 2.3. Culture specific dechlorination rates under non-limiting conditions in batch assays. a) The lactate-fed system and b) the formate-fed system.

Table 2.2. Maximum utilization rates (k_{\max}) for EV culture previously reported versus current study.

	k_{\max} ($\mu\text{mol}/\text{mg protein}/\text{day}$)		
	EV ^a	Lactate-fed ^b	Formate-fed ^b
TCE	125 \pm 14	70.1 \pm 6.5	105 \pm 8.6
cDCE	13.8 \pm 1.1	20.5 \pm 1.2	29.8 \pm 0.3
VC	8.1 \pm 0.9	5.1 \pm 0.7	11.2 \pm 0.4

^a Previously reported by Yu et al., 2005. Triplicate average \pm standard deviation.

^b Units converted from presented material for comparison. Duplicate average \pm range.

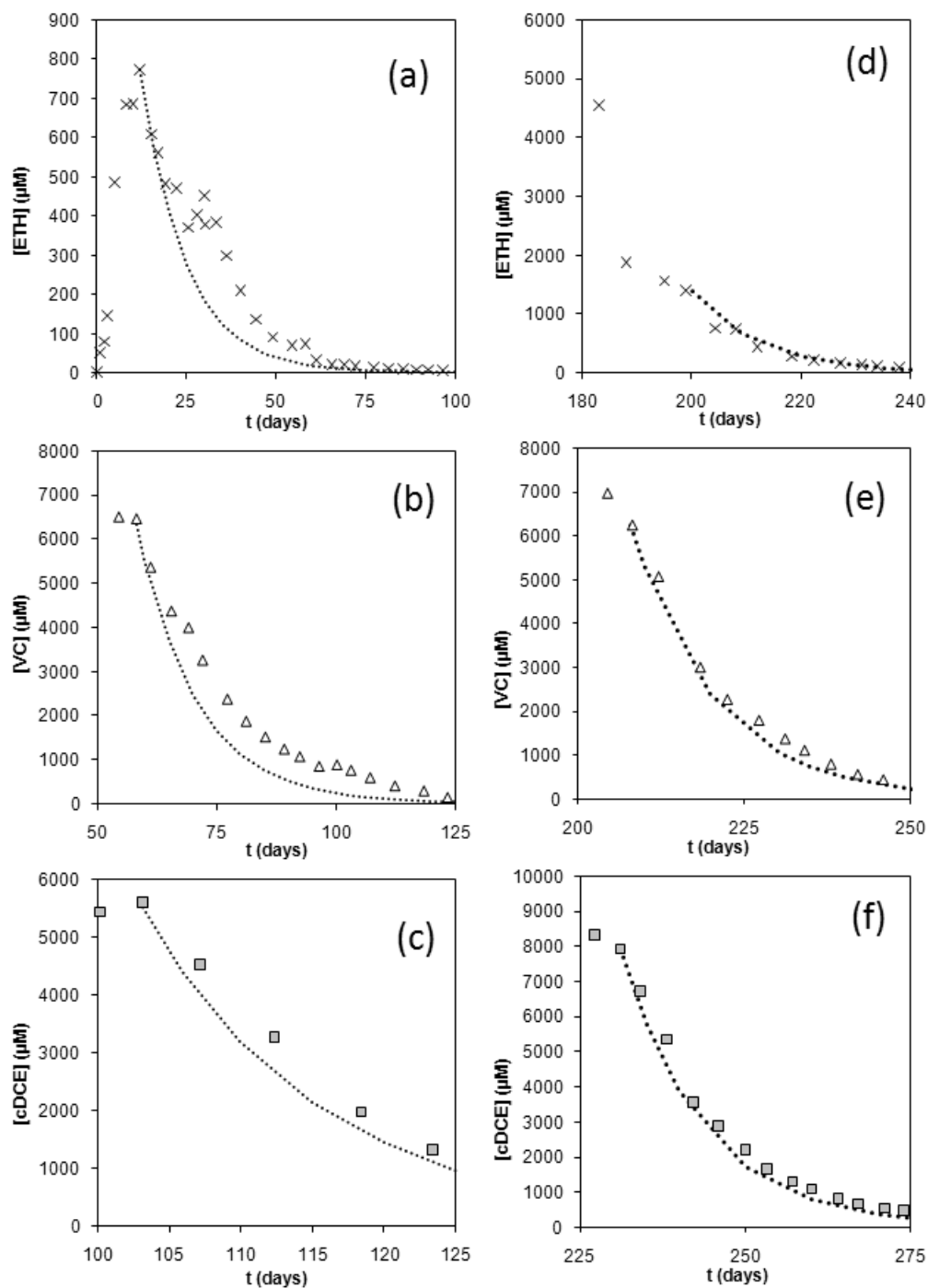


Figure 2.4. CAH monitoring compared to theoretical non-reactive washout. Theoretical curves and data are for the lactate-fed system with a) ETH, b) VC, and c) cDCE; or the formate-fed reactor with d) ETH, e) VC, and f) cDCE. Dashed lines represent theoretical non-reactive washout. Symbols are reactor effluent measurements. Note the differing time scales in each figure.

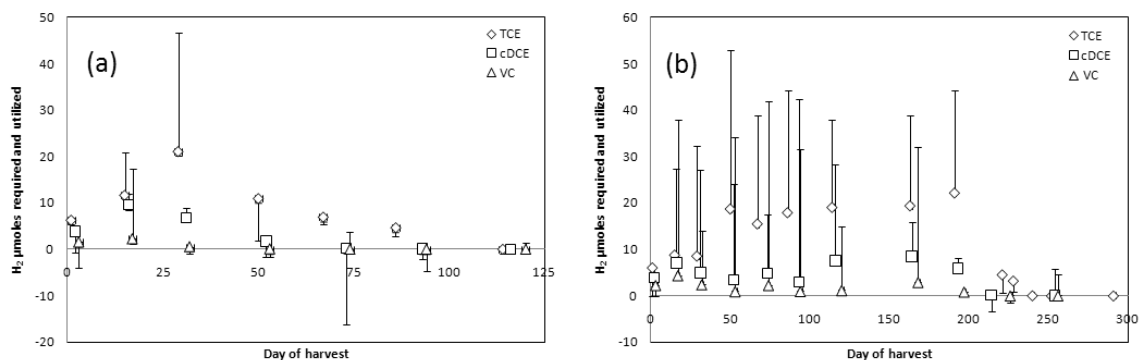


Figure 2.5. Endpoint hydrogen consumption during all CAH batch assays after 10 hours of incubation. a) The lactate-fed system, and b) the formate-fed system. Symbols are the stoichiometric H₂ requirements for the amount of dechlorination activity measured for the CAH indicated in figure legends, and whiskers are measured H₂ consumption. Whiskers extending below the symbols represent net H₂ formation (from fermentation or formate dehydrogenation), while whiskers extending above the symbols indicate net over-consumption of H₂ for non-dechlorinating processes.

Chapter 3

Gene quantification tracks electron donor and acceptor effects on multiple *Dehalococcoides* strains in mixed community chemostats and predicts cDCE and VC dechlorination rate potential

ABSTRACT

DNA quantification for 16S rRNA and functional genes, such as reductases, is gaining use in tracking multiple *Dehalococcoides* strains in mixed anaerobic dechlorinating cultures. Little is known, however, about how *Dehalococcoides* are impacted within mixed communities by different electron donors or acceptors, nor how different *Dehalococcoides* strains compete with each other. In this study, we tracked multiple reductase genes of *Dehalococcoides* species within a mixed anaerobic consortium to determine how different electron donors or acceptors affected the populations starting from the same culture. Three separate continuous flow stirred tank reactors (CFSTRs) were inoculated with the same culture, and fed either trichloroethene (TCE) and lactate, TCE and formate, or vinyl chloride (VC) and formate. TCE or VC were continuously supplied at their solubility limits in the media, with twice the stoichiometric electron donor requirements to dechlorinate the TCE or VC completely to ethene (ETH). *Bacteria* and *Dehalococcoides* 16S rRNA genes, plus the characterized *Dehalococcoides* reductase genes: *bvcA*, *vcrA*, *tceA*, and *pceA* were repeatedly analyzed by quantitative polymerase chain reaction (qPCR), and compared to reactor performance and separate batch dechlorination rate determinations with reactor-harvested cells. qPCR data demonstrated that the lactate- and TCE-fed reactor selected for decreasing amounts of *Dehalococcoides* over time, while the formate- and TCE-fed reactor maintained a consistent proportion of *Dehalococcoides* to total bacteria. With the short (12.5 day) retention time, the VC-formate-fed reactor quickly flushed *Dehalococcoides* from the reactor. In all three reactors, regardless of *Dehalococcoides* quantities, strain or dehalogenase gene dominance, qPCR data showed what appeared to be the presence of a single organism containing only *pceA* and *vcrA*, with a separate organism containing only the *tceA* gene. The lactate and TCE-fed reactor selected for domination of the *tceA* gene, while both formate-fed reactors selected for dominance of the *vcrA* gene. *bvcA* was not detected in any reactor. Additionally, *Dehalococcoides* 16S rRNA gene quantities correlated to batch-measured cDCE and VC dechlorination rates and could predict cDCE and VC dechlorination rates within the correct order of magnitude.

INTRODUCTION

Trichloroethylene (TCE) and the lesser chlorinated ethenes, cis-1,2-dichloroethene (cDCE) and vinyl chloride (VC), are ubiquitous groundwater contaminants of environmental concern (Ensley, 1991; McCarty, 1997; Kielhorn et al., 2000). Anaerobic reductive dechlorination is a well documented process for remediating TCE and other chlorinated aliphatic hydrocarbons (CAHs), which is desirable for its simplicity in implementation and success in completely dechlorinating CAHs to non-toxic ethylene (Aulenta et al., 2006). The process requirements are principally the addition of appropriate electron donor(s) and the presence of halorespiring organisms.

Many organisms are capable of reductive dechlorination of tetrachloroethylene (PCE) and TCE to cis-1,2-dichloroethylene (cDCE), including *Desulfitobacterium spp.*, *Dehalospirillum multivorans*, *Desulfomonile tiedjei*, *Desulfuromonas spp.*, *Dehalobacter restrictus*, (Holliger et al., 1999) *Sulfurospirillum spp.*, (Luijten et al., 2003) and *Geobacter lovleyi* (Sung et al., 2006a). However, *Dehalococcoides spp.* are of particular interest because they are the only organisms known to reductively dechlorinate PCE and lesser chlorinated CAHs to vinyl chloride (VC), and completely to ethylene (ETH) (Cupples, 2008). To date, six strains of *Dehalococcoides* with differing dechlorination capabilities have been described (as summarized in Cupples, 2008), five of which can dechlorinate chloroethenes to ETH, and only three of which have been shown to obtain energy for growth from dechlorination of VC to ETH (Adrian et al., 2000; Maymó-Gatell et al., 1997; He et al., 2003; He et al., 2005; Sung et al., 2006b; Müller et al., 2004).

Recent work has shown that the 16S rRNA genes of the various *Dehalococcoides* strains are too similar to distinguish between different strains, or to allow inference of what functional genes are present within a *Dehalococcoides*-containing community (Duhamel et al., 2004; He et al., 2005; Sung et al., 2006b; Daprato et al., 2007). Different functional genes, however, such as reductive dehalogenase genes have been successfully quantified in *Dehalococcoides*-containing communities as a way of monitoring dominance of different strains, but to date functional gene presence has not been correlated with activity (Holmes et al., 2006; Ritalahti et al., 2006; Lee et al., 2008;

Lee et al., 2006). Gene expression has been identified as an indicator of dehalogenation activity and can correlate with rates over a narrow range of activity, but a correlation between gene expression and dechlorination activity over a broad range has yet to be found (Fung et al., 2007; Rahm and Richardson, 2008a; Rahm and Richardson, 2008b; Lee et al., 2006).

Multiple dehalogenase gene quantification has been used to describe multiple distinct *Dehalococcoides* populations in field sites over large time scales (Lee et al., 2008), and different mixed cultures containing *Dehalococcoides* have been compared with quantitative functional gene presence analyses as a means of community comparison (Daprato et al., 2007). Few studies to date have analyzed shifts in multiple *Dehalococcoides* populations within a mixed community fed different CAH electron acceptors, and these have been restricted to endpoint analyses in enriched batch systems (Holmes et al., 2006; Ritalahti et al., 2006; Sung et al., 2006b). The effects of different electron donors on batch dechlorination performance has been previously evaluated, but in the absence of community genetic analyses (Lee et al., 2007; Heimann et al., 2007; Yang and McCarty, 1998). Studies are currently needed of a single mixed community receiving different electron donors and acceptors over long periods of time, and in continuous flowthrough systems, to determine how such operational differences affect the dehalogenation community genetics and performance.

In this study, our principle objective was to determine how different electron donors and CAHs affect shifts in community structure and performance over time within continuously fed reactors inoculated with the same mixed *Dehalococcoides*-containing anaerobic community. Additionally, we investigated whether qPCR analysis of gene presence could be correlated with temporal trends in maximum dechlorination rates repeatedly measured on cells harvested from the reactors. Specifically, we utilized qPCR analysis of the *Dehalococcoides*-specific reductive dehalogenase genes, 16S rRNA gene, and universal *Bacteria* 16S rRNA gene to track temporal changes of multiple *Dehalococcoides* strains within mixed culture continuous flow stirred tank reactors (CFSTRs). qPCR DNA analyses combined with periodic harvested cell rate

measurements described how different strains of *Dehalococcoides* competed with each other and within the total bacterial community as a function of different electron donors or acceptors, and temporal operation. Comparison of gene quantification with batch rate measurements on reactor harvested cells revealed gene presence quantification could be correlated with activity.

To achieve these objectives, three CFSTRs were operated with the same retention time, of 12.5 days and inoculated simultaneously with the same Evanite (EV) mixed culture, but fed different electron donor/acceptor combinations. The EV culture performance has been previously characterized and confirmed to contain at least one *Dehalococcoides* species as well as the reductase genes known as *bvcA*, *vcrA*, *tceA*, and *pceA* (Yu et al., 2005; Yu and Semprini, 2004; Behrens et al, 2008). Each culture received either TCE and lactate, TCE and formate, or VC and formate as the electron acceptors and donors, with TCE and VC in the influent at practical solubility limits. Results from this research have expanded our knowledge of impacts on dehalogenator population compositions and performance by different CAHs and soluble electron donors, and highlights the potential for dehalogenation performance predictions with gene presence quantification.

MATERIALS AND METHODS

Chemicals: The same stocks of CAHs and ETH were used for analytical standards, chemostat feeds, and batch kinetic tests. Stocks used were TCE (99.9%), and cDCE (97%) (Acros Organics, Pittsburg, PA), VC (99.5%) and ETH (99.5%) (Aldrich Chemical, Milwaukee, WI). Hydrogen gas and 10%CO₂/90%N₂ gases (Airco, Inc., Albany, OR) were anaerobically treated with copper filings at 600°C prior to use for media or culture sparging. A modified anaerobic basal medium for chemostat feed was prepared as described previously (Yang and McCarty, 1998; Yu et al., 2005) using reagent grade salts.

Analytics: CAHs and ETH were quantified on a HP 6890 gas chromatogram with a flame ionization detector (FID) and 30 m x 0.53 mm GS-Q column (J&W Scientific, Folsom, CA). Analyses were performed with helium as the carrier gas (15 mL/min.) and a temperature gradient as follows: 150°C initial temperature for 2 min., 45°C/min ramp to 220°C, hold for 0.7 min. Detection limits for ETH, VC, cDCE, and TCE were 0.04, 0.5, 2.3, and 0.9 µM aqueous concentrations, respectively. Hydrogen gas (H₂) was quantified on a HP 5890 GC with a thermal conductivity detector (TCD) and 15 ft x 1/8 in Carbonex 1000 column (Supelco, Bellefonte, PA). Analyses were conducted at a 220°C isotherm with an Argon carrier gas at 15 mL/min. The detection limit for H₂ was 43 nM (aqueous concentration).

Culture: The original Evanite (EV) culture enrichment, maintenance, and dechlorination performance has been described previously (Yu and Semprini, 2002; Yu et al. 2005). This culture has been confirmed to contain at least one species of *Dehalococcoides*; the *Dehalococcoides* reductase genes *bvcA*, *vcrA*, *tceA*, and *pceA*; and dechlorinate and grow on PCE, TCE, cDCE, and VC (Behrens et al, 2008; Yu et al., 2005; Yu and Semprini, 2004). A subculture of the EV culture was enriched for two years, with batch feedings and transfers as previously reported (Yu and Semprini, 2004), but with TCE as the electron acceptor.

CFSTRs: Three separate CFSTRs were constructed using GL-45 250 mL (nominal) Kimax bottles fitted with Teflon three-hole caps (Kontes Glass Co., Vineland, NJ).

Details and diagrams of the reactors have been supplied previously (Chapter 2). The culture was suspended in each reactor via a 1.5" Teflon stir bar and an IKA Ultra-Flat Lab Disc stir plate (IKA-Works, Inc., Wilmington, NC) with corrugated cardboard under each reactor to maintain temperatures at 21°C ($\pm 1.4^\circ\text{C}$ std dev). The influent for each reactor was continuously introduced with a 100 mL Hamilton gastight syringe (Leno, NV) on an Orion M361 syringe pump (Thermo Electron Corp., Beverly, MA). The pumps delivered very constant flows of 24 mL/day for cell residence times of 12.5 days for each reactor over the entire time of operation.

Inoculation of all reactors was conducted simultaneously from the same inoculum inside a Coy anaerobic glove box (Coy Laboratory Products, Inc., Grass Lake, MI) in a 5% H_2 /95% N_2 atmosphere. 500 mL of liquid EV culture and 500 mL of growth medium were added to a 1 L bottle, and well shaken. The mixture was distributed into the three CFSTRs (303 mL each) flush to the top of each reactor and capped. After inoculation, the CFSTRs were removed from the glove box and connected to feed and anaerobically prepared waste collection chambers. The influent lines were flushed with anaerobic media, and pumping was initiated.

Media preparation: Media for the chemostats was prepared as previously reported (Yang and McCarty, 1998; Yu et al., 2005), with the exception of the following modifications. Na_2S concentrations were increased to 0.45 mM, and pH buffer capacity was increased by augmenting media with an additional 0-880 mg/L anhydrous Na_2CO_3 . Na_2CO_3 concentrations were adjusted based upon effluent pH measurements. The pH values for Reactors 1, 2 and 3 (operating conditions are described in greater detail below) were 6.7 ± 0.5 , 7.1 ± 0.3 , and 7.8 ± 0.5 , respectively. pH values between 8.1 and 8.8 were observed in Reactor 3 from days 36 to 118 due to an initial overbuffering and slow pH decline resulting from loss of acidifying dechlorination activity, and possible acid consumption from formate dehydrogenation.

To achieve saturation concentrations of TCE and VC in the media for each CFSTR, 250 mL batches of feed media were augmented with either 0.5 mL of N_2 -purged neat TCE or pressurized with 65 mL of anaerobically prepared gaseous (99.5%) VC.

Electron donors were added as either 60% Na-lactate syrup, Baker grade (Mallinckrodt Baker, Inc., Phillipsburg, NJ), or 99+% reagent grade anhydrous Na-formate (Sigma-Aldrich, Inc., St. Louis, MO) plus analytical reagent grade Na-acetate·3H₂O (Mallinckrodt Baker, Inc., Phillipsburg, NJ) to concentrations summarized in Table 3.1. Acetate was added at 10% of the formate concentrations (on a carbon basis) to ensure ample carbon for growth was available, but at concentrations low enough to ensure formate served as the principle electron donor. After loss of VC dechlorination activity in the VC-fed reactor (plus formate and acetate), the feed was switched over to TCE with formate and acetate, and gradually transitioned from initial TCE concentration of 2.8 mM to a final TCE concentration of 8.8 mM. All varying feed parameters for this reactor are also summarized in Table 3.1.

CFSTR media stocks were prepared in separate designated 250 mL (nominal volume) GL-45 bottles containing Teflon-lined stir bars and fitted with three-hole Teflon caps as described previously (Chapter 2). Base media were augmented with respective electron donors and acceptors inside the anaerobic glove box. For TCE-fed reactors, media was stirred for approximately 30 minutes, and settled for approximately 30 minutes to obtain the chemostat feed at TCE solubility limits (~7.5mM). When VC was added as the electron acceptor, the feed was vigorously stirred for several hours, with no time devoted to settling. The feed bottles were then pressurized with anaerobic N₂ gas, and media were extracted with the designated 100 mL chemostat feed syringes.

Batch assays: Batch kinetic tests were performed to separately measure maximum dechlorination rates of TCE, cDCE, and VC under non-limiting (hydrogen and CAH) conditions. These tests were conducted with harvested effluent cells approximately once per reactor residence time. The batch assays consisted of a 10-hr incubation step, followed by an instantaneous rate measurement. 1.0 or 1.5 mL of liquid culture were then harvested from each bottle and fixed for DNA analyses. DNA samples were collected 15 to 18 hours after initial CAH augmentation.

Batch assays were prepared as described previously (Chapter 2). Briefly, 24-hr composite effluent samples were collected in N₂-sparged 28 mL crimp-top vials, divided

into two separate 28 mL crimp-top vials, sparged with an anaerobic gas mixture of 10% H_2 (electron donor), 90%{10% CO_2 /90% N_2 } and inoculated with TCE, cDCE or VC. The duplicate vials were shaken within an anaerobic glove box for 10 hrs at room temperature ($25.2^\circ\text{C} \pm 1.3^\circ\text{C}$ std dev) to fully activate reductase expression (Johnson et al., 2005; Rahm and Richardson, 2008a; Rahm et al., 2006b). The vials were sparged again with 10% H_2 , 90%{10% CO_2 /90% N_2 }, to remove daughter product accumulation, and reaugmented with the CAH of interest. After reaugmentation, CAHs were analyzed 5 times, generally within three hours, by GC-FID, and a linear regression of the product formation rate data was used to quantify the maximum utilization rates associated with each CAH. Rate measurements were made with TCE, cDCE, or VC at aqueous concentrations of 500 μM , 700 μM , or 1000 μM , respectively, and hydrogen headspace concentrations between 5% and 15% v/v. At the end of the kinetic assays, solution was extracted for DNA analysis as described below.

DNA sampling/extraction: 1.0 or 1.5 mL of liquid culture was extracted from each batch kinetic bottle for DNA analysis with new, sterile disposable syringes, transferred to individual 1.5 mL eppendorf tubes, and capped. These tubes were exported from the glove box and centrifuged for 5 min. at 14,000 rpm. The supernatants were then decanted via pipetting, and samples were resuspended in 500 μL AE buffer (20 mM Na-acetate, 1mM EDTA, pH 5.5), centrifuged at 14,000 rpm for 5 min., and decanted again by pipetting. The washed cell pellets were immediately placed in a -80°C freezer until DNA extraction could be performed at a later date. DNA extraction was performed with the Qiagen DNeasy kit (Qiagen, Valencia, CA) per manufacturer's instructions to yield final extracted DNA volumes of 100 μL .

qPCR analyses for DNA quantification: Genes were quantified using the iQ 156 SYBR Green Supermix (BioRad Laboratories, Hercules, CA), and gene specific primers. Genes quantified were *Dehalococcoides* 16S rRNA and universal *Bacteria* 16S rRNA genes, as well as the *Dehalococcoides* reductase genes known as *bvcA*, *vcrA*, *tceA*, and *pceA*. All primer sets for 16S rRNA and reductase genes were previously reported (Behrens et al., 2008). A standard curve was generated for each reductase gene and the

Dehalococcoides 16S rRNA (Dhc 16S) gene with a 5-gene plasmid (pCR2.1_rdh16S) constructed as reported previously (Behrens et al., 2008). Total *Bacteria* 16S (Bac 16S) rRNA genes were quantified with a separate plasmid (pCR4_VS16S) containing the full length *Dehalococcoides* sp. strain VS 16S rRNA gene fragment (PCR primers 8F to 1492R) inserted into the pCR4 vector (Invitrogen, Carlsbad, CA). qPCR amplification and quantification was conducted on a BioRad iCycler (BioRad Laboratories, Hercules, CA), with C_t determinations made by the BioRad iCycler IQ software version 3.1. Real-Time qPCR reactions were conducted with an initial incubation of 95°C for 3 minutes, followed by 50 cycles of 95°C for 10 seconds and 60.0°C for 45 seconds. Each qPCR analysis was performed in 25 µL reaction volumes containing, 1X iQ SYBR Green Supermix, 500 nM forward and reverse primers, 5 µL of the prepared DNA template, and nuclease free dilution water. DNA template was supplied as 1:100 dilution of original concentrated material to amplify within the linear range of calibration curves. All qPCR reactions (primer/template combinations) were performed in triplicate on a minimum of two independent DNA extracts unless otherwise indicated. The linear dynamic ranges for each gene, on a total copies per reaction basis were as follows: *vcrA* (10^1 to 10^6), *bvcA* (10^0 to 10^6), *tceA* (10^1 to 10^6), *pceA* (10^0 to 10^6), *Dehalococcoides* 16S rRNA (10^1 to 10^6), *Bacteria* 16S rRNA (10^0 to 10^8)

Calibration curves were generated as described previously (Behrens et al., 2008), plotting gene copies per reaction versus cycle threshold (C_t) values using dilutions of the pCR2.1_rdh16S and pCR4_VS16S plasmids, fitting linear regressions through the log data. Quantification of target genes was obtained from individual standard curves generated from each gene and scaled by appropriate dilution factors to obtain gene copies per mL of culture values.

The *bvcA* gene was present in the EV culture two years prior to this study (Behrens et al., 2008), but not detected in the inoculum culture for this study, or any other sample associated with this study. No numbers for *bvcA* are therefore reported. The pCR2.1_rdh16S plasmid containing *bvcA* was used as a positive control to confirm gene absence in samples. The *bvcA*-containing organism was apparently lost from the EV

culture during the multiple feedings with TCE and transfers over the EV culture history. Previous work by other researchers enriching with TCE or PCE in batch feedings has resulted in losing the *bvcA* gene or reducing its presence by at least 5 orders of magnitude from a mixed culture (Sung et al., 2006b; Ritalahti et al., 2006).

RESULTS AND DISCUSSION

Reactor performance: The chemostat effluent CAH monitoring data for all three reactors are shown in Figure 3.1a, 3.1c, and 3.1e. A more detailed account of Reactors 1 and 2 performances and effluent observations has been previously described in Chapter 2. Each reactor demonstrated different degrees of completeness regarding dechlorination, and different durations of successful treatment. As shown in Figure 3.1a, the TCE and lactate fed reactor (Reactor 1) began converting TCE to approximately 85% VC and 15% ETH, followed by sequential loss of each dechlorination step, starting on days 12, 44, and 72 for VC, cDCE, and TCE respectively. Lactate was generally fermented to approximately 50% acetate and 50% propionate during the first 58 days of operation followed by a decline in acetate production after day 58, and a decline in propionate production after day 96 (see Figure 3.1b).

The TCE and formate fed reactor (Reactor 2) initially converted TCE to approximately 66% ETH and 33% VC (Figure 3.1c). Relatively stable performance was maintained at approximately 66% ETH and 33% VC until day 195 with sequential loss of each dechlorination step for VC, cDCE, and TCE starting on days 195, 204, and 227, respectively. Approximately 20% of the formate carbon left the system as acetate, apparently via homoacetogenesis, to day 65 (Figure 3.1d). Varying degrees of homoacetogenesis were observed until day 185, as seen with effluent acetate concentrations exceeding influent acetate concentrations. Homoacetogenic activity has been previously reported in the EV culture (Pon et al., 2003). After day 185, 50% of influent acetate was consumed and formate began to increase in the effluent (see Figure 3.1d).

In the VC and formate fed reactor (Reactor 3), VC was initially dechlorinated almost completely to ETH, but VC began to rise in the effluent after 15 days, however, with virtually no dechlorination from day 15 to 99 (Figure 3.1e). All formate was consumed during this time, and CO₂ was present for acetogenesis, but not quantified due to complications associated with a carbonate-buffered system. Methanogenesis did not occur, but homoacetogenesis was observed, as indicated by effluent acetate

concentrations exceeding influent acetate to varying degrees from startup to day 245, after which time net acetogenesis ceased (Figure 3.1f). After day 337, less effluent than influent acetate indicated net acetate consumption occurred, which was accompanied by increasing effluent formate concentrations (see Figure 3.1f).

Batch rate tests between days 52 and 95 (to be discussed later) produced no detectable cDCE or VC dechlorination activity in Reactor 3, though a very low level of TCE-dechlorinating activity was consistently detected. The feed was then switched to TCE after day 99, when it was confirmed that essentially no VC dechlorination was occurring. This was indicated by the effluent VC concentration equalling the influent concentration for 2.5 cell residence times (see Figure 3.1e and influent concentration summary in Table 3.1). TCE concentrations rose in the effluent during an initial lag phase, as VC concentrations declined with flushing, followed by complete transformation to essentially 100% cDCE and trace VC and ETH by day 167. After steady dechlorination was achieved, influent TCE, formate, and acetate concentrations were increased on days 212 and 311 to ultimately receive similar TCE, formate, and acetate concentrations as Reactor 2. Shortly after increasing the influent to 8.8 mM TCE, Reactor 3 failed, as evident by increasing TCE in the effluent beginning on day 350 (Figure 3.1e).

qPCR 16S rRNA gene analyses: *Dehalococcoides* 16S rRNA and *Bacteria* 16S rRNA gene copy numbers are displayed in Figures 3.2a, 3.2b and 3.2c. The 16S rRNA gene quantity data agree with effluent monitoring data, with simultaneous declines in reactor performance, *Bacteria* 16S rRNA and *Dehalococcoides* 16S rRNA gene quantities as each reactor failed (see Figures 3.1a through 3.1f and Figures 3.2a, 3.2b, and 3.2c). Caution must be exercised when interpreting 16S rRNA gene copy quantification, however, due to the various 16S rRNA gene copy numbers possible in different species (Klappenbach et al., 2001). These data are used principally to determine how the relative amounts of *Dehalococcoides* shifted within the total *Bacteria* population, with 16S rRNA gene copy qPCR analysis being one of the most quantitative means available.

The qPCR 16S rRNA data illustrate how *Dehalococcoides* varied within the general mixed bacterial community as a function of electron donor, electron acceptor, and duration of operation within the CFSTRs. The proportion of *Dehalococcoides* within the mixed bacterial community differed greatly between the three reactors. In Reactor 1, the proportion of *Dehalococcoides* to total *Bacteria* 16S rRNA gene copies declined from 18% at day 2 to 0.7% by day 92 (Figure 3.2a), while proportions of *Dehalococcoides* to total *Bacteria* in Reactor 2 were typically maintained between 28% and 37% throughout the 291 days of operation (Figure 3.2b). In Reactor 3, the ratio of *Dehalococcoides* to *Bacteria* 16S rRNA gene copies was 45% on day 2 of operation, but declined below 1% by day 86, and to 0.001% by day 240 (Figure 3.2c). Thus, *Dehalococcoides* were well supported within the mixed community by formate and TCE (Reactor 2), compared to lactate and TCE (Reactor 1), but they could not be sustained in the 12.5 day residence time CFSTR with VC and formate (Reactor 3), nor could *Dehalococcoides* sufficiently recover once switched to TCE and formate in the cDCE-producing reactor.

In Reactor 1, *Dehalococcoides* and total *Bacteria* increased from startup to day 17, followed by a gradual decline in total *Bacteria*, and a sharper decline in *Dehalococcoides* (Figure 3.2a). This agrees with the most complete dechlorination observed in the reactor up to day 12, with sequential declines in cDCE and TCE dechlorination on days 44 and 72, respectively (Figure 3.1a). Previous analysis of Reactor 1 (Chapter 2) demonstrated a majority of electrons added as lactate left the reactor as acetate and hydrogen-rich propionate, with only 6% of added electron equivalents directed toward dechlorination. The sharper decline in *Dehalococcoides* 16S rRNA genes compared to total *Bacteria* 16S rRNA genes could therefore result from a population fermenting lactate and existing independently of dechlorination activity (see Figure 3.1b) or dominating the TCE dechlorination step. Many non-*Dehalococcoides* species are known to anaerobically dechlorinate TCE to cDCE (Holliger et al., 1999; Luijten et al., 2003; Sung et al., 2006a), and potentially were associated with this step. Partial fermentation and continued TCE dechlorination, while VC and cDCE

dechlorination failed (Figure 3.1a), is consistent with the greater declines in *Dehalococcoides* 16S rRNA gene copies compared to *Bacteria* 16S rRNA gene copies.

During stable performance in Reactor 2 from startup to day 195, *Bacteria* 16S rRNA and *Dehalococcoides* 16S rRNA measurements were quite constant (Figure 3.2b). The failure of Reactor 2, as illustrated by sequential increases in VC, cDCE, and TCE in the effluent starting on day 195 (Figure 3.1c) is accompanied by declines in both *Bacteria* and *Dehalococcoides* 16S rRNA gene quantities (Figure 3.2b). Loss of net acetogenesis, with effluent acetate being equal or less than influent acetate by day 156, and formate increasing in the effluent by day 195 (Figure 3.1d) is reflected in the three order of magnitude decline in *Bacteria* 16S rRNA gene copies observed between days 194 and 291 (Figure 3.2b). With consistent TCE dechlorination to approximately 33% VC and 66% ETH for the first 195 days of operation, and a relatively constant concentration of electron donors (formate) and acceptors (TCE), Reactor 2 should theoretically maintain constant amounts of biomass and dehalogenating cells, as observed (Figure 3.2b). Sustained dechlorination to VC and ETH in Reactor 2 was shown to maintain a *Dehalococcoides* population, the only organisms known to energetically perform these steps (As summarized by Cupples, 2008).

In Reactor 3, the initial decline in VC dechlorination over the first 100 days of operation (Figure 3.1e) was accompanied by a three order of magnitude decrease in *Dehalococcoides* 16S rRNA gene copies/mL and an order of magnitude decrease in *Bacteria* 16S rRNA gene quantities (Figure 3.2c). Once TCE dechlorination was established in Reactor 3 on day 161 (Figure 3.1e), an order of magnitude increase in *Bacteria* 16S rRNA gene copies was observed, though *Dehalococcoides* 16S rRNA gene copies continued to decline (Figure 3.2c). Increases in influent TCE on days 212 and 311 resulted in greater net rates of TCE dechlorination (see Figure 3.1e), though not in increased *Bacteria* 16S rRNA gene copies (Figure 3.2c). Increasing TCE and, perhaps more importantly, produced cDCE did correspond to over a two order of magnitude increase in *Dehalococcoides* 16S rRNA gene copies from days 240 to 327. The loss of TCE dechlorination observed by day 350 corresponded to declines in both *Bacteria* and

Dehalococcoides 16S rRNA genes by approximately two orders of magnitude each between days 327 and 387.

Increased *Bacteria* 16S rRNA gene quantities in Reactor 3 after day 94 (Figure 3.2c) and sustained TCE dechlorination for over 190 days (Figure 3.1e) indicates TCE dechlorination supplied energy for growth for the TCE-dechlorinating population. We have not found a documented case where a *Dehalococcoides* spp. transforms TCE to only cDCE in the presence of excess electron donor, as was the case for Reactor 3, though numerous other species have been shown to do this. It is therefore highly likely some species other than *Dehalococcoides* capable of TCE to cDCE dechlorination was present in the EV inoculum and able to dominate Reactor 3. A limited clone library conducted with soils from a packed column study inoculated with the EV culture did detect a *Eubacterium* species with 97% similarity to the *Eubacterium limosum*, shown to dechlorinate methoxychlor and DDT, as a possible organism present capable of the TCE to cDCE dechlorination observed (Behrens et al., 2008; Yim et al., 2008).

Declines in dechlorination performance and *Dehalococcoides* 16S rRNA genes earlier and to a greater extent in Reactor 1 than Reactor 2 indicate the *Dehalococcoides* population were better sustained with formate than lactate in the TCE-fed mixed community CFSTRs. The reason for this difference in *Dehalococcoides* fractions between the two systems is likely that formate is virtually a direct source of hydrogen through its dehydrogenation, while lactate must be fermented to produce hydrogen. Lactate fermentation in Reactor 1 was incomplete, with production of both acetate and propionate (Figure 3.1b). Fermentation of propionate to acetate can potentially produce 3 moles of H₂ per mole of acetate formed. Thus, fermentative organisms were present and obtaining energy from the observed partial fermentation, but insufficient hydrogen was released for cDCE and VC dehalogenation mediated by the *Dehalococcoides* population.

The TCE and formate fed Reactor 2 sustained *Dehalococcoides* populations better than Reactor 3 fed VC and formate (See Figures 3.2b and 3.2c). Given the dechlorination kinetics for the EV culture are approximately 10 times faster for TCE dechlorination than VC dechlorination, it is reasonable that better *Dehalococcoides* cell retention occurred

with TCE (Yu and Semprini, 2004; Yu et al., 2005). Modeling with protein-specific kinetic parameters (Yu and Semprini, 2004; Yu et al., 2005) indicates such an outcome was likely in this attempt to enrich for a robust VC-dechlorinating community, but total *Bacteria* 16S rRNA gene quantification and acids monitoring shows formate dehydrogenation and homoacetogenesis sustained other *Bacteria* within Reactor 3 (Figures 3.1f and 3.2c). Thus, TCE was better able to maintain *Dehalococcoides* compared to VC in these CFSTRs, though VC and formate was able to sustain and select for an unidentified population capable of TCE dechlorination to cDCE within the 12.5 day retention time CFSTR, as indicated by batch-measured TCE dechlorination rates in the absence of cDCE and VC batch-measurable dechlorination rates.

qPCR reductase gene analyses: The measured reductase gene copies of *vcrA*, *tceA*, and *pceA* for all three reactors are presented in Figures 3.3a, 3.3b and 3.3c. Temporal shifts in magnitude of the reductase gene quantities generally followed the shifts in *Dehalococcoides* 16S rRNA gene copies (Figures 3.2a, 3.2b, and 3.2c). Each system showed different patterns of which functional genes were present in greater numbers, however. In Reactor 1, *vcrA* and *pceA* gene quantities initially exceeded *tceA* gene copies by approximately an order of magnitude (Figure 3.3a). By day 16, however, the *tceA* gene was detected in greater numbers, and was the dominant reductase gene for the remainder of operation. In Reactor 2, the *vcrA* and *pceA* gene copies were initially present at approximately an order of magnitude greater than *tceA* gene copies, and remained the predominant reductases throughout operation (Figure 3.3b). In Reactor 3, similar to the other formate-fed Reactor 2, *vcrA* and *pceA* gene copies maintained dominance among the reductase genes, and *tceA* gene copies were two full orders of magnitudes lower than *vcrA* and *pceA* copies by day 94, remaining in a similar proportion to day 240 (Figure 3.3c). A shift to *tceA* dominance occurred by day 327, when Reactor 3 had been transforming TCE to cDCE with no significant VC or ETH formation for 171 days.

Note that all *Dehalococcoides* reductase and 16S rRNA genes quantified in Reactor 3 declined by approximately 5 orders of magnitude compared to a zero to one

order of magnitude change in Reactors 1 and 2 during their peak performance. Interestingly, after switching the feed to TCE, trace amounts of VC and ETH were always present in the effluent, which could conceivably be due to cometabolism by the TCE-dechlorinating population. However, 16S rRNA gene quantification reveals *Dehalococcoides* were never completely flushed from the system and likely performing the low levels of cDCE dechlorination to VC and ETH observed, in addition to possibly contributing low levels of TCE dechlorination.

While different electron donor and acceptor combinations promoted domination by different reductase containing populations, common to all three reactors was an apparent pairing of *vcrA* and *pceA* genes. Increases or decreases in *vcrA* and *pceA* quantities were simultaneous and within the same order of magnitude, while the *tceA* gene quantities increased or decreased independently of either *vcrA* or *pceA* (Figures 3.3a, 3.3b and 3.3c). Despite the broad range of *Dehalococcoides* 16S rRNA gene quantities present in all three systems, from 1.7×10^3 16S rRNA gene copies/mL to 1.7×10^8 16S rRNA gene copies/mL, (see Figures 3.2a, 3.2b, and 3.2c) the ratios of *pceA/vcrA* gene copies were consistently 0.4 to 0.6 in all reactors, with few exceptions in Reactor 3 (see Figures 3.3a, 3.3b, and 3.3c). To confirm the correlation between *vcrA* and *pceA*, log-log regressions of gene copies/mL were made of *pceA* vs. *vcrA*, *tceA* vs. *vcrA*, and *pceA* vs. *tceA* for each reactor separately. For all three reactors, a linear regression of *pceA* vs. *vcrA* data produced R^2 values greater than 0.91. R^2 values for *tceA* vs. *pceA* or *tceA* vs. *vcrA* in all three reactors ranged from 0.09 to 0.85. This correlation analysis indicates there is likely a dominant *Dehalococcoides* population in the EV culture that contains both the *vcrA* and *pceA* genes, but lacks the *tceA* gene. The lack of strong correlation between *tceA* and the other reductases, despite *tceA* often occurring in similar abundance, possibly indicates a *tceA*-containing organism is a separate co-dominant *Dehalococcoides* strain within the EV culture that lacks the *vcrA* and *pceA* genes. Whether other dehalogenase genes were present, expressed, shared by the two dominant *Dehalococcoides* communities, or relevant to TCE, cDCE, or VC dechlorination is unknown. However, a single organism containing both *vcrA* and *pceA* can explain why

the *pceA* gene was retained in all three CFSTRs that produced CAH substrates for the *vcrA* gene product, but were never supplied known substrates for the *pceA* gene product (Magnuson et al., 1998)

Previous work with the EV culture in a PCE-fed soil packed column also showed presence of the *pceA* gene in similar proportions to the *vcrA* gene in the effluent end of the column, which contained predominantly VC and ETH (Behrens et al, 2008; Azizian et al., 2008). Our current understanding of the dechlorinating process is that the *pceA* gene product is responsible for dechlorinating PCE to TCE, that the *tceA* gene product dechlorinates TCE and cDCE to VC, and that the *vcrA* gene product dechlorinates cDCE and VC to ETH (Magnuson et al., 1998; Magnuson et al., 2000 ; Müller et al., 2004; Sung et al., 2006b). Thus, the previous column study (Azizian et al., 2008; Behrens et al., 2008) combined with the current study shows multiple systems where the EV culture maintained *pceA* gene presence in the absence of a known substrate for the *pceA* gene product, but in the presence of the *vcrA* gene and substrate for the *vcrA* gene product. Other work has shown detection of the *bvcA* gene in zones not associated with known substrates (VC) for that gene product (Lee et al., 2008), and this work supplies further evidence that reductase-containing organisms can have genes relevant to observed dechlorination activity that are not yet identified or possess multiple reductase genes, of which some are irrelevant for the CAHs available.

Previous analysis of the EV culture , and pure cultures of *Dehalococcoides* strains CBDB1, FL2, BAV1, VS, and 195 showed that only *tceA* was detectable in strain FL2, only *bvcA* was detectable in strain BAV1, only *pceA* was detectable in CBDB1, and that strain VS contains both *pceA* and *vcrA*, but not *bvcA* or *tceA* (Behrens et al., 2008). These analyses are summarized in Figure B1. Additionally, strain VS contained approximately twice the number of *vcrA* genes as *pceA* genes (Behrens et al., 2008). It therefore appears that the CFSTR inocula contained mixtures of FL2-type and VS-type organisms. Note that initial operation with VC and formate in Reactor 3 would not supply a substrate relevant to the *pceA* gene product. Therefore, if a *pceA* containing organism existed in the EV culture that did not also contain the *vcrA* (or other VC

reductase) gene, one would expect the ratio of *pceA* to *vcrA* genes to decline in a manner similar to the decline of *tceA* relative to *vcrA* over time. This was not observed, again suggesting that the *vcrA* containing organism within the EV culture is a VS-type *Dehalococcoides* which contains both *vcrA* and *pceA* genes.

Other research has shown that qPCR analysis of reductase genes can track shifts in multiple *Dehalococcoides* strains within a mixed community (Ritalahti et al; 2006; Lee et al., 2008), and such analyses of our CFSTRs showed that there were likely two different *Dehalococcoides* populations within the original culture, and that different *Dehalococcoides* populations prevailed under different conditions established by the multiple CFSTRs. Discerning two distinct *Dehalococcoides* populations with only reductase gene quantification would not have been apparent without the temporal tracking of reductases in the CFSTRs, highlighting one of the strengths of continuous flow and measurement applications, versus endpoint analysis.

Reductase quantification corroborated reactor performance observations, and supplied greater detail about the dechlorinating population as it relates to observed performance. In Reactor 1 TCE was fully dechlorinated from startup to day 72, though VC and cDCE dechlorination declined by days 12 and 44, respectively (Figure 3.1a). One would thus expect a gene associated with TCE dechlorination to dominate, and the *tceA* gene was the dominant reductase measured (Figure 3.3a). Incomplete fermentation was observed in Reactor 1 (see Figure 3.1b, and Chapter 2), resulting in insufficient H₂ availability to dechlorinate TCE completely to ETH. With TCE in the influent, and therefore the principle CAH available for dechlorination, it is likely that the *tceA*-containing organisms could dominate within the *Dehalococcoides* population.

In Reactor 2, where prolonged dechlorination to roughly 66% VC and 33% ETH was observed, a mixture of the *tceA*-containing (FL2-type) and *vcrA*-containing (VS-type) organisms could conceivably coexist. There was likely a non-*Dehalococcoides* population competing for TCE within Reactor 2, as Reactor 3 (inoculated the same day from the same bottle) enriched for a population incapable of measurable cDCE and VC dechlorination, and *Bacteria* 16S rRNA gene quantities correlated better with batch-

measured TCE dechlorination rates than *Dehalococcoides* 16S rRNA gene quantities (to be discussed below). Given that the EV culture is a mixed anaerobic community, with a likely non-*Dehalococcoides* species present that could dechlorinate TCE to cDCE, it would be possible for the FL2-type organism to suffer from TCE competition with some community members, and hydrogen competition with others, such as acetogens, and the VS-type dechlorinators. It is therefore reasonable to expect and observe dominance by the VS-type organism.

Reactor 3, which was initially fed VC and formate, maintained dominance of the VS-type organism, which agrees with our understanding that VC is not a substrate for the *tceA* gene product. Once *Dehalococcoides* cells began to increase within the total population after day 240, and after over 11 cell residence times of TCE addition, the *tceA*-containing cells began to dominate within the *Dehalococcoides* population (see Figures 3.2c and 3.3c).

DNA correlations with rate measurements: Batch dechlorination rate tests were conducted under non-limiting CAH and hydrogen conditions to determine maximum dechlorination rates. Batch measured maximum dechlorination rates are plotted with quantified *Bacteria* and *Dehalococcoides* 16S rRNA genes on log plots versus time in Figures 3.4a, 3.4b and 3.4c. Note that the maximum and minimum log values on both axes are adjusted to overlay rate and DNA data, with 1×10^8 gene copies/mL aligned to 1.0×10^0 $\mu\text{moles/day/mL}$ rate measurements in all three figures. However, both axes mark the same number of log units, in all three figures, demonstrating similar magnitude shifts between DNA and rate measurements. The same scale adjustment is used in Figure 3.5 (below).

In all three reactors, TCE dechlorination rates tend to follow *Bacteria* 16S rRNA gene quantities better than *Dehalococcoides* 16S rRNA gene quantities, while cDCE and VC rate measurements tend to follow *Dehalococcoides* 16S rRNA gene quantities. TCE dechlorination rates likely correlate with *Bacteria* 16S rRNA gene quantities better than *Dehalococcoides* 16S rRNA genes because of the low ratios of *Dehalococcoides*:*Bacteria* 16S rRNA genes in Reactors 1 and 3 (Figures 3.2a and 3.2c),

and the variety of different bacteria known to reductively dechlorinate TCE to cDCE (Holliger et al., 1999; Luijten et al., 2003; Sung et al., 2006a). The similar trends between TCE dechlorination rates and *Dehalococcoides* 16S rRNA gene copies for Reactor 2 (Figure 3.4b) could be due to the relatively constant fraction of *Dehalococcoides* 16S genes compared to total *Bacteria* 16S rRNA gene copies during the entire time of operation (Figure 3.2b).

In Reactors 1 and 2, cDCE and VC rate measurements exhibit similar magnitude and temporal changes as the *Dehalococcoides* 16S rRNA gene quantities (Figures 3.4a and 3.4b). There were too few measurable cDCE and VC dechlorination rates in Reactor 3 to observe temporal trends, though the initial decline in cDCE and VC rates between startup and day 32 reflected *Dehalococcoides* 16S rRNA gene declines in the same time frame (Figure 3.4c). As Reactors 1 and 2 began to fail (after day 94 in Reactor 1 and day 254 in Reactor 2), cDCE and VC dechlorination rates were not measurable and thus could not be plotted on the log-figures. Undetectable cDCE and VC dechlorination rates occurred when *Dehalococcoides* 16S rRNA gene copies fell below 10^6 copies per mL (Figures 3.2a and 3.2b). *Dehalococcoides* 16S rRNA gene copy numbers were below 10^6 /mL in Reactor 3 from day 86 to the end of operation (Figure 3.2c), indicating a likely population threshold before dechlorination activity could be detected within the 18 hours of incubation. A single cDCE dechlorination rate was detectable in Reactor 3 on day 327, when *Dehalococcoides* 16S rRNA gene quantities increased to 4.5×10^5 copies/mL. cDCE and VC dechlorination rates were otherwise too low to measure in the batch rate tests for Reactor 3 from day 53 to 389.

Batch measured maximum dechlorination rates with reductase gene quantities are presented in log plots versus time (Figures 3.5a, 3.5b and 3.5c). Simultaneous shifts, by similar orders of magnitude, in cDCE and VC dechlorination rates compared to *vcrA*, *tceA* and *pceA* gene copy numbers, were observed in Reactor 1 (Figure 3.5a). TCE rates did not mirror reductase gene quantities, but were better correlated with the total *Bacteria* 16S rRNA gene quantities, of which *Dehalococcoides* 16S rRNA genes had declined from a maximum of 29% on day 29 to less than 1% by day 92 (Figure 3.2a), again

indicating non-*Dehalococcoides* domination of this dechlorination step. For Reactor 2 (Figure 3.5b), all rate data, including TCE dechlorination rates demonstrated reasonable fits to all reductase gene measurements. Because the proportion of *Dehalococcoides* 16S rRNA genes to total *Bacteria* 16S rRNA genes remained fairly constant, TCE rate data in the mixed community would likely compare well to *Dehalococcoides* parameters such as each of the reductase genes quantified, regardless of whether *Dehalococcoides* or other bacteria were responsible for this dechlorination step. For Reactor 3, similar to Reactor 1, TCE rate data did not appear to correlate with any of the reductase genes quantified (Figure 3.5c). The apparent dominance of non-*Dehalococcoides* bacteria, as indicated by the minor fraction of *Dehalococcoides* 16S rRNA gene copies compared to total *Bacteria* 16S rRNA gene copies (Figure 3.2c), would support the lack of correlation between the high TCE dechlorination rates and low *Dehalococcoides* reductase gene presence, further implicating non-*Dehalococcoides* organism(s) dominating TCE dechlorination activity in Reactor 3. As discussed previously, there was a lack of measurable cDCE and VC dechlorination rates in Reactor 3, but initial declines in the rates agreed with the declines in *vcrA*, *tceA*, and *pceA* gene copies measured between days 2 and 86 (Figure 3.5c).

To test the comparability of dechlorination rates in the different reactors, dechlorination rates were normalized to quantified *Dehalococcoides* 16S rRNA genes (Table 3.2). There is poor agreement among the reactors for *Dehalococcoides*-normalized TCE dechlorination rate data possibly from bacteria other than *Dehalococcoides* dominating the TCE dechlorination. There is reasonable agreement, however in cDCE and VC dechlorination rate determinations between Reactors 1, 2 and 3 once rates are normalized to *Dehalococcoides* 16S rRNA gene quantities. Despite rate measurements spanning three orders of magnitude when normalized per mL of culture (Table 3.2), rates per copy of *Dehalococcoides* 16S rRNA genes are within one order of magnitude of each other for cDCE and VC dechlorination, indicating the *Dehalococcoides* 16S rRNA gene is an appropriate factor to normalize cDCE and VC dechlorination rates. Measurable cDCE and VC dechlorination rates normalized to *Dehalococcoides* 16S rRNA gene quantities in Reactor 3 were within one order of

magnitude of those in Reactors 1 and 2. This is good agreement considering few measurements were made prior to washout of significant cDCE and VC dechlorination activity, and the larger errors associated with the low rates and low quantities of DNA present.

VC dechlorination rate data from a previous column study with the EV culture (Azizian et al., 2008) is also compared in Table 3.2. In the previous study, the EV culture was bioaugmented to a soil column packed with aquifer material from the Hanford DOE site and continuously fed PCE and lactate as a fermenting substrate. At the end of the study (170 days), PCE was converted to approximately 66% ETH and 33% VC, and the column was sacrificed and divided into six sections along its length, in 5 cm increments. Solids from each of the 5 cm increments were distributed into separate microcosms, and batch rate measurements were conducted for VC dechlorination with excess hydrogen, and an aqueous VC concentration of 12 μM . In Table 3.2, those rates are adjusted to equivalent rates at conditions tested in this study ($[\text{VC}_{\text{aq}}] = 1000 \mu\text{M}$) based upon the previously reported half-saturation coefficient for EV of 62.6 μM (Yu et al., 2005) by a scaling factor of 5.85 (the ratio of $d\text{VC}/dt$ at $[\text{VC}]_{\text{aq}} = 1000 \mu\text{M}$ versus $d\text{VC}/dt$ at $[\text{VC}]_{\text{aq}} = 12 \mu\text{M}$). The adjusted average of all six VC dechlorination rates normalized to *Dehalococcoides* 16S rRNA gene quantities from those microcosms are presented in Table 3.2. VC dechlorination rates normalized to *Dehalococcoides* 16S rRNA gene measurements between this study and the column study are within one order of magnitude, indicating a good agreement across different electron donor supplies and operating systems (CFSTR grown vs. attached growth cells).

To test for relationships between the genes quantified and rate measurements, $\log(\text{dechlorination rate})$ versus $\log(\text{DNA})$ linear regressions were performed for each reactor with all rate measurements and genes quantified. R^2 values for all tested relationships are supplied in Table 3.3. In Reactor 1, *Bacteria* 16S rRNA genes correlated best with TCE dechlorination rate measurements, and better than *Dehalococcoides* 16S rRNA, *pceA*, *tceA*, or *vcrA* genes, as indicated by the higher R^2 value (Table 3.3). All quantifiable *Dehalococcoides* parameters (16S rRNA, *vcrA*, *tceA*,

and *pceA*) showed reasonable agreement with cDCE and VC rate measurements for Reactor 1, with R^2 values generally above 0.6. The higher R^2 associated with the cDCE rate data for the *tceA* gene compared to *vcrA* and *pceA*, could be an indication of which gene within the community was principally responsible for this reaction. While gene products for *vcrA* and *tceA* are both associated with cDCE dechlorination (Magnuson et al., 2000; Müller et al., 2004), the *tceA* gene was generally present at 10 times the quantity of *vcrA* in Reactor 1 (Figure 3.3a). For VC dechlorination rates in Reactor 1, the *vcrA* gene has a higher R^2 compared to the *tceA* gene. Thus, although the *tceA*-containing organisms dominated this reactor over time, these data suggest VC dechlorination rates correlate best with the *vcrA* gene. This agrees with our current knowledge of substrates for each of those genes (Magnuson et al., 2000; Müller et al., 2004). VC dechlorination rates correlated strongly with *pceA* quantities as well, but as discussed previously, it is highly likely the same organism contains both *vcrA* and *pceA* in the EV culture.

In Reactor 2, all detectable genes, including *Bacteria* 16S rRNA, correlated reasonably well with TCE. Higher R^2 for *Dehalococcoides* 16S rRNA genes compared to *Bacteria* 16S rRNA for cDCE and VC dechlorination (see Table 3.3) supports our understanding that *Dehalococcoides* are the principle, if not the only, organisms responsible for these reactions (Cupples, 2008). The similar R^2 for *Dehalococcoides* and *Bacteria* 16S rRNA genes compared to TCE dechlorination could be due to *Dehalococcoides* proportions remaining fairly constant within the total bacterial community, or an indication that *Dehalococcoides* had a significant role in TCE dechlorination rates in Reactor 2. Similar R^2 values for all functional genes is likely due to the proportions of these functional genes remaining fairly constant throughout operation, though Reactor 2 was dominated by the *vcrA* and *pceA* genes (Figure 3.3b). The fairly constant ratios of different genes throughout operation of Reactor 2 illustrates one of the possible challenges in attempting to correlate DNA quantification with rate measurements, and the risk of assuming correlation necessitates causation. The differences in Reactor 2 are too small to draw conclusions, but the slightly higher R^2 for

the *tceA* gene compared to cDCE dechlorination rates and *vcrA* gene compared to VC dechlorination rates again may indicate dominant genes within the *Dehalococcoides* community responsible for each of these steps.

In Reactor 3, there were insufficient measurable rate data associate with cDCE and VC dechlorination to test for relationships with DNA. The TCE dechlorination rate data correlated well with total *Bacteria* 16S rRNA gene quantification, though no *Dehalococcoides*-specific genes could be correlated to TCE dechlorination rates (Table 3.3). Given that numerous anaerobes can dechlorinate TCE, but only *Dehalococcoides* are known to reductively dechlorinate cDCE and VC, it is somewhat expected that the above observations could be made in Reactor 3, where *Dehalococcoides* comprised less than 0.01% of the total population and the reactor dechlorinated TCE to cDCE with virtually no VC or ETH formation during a majority of operation.

The linear regressions that were generated were used to calculate expected dechlorination rates based upon DNA measurements. Predicted rates based upon measured *Dehalococcoides* 16S rRNA gene quantities and log-log regression equations are supplied with the temporal cDCE and VC dechlorination rates in Figures 3.6a through 3.6f. Regression curves for *Dehalococcoides* 16S rRNA genes from both Reactors 1 and 2 were used to model expected cDCE and VC dechlorination rates in all three reactors. No regression equations from Reactor 3 could be used because there was an insufficient number of measurable cDCE and VC dechlorination rates. Detailed example calculations are supplied Appendix B. Essentially, the regression equations fit to the log data of *Dehalococcoides* 16S rRNA gene quantities and rate measurements from one reactor were used to calculate predicted rates based only on the measured *Dehalococcoides* 16S rRNA gene quantities in the other reactors, and compared to actual measured rates.

In Figures 3.6a and 3.6b, cDCE and VC dechlorination rates for Reactor 1 are plotted with the regression-based predictions. The regression fits using Reactor 1 data serve as method controls because those relationships were derived from data within that reactor, and illustrate reliability of the method. The rate predictions derived from Reactor 2 regressions are also presented in Figures 3.6a and 3.6b. A similar approach is used for

Reactor 2, shown in Figures 3.6c and 3.6d. In Figures 3.6e and 3.6f, Reactor 3 cDCE and VC dechlorination rate data, is plotted with regression-based predictions from both Reactor 1 and Reactor 2, with no control model from Reactor 3 due to too few measurable rates.

Predictions for VC and cDCE dechlorination rates are within an order of magnitude of the measured rates in all three reactors. Predicted rates extending beyond day 94 in Reactor 1 (Figures 3.6a and 3.6b) and 254 in Reactor 2 (Figures 3.6c and 3.6d) correspond to times when dechlorination rates were not measurable, yet qPCR DNA was measurable. The lowest detectable dechlorination rate in any experiment was 1.0×10^{-3} $\mu\text{moles/day/mL}$. In Reactor 3, rate measurements conducted from day 32 to 389 for cDCE and VC dechlorination were below the lower limits of detection, with one exception. The predicted rates based on regression analyses of Reactor 1 and Reactor 2 data are near or below the 1.0×10^{-3} $\mu\text{moles/day/mL}$ threshold during this time frame. The measurable increase in cDCE dechlorination on day 327 in Reactor 3 (Figure 3.6e) is predicted within the correct order of magnitude using the regression-based models. For VC dechlorination (Figure 3.6f), the predicted increase corresponding to day 327 remains below the measurable threshold.

Predictions based upon time-independent regression analyses of rates versus *Dehalococcoides* 16S rRNA genes in separate reactors accurately captured temporal shifts in dechlorination rate magnitudes. This indicates that *Dehalococcoides* 16S rRNA genes can be used to predict dechlorination cDCE and VC dechlorination rate potentials. The gene-based maximum dechlorination rate predictions supplied order of magnitude estimates for cDCE and VC dechlorination activity for all three reactors, and was independent of which reductase system dominated, or which electron donors or CAHs the mixed cultures were enriched upon. An order of magnitude prediction is a reasonably accurate and valuable tool in assessing potential rates in the field. Higher R^2 values for some reductase genes regressed to rate data were obtained (see Table 3.3), which should potentially produce more accurate predictions, but the 16S rRNA-based prediction provides a simple approach that is within reasonable tolerance for field predictions.

SUMMARY

All three reactors were simultaneously started with the same inoculum, but fed different electron donor/acceptor combinations. Performance differences in dechlorinating mixed cultures enriched on different electron donors has been shown previously in batch fed cultures (Lee et al., 2007; Heimann et al., 2007; Yang and McCarty, 1998). The performance in our CFSTRs also showed clear differences in community capabilities to dechlorinate (Figures 3.1a, 3.1c, and 3.1e). The dechlorination abilities, as measured in non-limiting harvested cell batch rate tests, also changed over the time of operation, demonstrating temporal shifts in community capabilities independent of extant reactor conditions. Similar temporal shifts between batch rates and CFSTR performance reported previously (Chapter 2) indicates the non-limiting batch tests are an effective way to assess culture capabilities and reflect *in situ* reactor performance, though they reveal little about specific organisms or enzymes involved. This work demonstrates that quantities of relevant reductase genes to perform each dechlorination step, as well as *Dehalococcoides* and *Bacteria* 16S rRNA genes, exhibited temporal shifts (Figures 3.2a through 3.2c, and 3.3a through 3.3c) and were associated with reactor performance and batch rate measurements.

Numerous studies have measured electron donor effects on dechlorination performance in mixed communities, but at a single timepoint and in the absence of molecular data, generally limited to batch fed systems (Fennell et al., 1997; Yang and McCarty, 1998; Lee et al., 2007; Aulenta et al., 2006). Previous researchers have used qPCR analysis of reductase genes to demonstrate how mixed populations containing multiple *Dehalococcoides* strains shifted at the end of batch fed enrichments on different CAH electron acceptors (Holmes et al., 2006; Ritalahti et al., 2006; Sung et al., 2006b). However, no similar comparisons devoted to electron donor effects have been made. In this research, 16S rRNA and reductase gene quantification supplied details about how the populations in the different CFSTRs shifted temporally in response to different CAH electron acceptors and soluble electron donors. The temporal shifts in dechlorination performance were accompanied by shifts in total numbers of *Dehalococcoides*,

proportions of *Dehalococcoides* within the total bacterial community, and proportions of different reductase genes present. Which reductase-containing *Dehalococcoides* dominated was associated with different electron donors and CAHs supplied. Understanding what conditions favor the different dechlorination processes and relevant reductases is important for optimizing conditions that favor complete dechlorination to ETH in remediation sites.

This study showed that qPCR analyses of 16S rRNA and reductase genes were effective in tracking *Dehalococcoides* within the total population, and discerning two separate *Dehalococcoides* populations within the mixed community. Analysis using only the characterized reductase genes agreed with performance characterization, indicating that a small collection of genes quantified may be sufficient to characterize and understand dechlorinating populations and optimize performance for complete dechlorination. When added on an equivalent hydrogen production potential, formate (a more direct source of hydrogen), versus lactate, favored *Dehalococcoides* growth, and perhaps more importantly, a *vcrA*-containing population. The failure to maintain substantial *Dehalococcoides* and *vcrA* numbers in the VC-fed CFSTR illustrates that sufficient growth kinetics and reaction times are important factors.

qPCR analyses showed initial loss of measurable VC dechlorination was accompanied by a 5 order of magnitude decrease in *Dehalococcoides* 16S rRNA genes, but did not completely eliminate the organisms. Switching Reactor 3 to more energetically favorable TCE led to increased *Dehalococcoides* populations in the CFSTR, from 1.7×10^3 to 4.5×10^5 16S rRNA gene copies/mL, though significant measurable cDCE and VC dechlorination activity did not occur prior to the reactor failure. cDCE and VC dechlorination activity in batch test were generally too low to detect when *Dehalococcoides* 16S rRNA gene quantities were below 1×10^6 copies/mL. The significance of the 260-fold increase in *Dehalococcoides* after switching Reactor 3 to TCE is that sites containing measurable *Dehalococcoides* 16S rRNA genes but immeasurable cDCE or VC dechlorination may contain relevant reductases and activity

at low levels. Biostimulation could be as effective as bioaugmentation given adequate electron donors and time for growth.

With the understanding that gene presence does not necessitate gene expression (Lovely, 2003), it has been argued that DNA quantification is unlikely to correlate with activity measurements. Attempts have therefore been made to correlate RNA measurements with dechlorination rates, with minor to no success over a narrow range of concentrations (Lee et al., 2006; Rahm and Richardson, 2008a; Rahm and Richardson 2008b). This work has shown that correlation with DNA over a broad range of activity is a possibility, especially with respect to cDCE and VC dechlorination.

Order of magnitude predictions of dechlorination rates in dynamic systems were achieved, and qPCR analyses of DNA were more sensitive than our rate measurements. cDCE and VC dechlorination activity was undetectable in 18-hour incubations when *Dehalococcoides* 16S rRNA gene copies were below 10^6 copies/mL.

Although different reductase-containing *Dehalococcoides* populations prevailed under different conditions, the *Dehalococcoides* 16S rRNA gene served as an adequate predictor of cDCE and VC dechlorination rates. This is of interest since not all putative reductase genes have been characterized, though transcription for some putative reductases has been demonstrated in the presence of varying CAHs (Johnson et al., 2008; West et al; 2008; Waller et al., 2005). Quantifying specific reductase genes may produce more accurate predictions of dechlorination activity, as indicated by higher regression R^2 values for some of the genes (summarized in Table 3.3 of this study). However, such an approach presents the risk of quantifying a gene that is not the dominant reductase gene for that process within a mixed community or failing to quantify a reductase gene important to an observed dechlorination step.

Our work has shown that cDCE and VC dechlorination rates can be normalized to *Dehalococcoides* 16S rRNA genes, regardless of the *Dehalococcoides* strain dominating under extant conditions within a mixed community. Previous work has shown an order of magnitude greater expression of *vcrA* compared to *bvcA* despite gene presence being essentially equal (Lee et al., 2008), and up to four orders of magnitude changes in

expression levels of reductases have been observed between starvation and full expression (Johnson et al., 2005; Lee et al., 2006). Thus, as long as a portion of *Dehalococcoides* are present with the relevant reductase genes, increases in expression could overwhelm the difference in proportions of reductase genes present. This seemed possible in our systems where each reductase was present at a minimum of 1% the concentration of other reductase genes quantified, perhaps explaining why *Dehalococcoides* 16S rRNA gene quantities were sufficient in predicting cDCE and VC dechlorination rates.

The correlation of selected genes to maximum dechlorination rates, and reflection of batch-measured dechlorination rates and DNA quantification to reactor performance illustrates that site remediation potential can be adequately predicted by simple measurements such as *Dehalococcoides* 16S rRNA gene quantification. The simplicity of DNA quantification compared to RNA quantification, microcosm experiments, or pilot scale evaluations is an exciting development toward simplifying field remediation assessment.

ACKNOWLEDGEMENTS

We thank Alfred Spormann at Stanford University for invaluable use of his laboratory facilities and expertise. We also thank Sebastian Behrens for his qPCR primer and method development at Stanford University, as well as his qPCR training and expertise. Funding for this research was provided by NSF Integrative Graduate Education and Research Traineeship Program (IGERT), U.S. EPA Western Region Hazardous Substance Center (Grant # R-828772), and National Institute of Environmental Health Sciences (Graduate Training Grant #1P42 ES10338). This article has not been reviewed by the above agencies and no endorsement should be inferred.

Table 3.1. CFSTR influent electron donor/acceptor conditions.

Reactor	Operation (days)	Electron donor (mM) ^a	Electron Acceptor (mM) ^a
#1	0-125	Lactate: 25.7 ± 3.3	TCE: 7.0 ± 1.2
#2	0-305	Formate: 39.5 ± 9.0 Acetate: 2.2 ± 0.3	TCE: 7.7 ± 1.3
#3	0-99	Formate: 14.1 ± 4.4 Acetate: 0.77 ± 0.35	VC: 9.8 ± 2.2
	99-212	Formate: 17.4 ± 2.1 Acetate: 0.68 ± 0.10	TCE: 2.8 ± 0.4
	212-311	Formate: 22.5 ± 6.4 Acetate: 1.5 ± 0.4	TCE: 5.9 ± 1.0
	311-390	Formate: 28.3 ± 0.9 Acetate: 2.5 ± 0.3	TCE: 8.8 ± 1.4

^a Average of all measurements during period of operation \pm corresponding standard deviation.

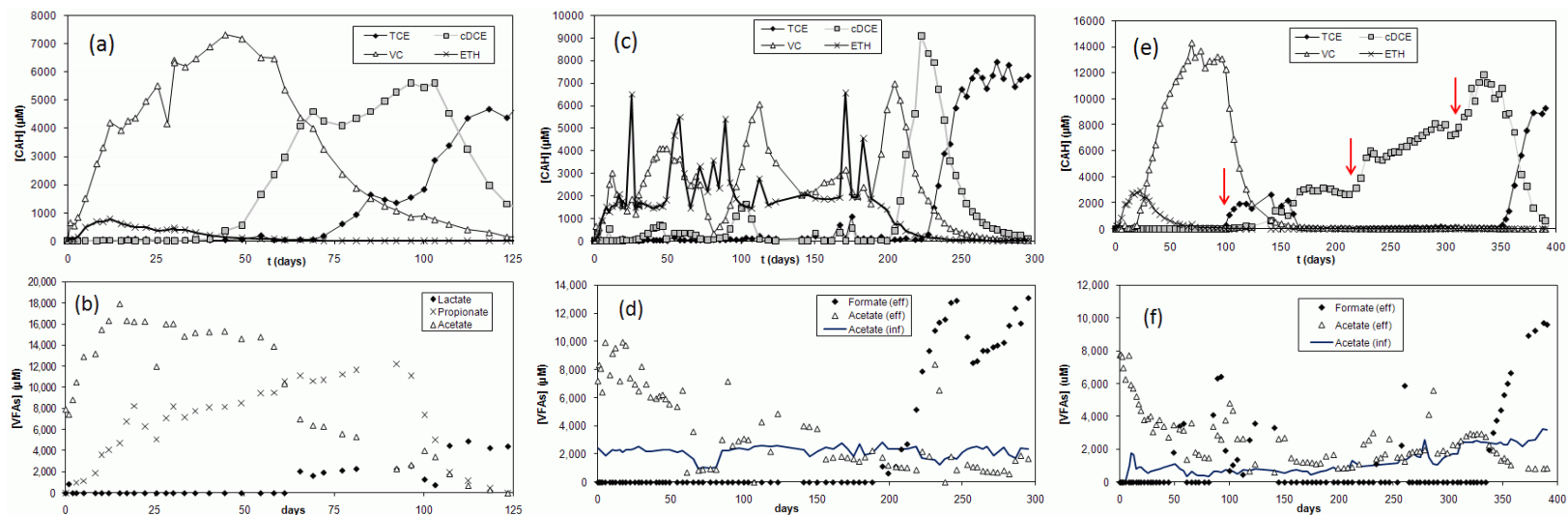


Figure 3.1. Effluent CAH and organic acids monitoring. Reactor 1 (a and b), Reactor 2 (c and d), and Reactor 3 (e and f). Arrows in Figure 3.1e represent operational changes for Reactor 3 as follows: day 99 change to 2.8 mM TCE, day 212 change to 5.9 mM TCE, and day 311 change to 8.8 mM TCE. Symbols as indicated in figure legends.

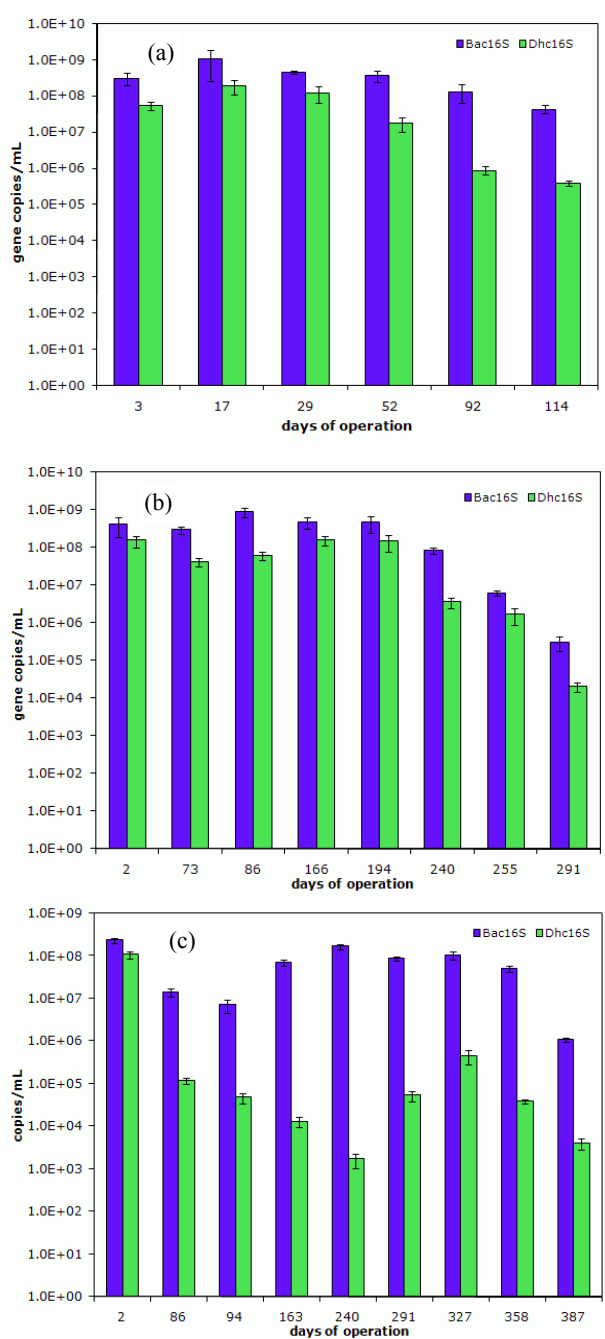


Figure 3.2. Total *Bacteria* and *Dehalococcoides* 16S rRNA gene quantities. Reactor 1 (a), Reactor 2 (b), and Reactor 3 (c). Dark blue bars are universal *Bacteria* 16S rRNA genes quantified. Light green bars are *Dehalococcoides* 16S rRNA genes quantified. Error bars indicate standard deviation of independent samples analyzed in triplicate qPCR reactions.

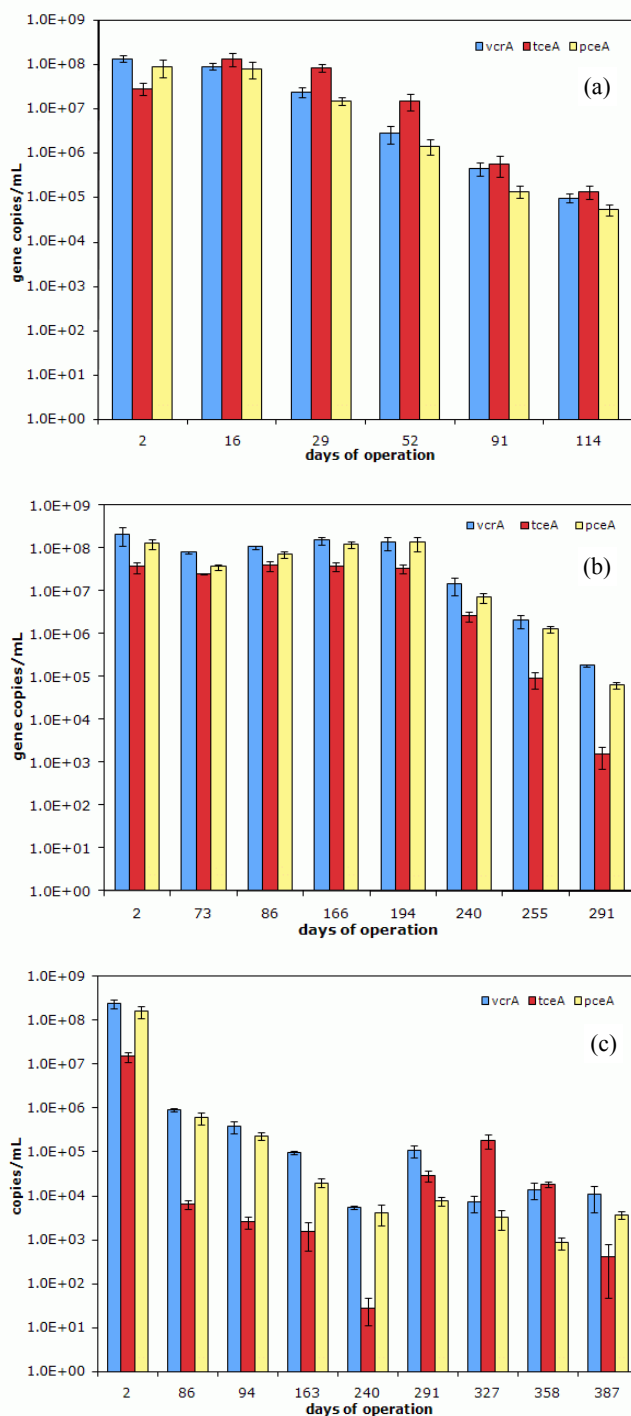


Figure 3.3. Reductase genes quantities. Reactor 1 (a), Reactor 2 (b), and Reactor 3(c). Light blue bars are quantities of the *vcrA* gene. Red bars are quantities of the *tceA* gene, and yellow bars are quantities of the *pceA* gene. Error bars indicate standard deviations of independent samples analyzed in triplicate qPCR reactions.

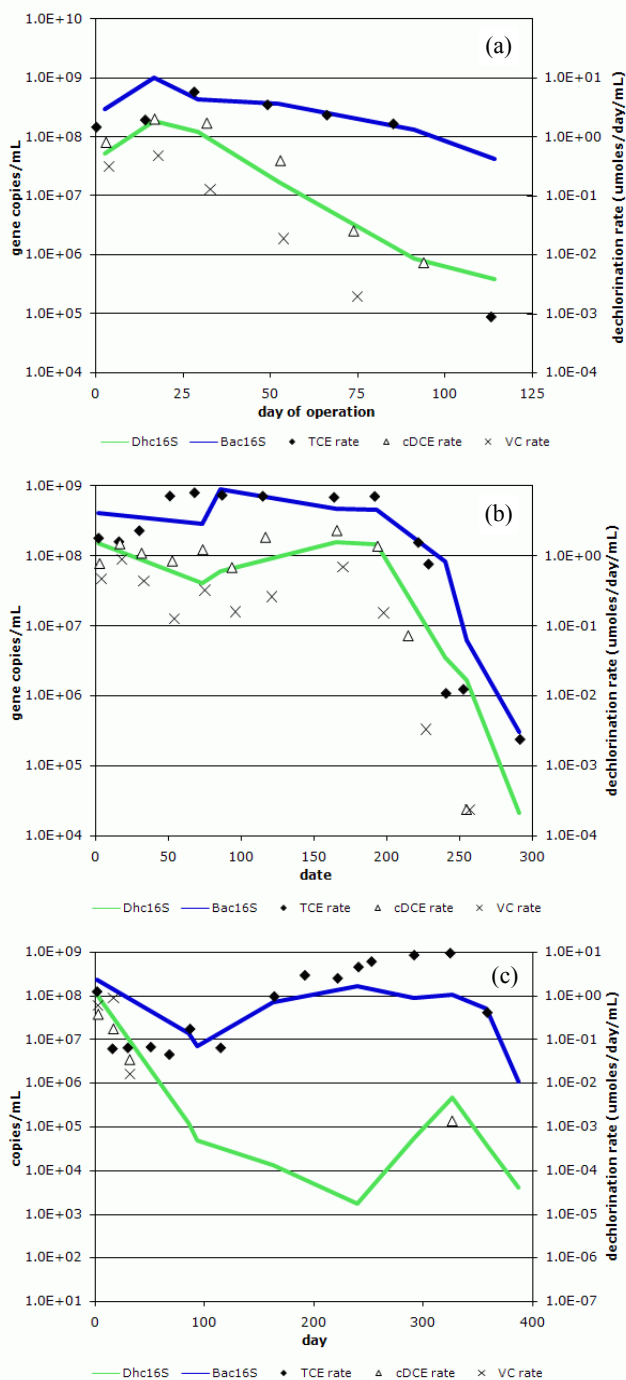


Figure 3.4. *Dehalococcoides* and total *Bacteria* populations compared to dechlorination rates. Reactor 1 (a), Reactor 2 (b), and Reactor 3 (c). Symbols correspond to batch rate measurements of TCE, cDCE, and VC dechlorination as indicated in figure legends. Dark blue lines correspond to total *Bacteria* 16S rRNA gene quantities. Light green lines correspond to *Dehalococcoides* 16S rRNA gene quantities.

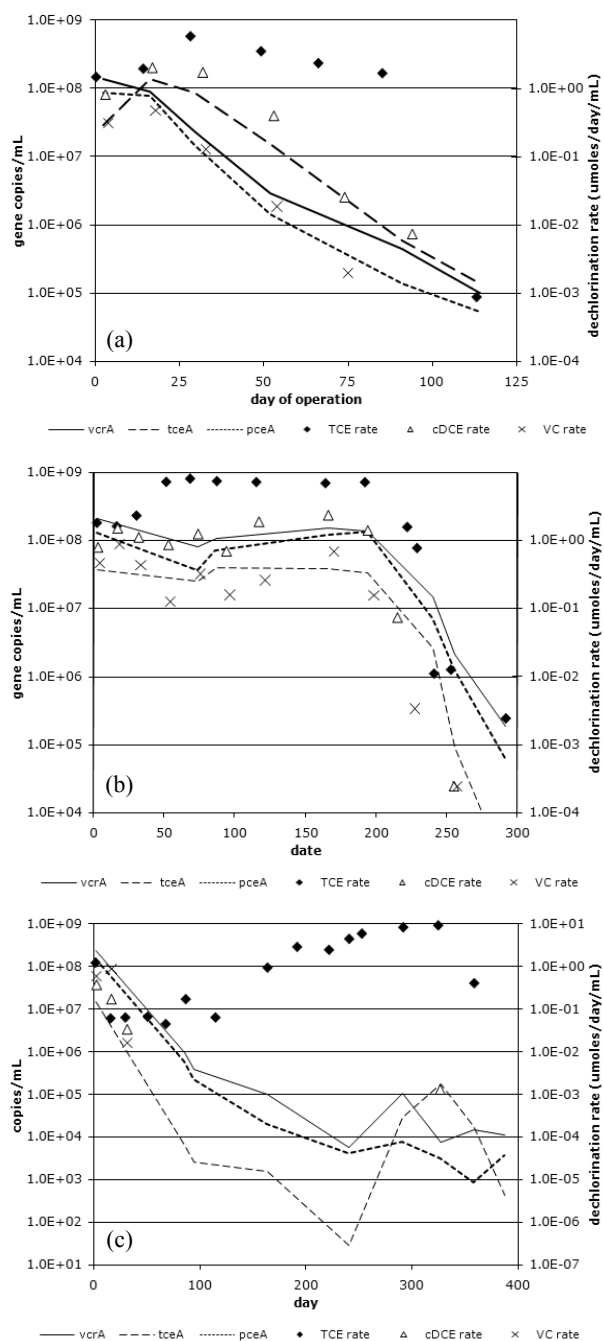


Figure 3.5. Reductase gene presence compared to dechlorination activity. Reactor 1 (a), Reactor 2 (b), and Reactor 3 (c). Symbols correspond to batch rate measurements of TCE, cDCE, and VC dechlorination as indicated in figure legends. Solid lines correspond to *vcrA* gene quantities; long dashed lines correspond to *tceA* gene quantities, and short-dashed lines correspond to *pceA* gene quantities

Table 3.2. Comparability of dechlorination rates normalized to *Dehalococcoides* 16S rRNA gene copies.^a

Reactor	μmoles TCE/day/Dhc16S	μmoles cDCE/day/Dhc16S	μmoles VC/day/Dhc16S
#1	$3.7 \times 10^{-7} \pm 7.7 \times 10^{-7}$ { $8.8 \times 10^{-4} - 5.8 \times 10^0$ }	$1.4 \times 10^{-8} \pm 5.5 \times 10^{-9}$ { $7.3 \times 10^{-3} - 2.0 \times 10^0$ }	$2.6 \times 10^{-9} \pm 2.3 \times 10^{-9}$ { $2.0 \times 10^{-3} - 4.7 \times 10^{-1}$ }
#2	$6.9 \times 10^{-8} \pm 6.9 \times 10^{-8}$ { $2.4 \times 10^{-3} - 8.2 \times 10^0$ }	$1.9 \times 10^{-8} \pm 1.4 \times 10^{-8}$ { $7.2 \times 10^{-2} - 2.3 \times 10^0$ }	$3.7 \times 10^{-9} \pm 2.5 \times 10^{-9}$ { $3.4 \times 10^{-3} - 8.7 \times 10^{-1}$ }
#3 ^b	$4.3 \times 10^{-4} \pm 1.2 \times 10^{-3}$ { $4.5 \times 10^{-2} - 9.6 \times 10^0$ }	3.3×10^{-9} { $1.3 \times 10^{-3} - 3.7 \times 10^{-1}$ }	1.7×10^{-8} { $1.3 \times 10^{-3} - 8.7 \times 10^{-1}$ }
Azizian et al., 2008 ^c			$7.8 \times 10^{-10} \pm 4.5 \times 10^{-10}$ { $9.0 \times 10^{-5} - 1.7 \times 10^{-4}$ }

^a **Average of all measurable rates \pm corresponding standard deviation (μmoles**

CAH/day/Dhc16S copies). {Range of rates expressed as $\mu\text{moles/day/mL}$ culture}.

^b cDCE and VC rates are based upon only two measurable rates. No standard deviation can be supplied.

^c Values based upon rate and DNA measurements in all 6 microcosms published.
{Range of rates expressed as $\mu\text{moles/hr/g}$ of soil}

Table 3.3. Dechlorination rates and gene quantity correlations.

Reactor	Gene	TCE R^2	cDCE R^2	VC R^2
1	Eub16S	0.66	0.75	0.23
	Dhc16S	0.50	0.98	0.68
	<i>vcrA</i>	0.44	0.74	0.95
	<i>tceA</i>	0.57	0.98	0.53
	<i>pceA</i>	0.38	0.78	0.98
2	Eub16S	0.78	0.56	0.60
	Dhc16S	0.82	0.83	0.84
	<i>vcrA</i>	0.82	0.78	0.88
	<i>tceA</i>	0.80	0.83	0.87
	<i>pceA</i>	0.82	0.76	0.77
3	Eub16S	0.67	N/A	N/A
	Dhc16S	0.00	N/A	N/A
	<i>vcrA</i>	0.11	N/A	N/A
	<i>tceA</i>	0.01	N/A	N/A
	<i>pceA</i>	0.12	N/A	N/A

R^2 values correspond to linear regression best fits through log(gene copies/mL) versus log(dechlorination rate). Dechlorination rates calculated on μ moles CAH/mL culture/hr. Less than four data points were available for cDCE and VC dechlorination rate correlations in Reactor 3.

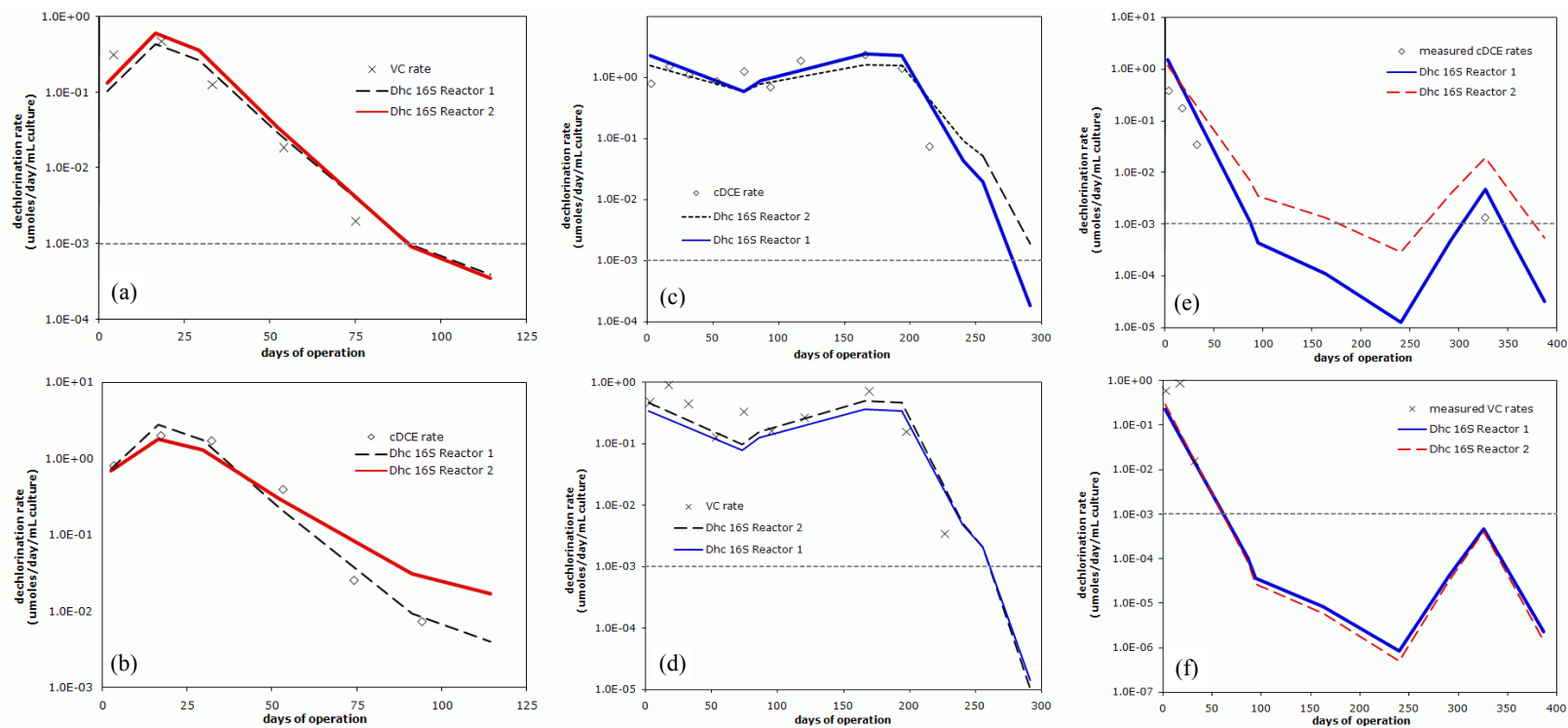


Figure 3.6. Predicted dechlorination rates based upon DNA quantification compared to measured dechlorination rates from reactor harvested cells. Reactor 1 cDCE (a) and VC (b), Reactor 2 cDCE (c) and VC (d), and Reactor 3 cDCE (e) and VC (f).

Chapter 4

**Trichloroethene and *cis*-1,2-dichloroethene concentration-dependent toxicity model
fits activity loss in batch-fed, continuous flow, and attached growth anaerobic
cultures**

ABSTRACT

The reductively dechlorinating anaerobic Evanite culture (EV) was fed trichloroethene (TCE) and excess electron donor in three different growth modes (batch-fed, continuous flow stirred tank reactor (CFSTR), and an attached growth recirculating packed column) to accumulate cis-1,2-dichloroethene (cDCE). The study evaluated the effects of high concentrations of chlorinated aliphatic hydrocarbons (CAHs) on culture viability. A second Point Mugu (PM) culture was additionally studied in the cDCE accumulating batch-fed experiment. Both cultures and all reactor systems accumulated cDCE to concentrations ranging from 9 to 12 mM before cDCE production from TCE ceased. Various inhibition models were analyzed, including the previously proposed Haldane inhibition model for the two cultures studied, but none adequately fit the observations from the reactors studied. A concentration-dependent toxicity model is proposed, which fit the data for both cultures and all three reactor growth modes. The toxicity model incorporates cDCE and TCE toxicity terms that directly increase the endogenous decay coefficient in proportion with cDCE and TCE concentrations. Modeled estimates for cDCE and TCE toxicity parameters suggest reductively dechlorinating cells are most sensitive to high concentrations of cDCE and TCE in batch-fed growth, followed by CFSTR, and attached growth, and that TCE is more toxic than cDCE. The different sensitivities were associated with the toxicity coefficients obtained by model fitting.

INTRODUCTION

Trichloroethylene (TCE) and the lesser chlorinated aliphatic hydrocarbons (CAHs), such as *cis*-1,2-dichloroethene (cDCE) and vinyl chloride (VC) are prevalent groundwater contaminants of environmental concern known to be, toxic and/or carcinogenic (Ensley, 1991; McCarty, 1997; Kielhorn et al., 2000; Moran et al., 2007). Anaerobic biological reductive dechlorination is a well documented and desirable treatment strategy for TCE and other chlorinated aliphatic hydrocarbons (CAHs) due to its simplicity, and the abundance of organisms capable of this process (Aulenta et al., 2006). The various CAHs have different chemical properties, and multiple factors affect the separate reductive dechlorination steps of TCE to cDCE, VC and ETH such as: different organisms capable of each dechlorination step, faster dechlorination rates of the higher chlorinated compounds (Yu et al., 2005), energetics associated with each dechlorination step (He et al., 2002), usable electron donors sources, advection of contaminants in a groundwater plume, and lower hydrogen thresholds for the higher chlorinated compounds (Lu et al., 2001; Yang and McCarty 1998; Luijten et al., 2004). It is therefore common to see separate zones of each different CAH at field sites (e.g., Ling and Rifai, 2007; Chapelle et al., 2005), often resulting in high cDCE concentrations (as summarized by Gerritse et al., 1995 and van Eekert and Schraa, 2001).

With the high solubility limits of TCE (8 mM) and cDCE (53 mM), and the demonstration of enhanced dissolution of non-aqueous phase liquids (NAPLs) such as TCE or PCE (Cope and Hughes, 2001; Yang and McCarty, 2000), it is possible to achieve separate zones with cDCE concentrations theoretically exceeding the molar solubility limit of TCE near a NAPL source zone. cDCE concentrations ranging from 3 to 9 mM cDCE have been produced biogenically from PCE dechlorination and been shown to have a toxic effect on dechlorinating cultures (Chu, 2004; Adamson et al., 2004). High concentrations of PCE, TCE, and cDCE on the order of 1 mM have been shown to reduce activity of reductively dechlorinating cultures (Yang and McCarty, 2000; Duhamel et al., 2002), and elevated decay coefficients have been demonstrated for two reductively dechlorinating mixed cultures in the presence of cDCE above 8 mM

(Chu, 2004). Competitive inhibition of higher chlorinated CAHs on the reductive dechlorination of lesser chlorinated CAHs has also been demonstrated (Yu et al., 2005; Cupples et al., 2004; Lee et al., 2004) and Haldane inhibition by high concentrations of CAHs reducing their own dechlorination rates has been proposed in model fits to reductive dechlorination data (Yu and Semprini, 2004). High CAH concentrations therefore produce complicated and negative interactions that are important to understand more fully.

The objective of this research was to determine the effects of high cDCE concentrations (~10 mM) in different reductively dechlorinating cultures and modes of growth. In this work, a cDCE and TCE concentration-dependent toxicity model was developed to simulate observed declines in dechlorination activity for different growth modes, and two different dechlorinating cultures. cDCE accumulation effects on dechlorination activity were studied in three different culture growth modes: batch fed reactors, a continuous flow stirred tank reactor (CFSTR), and a recirculating packed column (RPC). Two cultures tested were a (previously undescribed) subculture enriched from the Evanite (EV) culture capable of PCE and TCE dechlorination to cDCE, with no detectable VC or ETH formation, and the Point Mugu (PM) culture previously shown to dechlorinate PCE, TCE and cDCE to VC with cometabolic ETH formation (Yu et al., 2005). Both cultures were used in cDCE accumulation batch-fed experiments, and the EV cDCE-producing subculture (EV-cDCE) was additionally tested in a CFSTR and an RPC to study the effects of cDCE accumulation on dechlorination ability in the different reactor systems, or modes of growth. An empirical toxicity model was able to simulate the observed cDCE and TCE concentrations across all above systems, while inhibition models could not. This work has produced a mathematical and conceptual relationship between a long-observed problem of high concentration CAH inhibition or toxicity (Duhamel et al., 2002; Yang and McCarty, 2000; Chu, 2004), and observed declines in dechlorination activity.

MATERIALS AND METHODS

Chemicals: Liquid TCE (99.9%, Acros Organics, Pittsburgh, PA) was used for both feed stocks and analytic standards. Liquid cDCE (97%, Acros Organics, Pittsburgh, PA), gaseous VC (99.5%,) and gaseous ETH (99.5%) (Aldrich Chemical, Milwaukee, WI) were used for creation of analytic standards. Hydrogen gas (99%) and 10%CO₂/90%N₂ gasses were supplied by Airco, Inc., Albany, OR. Reagent grade salts or better were used in culture media.

Analytical Methods: Chlorinated ethenes and ethene were quantified by gas chromatography with a HP-6890 gas chromatogram (GC), using a flame ionization detector (FID) and 30 m x 0.53 mm GS-Q column (J&W Scientific, Folsom, CA). 100 µL gas samples were collected with a Hamilton 100 µL gastight syringe (Leno, NV), and analyzed on the GC with a 15 mL/min. flow of helium carrier gas. The GC oven was programmed with an initial temperature of 150°C, held for 2 min., increased to 220°C at 45°C/min, and held for 0.7 min at 220°C. Hydrogen was analyzed by GC thermal conductivity detection (GC-TCD) with a Carbonex 1000 column (15 ft x 1/8 in., Supelco, Bellefonte, PA) using an argon carrier gas at 15 mL/min at 220°C isothermal operation. Lactate, propionate, and acetate were analyzed by high pressure liquid chromatography (HPLC) on a Dionex-500 HPLC with a UV detector at 210 nm and a Prevail Organic Acid 5u column (250 mm x 4.6 mm I.D., Alltech, Deerfield, IL). HPLC analyses of 0.5 mL samples were performed with a 25.0 mM KH₂PO₄ and 17.3 mM H₃PO₄ elluent.

Culture: A subculture of the Evanite culture (EV-cDCE), which exhibited virtually no cDCE and VC dechlorination ability but maintained effective TCE dechlorination activity, was used in the CFSTR, RPC, and batch fed experiments. The EV culture was originally enriched by adding harvested groundwater from the TCE-contaminated Evanite site in Corvallis, OR (Yu and Semprini, 2004; Yu et al., 2005) and enriching in a modified basal medium (Yang and McCarty, 1998) for 5 years with batch feedings of tetrachloroethene (PCE) at 100mg/L, butanol (40 mg/L) and hydrogen (up to 10% in the headspace gas). The cDCE accumulating subculture developed over months of enrichment in the same fashion, and was maintained with the same PCE, butanol, and

hydrogen augmentation. The reason for the shift in behavior is presently unknown, but may have resulted from exposure of the original culture to oxygen. The Point Mugu (PM) culture was used in batch fed experiments reported here. The PM culture was originally enriched under anaerobic conditions from aquifer solids and groundwater from the Point Mugu Naval Weapon Facility, CA under conditions previously reported, similar to those for the EV culture, with the same growth medium and electron donors, but with TCE as the electron acceptor to 100 mg/L (Yu and Semprini, 2004; Yu et al., 2005).

CFSTR: A zero-headspace 303 mL CFSTR was completely mixed via a teflon stirbar (Figure 4.1). The reactor consisted of a 303 mL Kimax bottle fitted with a 3-hole stainless steel cap, connected to a syringe pump. Holes in the stainless cap were bored for ¼-28 threads to accommodate PEEK fittings, valves and tubing (Upchurch Scientific, Oak Harbor, WA). The influent was fitted with 1/8" PEEK tubing, and a three-way T-valve. The influent tube was inserted to within ¼" of the bottom of the bottle. The effluent line from the CFSTR consisted of 1/16" PEEK tubing flush with the stainless steel cap to create a zero-headspace reactor, and a 2-way L-valve was installed to switch between effluent flow and effluent sampling. The CFSTR was inoculated from inside an anaerobic glove box with 5% H₂, 95 N₂ atmosphere (Coy Laboratory Products, Inc., Grass Lake, MI) with 303 mL of the EV-cDCE subculture to create a zero-headspace reactor. The reactor was then capped, exported from the glove box, wrapped in aluminum foil (to avoid phototrophic activity), and connected to influent and effluent waste collection lines as illustrated in Figure 4.1.

The influent was introduced to the chemostat with a 100 mL gastight syringe on an Orion M361 syringe pump (Thermo Electron Corp., Beverly, MA). Batches of feed were made by augmenting basal medium with excess neat TCE (for an average aqueous concentration of 7.4 mM ±0.95 mM std dev) and sodium lactate to 25.6 mM (±4.0 mM std dev). Batches were stirred for at least one hour, settled for at least 30 minutes (to remove TCE NAPL from suspension), and one syringe-volume of feed stock was extracted. The feed syringe was refilled, and more TCE-lactate amended medium was prepared periodically as necessary. To ensure no oxygen entered the system, each time

the feed syringe was replaced, the reactor influent valve was closed, the syringe was refilled, placed back online, and 2 mL of feed were flushed through the influent line prior to opening the influent valve to the CFSTR. Resazurin was added as an oxygen indicator and was never oxidized during reactor operation, according to the colorimetric reaction. Influent pumping was varied for the CFSTR as summarized in Table 4.1. The majority of operation was at an influent flow rate of 18 mL/day, for a hydraulic retention time of 16.8 days. pH was monitored periodically and remained between 6.8 and 7.6 throughout operation

RPC: The RPC was constructed using a 30 cm x 2.5 cm (I.D.) glass Kontes Chromaflex column with PTFE end fittings and 20 μ m polyethylene bed support frits (Kontes, Vineland, NJ). The column was packed with 2 mm glass beads and connected with 1/8" PEEK tubing (0.062" I.D.) to a recirculating pump consisting of a Masterflex L/S 7550 computerized driver and Masterflex Micropump (Cole-Parmer Instrument Co., Vernon Hills, IL). The glass beads were previously etched (to enhance roughness and cellular attachment) with a chromic and hydrochloric acid procedure as described by Shellenberger and Logan (2002), thoroughly rinsed, and autoclave sterilized and oven dried. Multiple aliquots of beads were weighed to determine average bead weight prior to packing the column. Column weights before bead addition, after addition of dry beads, and after flushing with 25%CO₂/75%N₂-sparged autoclaved nano-pure water allowed determination of the number of beads added and the void/liquid volume. The total liquid pore volume of the column was 65.8 mL. The liquid volume of the entire assembled RPC, including the packed column and recirculating tubing was 70.8 mL, based on a bromide tracer test. The recirculating pump speed was set to operate at 2 mL per minute, to achieve a 35 minute circulation time through the assembled system.

The column was oriented vertically for upflow operation. T-valve PEEK connections below and above the column allowed influent and effluent liquid sampling. A 25 mL gastight syringe (Hamilton, Leno, NV) on an Orion M361 syringe pump was used for feed addition and connected to the influent T-valve connection. A T-connection at the top of the recirculating column system allowed effluent to leave the reactor by

pressure into an anaerobically prepared waste collection bottle. Inline mini-column cartridges were constructed of 1/4" (I.D.) glass tubing filled with the 2 mm glass beads, and placed below and above the column, with T-valve connections and 1/16" PEEK tubing bypass loops, to allow periodic culture assessment without interrupting RPC operation. Each mini-column had a liquid volume of 0.72 mL. The main column and mini-column cartridges were wrapped in aluminum foil to avoid phototrophic activity. A schematic diagram of the system is supplied in Figure 4.2.

Prior to column inoculation and startup, the assembled system was flushed and filled with autoclaved anaerobic media. The inoculum was transferred in the anaerobic glove box (5% H_2 /95% N_2 atmosphere) by adding 120 mL of the EV-cDCE subculture to a 156 mL serum bottle, augmenting with 490 mg of 60%Na-lactate syrup and 2.0 μL of neat TCE, shaking, and withdrawing 100 mL of the EV culture mixture into a 100 mL gastight syringe. The column was inoculated by injecting the culture up through the column at a rate of 2 mL/min without recirculation, until 90 mL of culture had been flushed up through the 70.8 mL system. The 25 mL influent syringe was then connected, and the recirculating and influent pumps were turned on to start operation. Influent feed was introduced at a rate of 6 mL/day to achieve a hydraulic retention time of 11.8 days. The syringe was refilled as needed, flushing influent lines each time to maintain anaerobic conditions. On day 101 the influent feed rate was increased to 12 mL/day, to obtain a hydraulic retention time of 5.9 days. The 12 mL/day feed rate was maintained until day 155 when operation was terminated. Compared to the 2 mL/min recirculation rate, this flow increase is insignificant and is not expected to impact shear forces on biomass in the column.

Twice during operation, the mini-columns from the RPC were taken offline, flushed with fresh media, injected with TCE- and lactate-augmented medium, incubated 18 hours, and analyzed for dechlorination activity by extracting the aqueous contents and analyzing on a GC-FID fitted with a purge and trap apparatus. These analyses (data not shown) confirmed that TCE dechlorination to cDCE was associated with cells attached to the beads in the mini-columns. These analyses also confirmed that dechlorination rates

were equal at the influent and effluent ends of the column, demonstrating that the RPC had successfully distributed activity throughout the length of the column, with no spatial separation of activity along the length of the column.

Growth medium for the RPC was prepared in the same fashion as the CFSTR, by augmenting the basal medium with excess TCE and 60% sodium lactate syrup for an average concentration of 11.3 mM TCE (± 2.5 std dev) and 22.6 mM lactate (± 6.2 mM std dev). For both the RPC and CFSTR, lactate was supplied at approximately 5 to 6 times the hydrogen formation potential requirement to dechlorinate TCE to cDCE for lactate fermentation to acetate and hydrogen, in order to avoid hydrogen limitations on dechlorination.

Chemostat and packed column liquid samples were collected by pushing an extra 1.5 mL from the influent syringe into the system, extracting 1.5 mL of effluent or influent instantaneously from the appropriate sampling port (in a disposable 3.0 mL syringe), and injecting 1.0 mL of liquid sample into a 2.0 mL crimp-top clear glass vial. The liquid samples were vortexed for 1 minute at room temperature, and 100 μ L of headspace was extracted and injected into the GC-FID injection port for CAH and ETH quantification. A second 100 μ L headspace sample was extracted and injected into a HP5890 GC-TCD for H₂ quantification. The liquid from the 2 mL sample vial was then stored in a 1.5 mL Eppendorf tube at -20°C until 0.5 mL of liquid sample could be analyzed by HPLC for organic acids at a later date. Influent and effluent sampling for both the CFSTR and RPC was conducted approximately every 2 to 3 days. Acids and H₂ data were monitored to ensure the systems were not electron donor limited.

Batch cDCE accumulation reactors: Batch reactors were constructed in the anaerobic glove box with either PM or EV culture in 156 mL serum bottles in triplicate, adding 80 mL of culture (EV-cDCE or PM) and 0.05 mL of 60% Na-lactate syrup to each bottle at startup. All batch bottles were sparged with 10% H₂, 90% {10%CO₂/90%N₂}, and then augmented with 2 μ L of neat TCE for an initial aqueous TCE concentration of 250 μ M. Each batch bottle was monitored daily for CAHs and H₂. TCE was added to each bottle approximately once per day to aqueous concentrations of 200 to 800 μ M, depending on

observed rates of dechlorination, with the intent of letting cDCE accumulate. TCE and cDCE have been shown to competitively inhibit dechlorination of less-chlorinated CAHs in the EV and PM cultures (Yu and Semprini, 2004; Yu et al., 2005), and VC accumulation was minimal in the PM culture, with no detectable ETH accumulation during this experiment. The EV-cDCE culture had lost the ability to dechlorinate cDCE, and no VC or ETH formation was detected in the EV batch experiments. TCE and H₂ were added as needed, in order to avoid accumulation of either TCE or H₂, such that amounts and frequency of additions declined later in the 67-day experiment as activity declined. TCE aqueous concentrations were generally maintained above 100 µM to ensure TCE dechlorination was not TCE-limited. TCE additions were performed inside the anaerobic glove box with injections of 2 to 6 µL of neat TCE. H₂ additions were performed with anaerobically prepared H₂ gas injected via H₂-flushed disposable syringes and 22 gage needles. pH was maintained between 6.5 and 7.3 during the batch experiments with a single addition of anaerobically prepared 100.3 mM Na₂CO₃ stock solution in autoclaved deionized water. pH values at the end of the experiment were between 6.8 and 7.2 for all batch-fed bottles. To ensure adequate carbon was available, 0.2 mL of anaerobically prepared 60% Na-lactate syrup was injected approximately every 20 days into all batch reactors. All batch reactor bottles were shaken in the dark at 200 rpm and 20°C.

MODEL DEVELOPMENT

Michaelis-Menten kinetics for Reductive Dechlorination: The anaerobic reductive dechlorination of volatile CAHs, by the EV and many other cultures, has been described using Michaelis-Menten kinetics as follows (Yu and Semprini, 2004; Lee et al., 2004; Cupples et al., 2004; Fennell and Gossett, 1998; Haston and McCarty, 1999).

$$\frac{dC_{L,j}}{dt} = -\frac{k_{\max,j}XC_{L,j}}{K_{S,j} + C_{L,j}} + \frac{k_{\max,i}XC_{L,i}}{K_{S,i} + C_{L,i}} \quad (1)$$

Where C_L is the CAH aqueous concentration ($\mu\text{mol/L}$), k_{max} is the maximum specific utilization rate ($\mu\text{mol/mg protein/day}$), X is the biomass concentration (mg protein/L), and K_S is the half-velocity coefficient ($\mu\text{mol/L}$). Coefficient i relates to production of one CAH by dechlorination of its more chlorinated parent compound, and coefficient j relates to removal by dechlorination of the CAH whose rate is being calculated. C_L is related to total mass in experiments containing both gas and aqueous phases by the Henry's coefficient relationship $C_L = M/(V_L + V_G/H_{CC})$, where M is the total mass of the volatile CAH in the reactor, V_L is the gas phase volume, V_G is the liquid phase volume, and H_{CC} is the dimensionless Henry's coefficient. The ETH and CAH Henry's coefficients utilized have been published previously (Gossett, 1987; Perry et al., 1997).

Growth of biomass can be related to dechlorination rates by the yield coefficient, Y ($\text{mg protein}/\mu\text{mol Cl}^-$ released) and decay coefficient, k_d (day^{-1}) as follows.

$$\frac{dX}{dt} = Y \sum_i \frac{dC_i}{dt} - k_d X \quad (2)$$

Where C_i represents each CAH that yields energy for growth from its dechlorination. Because previous modeling of the EV and PM cultures was successful with a single X population (Yu and Semprini, 2004; Yu et al., 2005), a single population X for this study is assumed.

Michaelis-Menten with inhibition: Previous work with the EV and PM culture, as well as other reductively dehalogenating cultures, has shown higher chlorinated compounds inhibit dechlorination of the lesser-chlorinated compounds, and that the nature of the inhibition is competitive (Yu and Semprini, 2004; Lee et al., 2004; Cupples et al., 2004). It has also been shown that lesser-chlorinated compounds do not inhibit dechlorination rates of higher-chlorinated compounds for the EV and PM cultures (Yu and Semprini, 2004). Cupples et al. (2004) did find competitive inhibition was exerted by lesser-chlorinated CAHs upon dechlorination of the higher-chlorinated CAHs in their study. Competitive inhibition of cDCE on TCE dechlorination was therefore evaluated in this

study, but did not fit data and is thus not discussed in detail here. Thus reductive dechlorination of TCE, cDCE, and VC, in the absence of PCE, can be modeled by the following three equations.

$$\frac{dC_{L,TCE}}{dt} = -\frac{k_{\max,TCE}XC_{L,TCE}}{K_{S,TCE} + C_{L,TCE}} \quad (3)$$

$$\frac{dC_{L,cDCE}}{dt} = -\frac{k_{\max,cDCE}XC_{L,cDCE}}{K_{S,cDCE}\left(1 + \frac{C_{L,TCE}}{K_{I,TCE}}\right) + C_{L,cDCE}} + \frac{k_{\max,TCE}XC_{L,TCE}}{K_{S,TCE} + C_{L,TCE}} \quad (4)$$

$$\frac{dC_{L,VC}}{dt} = -\frac{k_{\max,VC}XC_{L,VC}}{K_{S,VC}\left(1 + \frac{C_{L,cDCE}}{K_{I,cDCE}} + \frac{C_{L,TCE}}{K_{I,TCE}}\right) + C_{L,VC}} + \frac{k_{\max,cDCE}XC_{L,cDCE}}{K_{S,cDCE}\left(1 + \frac{C_{L,TCE}}{K_{I,TCE}}\right) + C_{L,cDCE}} \quad (5)$$

Where $K_{I,TCE}$, for instance, is the competitive inhibition coefficient of TCE on dechlorination of the lesser chlorinated compounds ($\mu\text{mol/L}$). Previous work with the EV and PM cultures has shown the K_I for each CAH can be adequately modeled as equivalent to the K_S for that CAH, and other researchers have shown very similar values between these parameters as well (Yu and Semprini, 2004; Yu et al.; 2005; Cupples et al., 2004).

When assessing high concentration effects of CAHs on dechlorinating organisms, a Haldane type inhibition of a CAH on its own dechlorination has been used to fit experimental data (Yu and Semprini, 2004). Haldane inhibition combined with competitive inhibition can be represented as follows for cDCE dechlorination in the presence of TCE.

$$\frac{dC_{L,cDCE}}{dt} = - \frac{k_{\max,cDCE} X C_{L,cDCE}}{K_{S,cDCE} \left(1 + \frac{C_{L,TCE}}{K_{I,TCE}} \right) + C_{L,cDCE} + \frac{C_{L,cDCE}^2}{K_{I,H-cDCE}}} + \frac{k_{\max,TCE} X C_{L,TCE}}{K_{S,TCE} + C_{L,TCE} + \frac{C_{L,TCE}^2}{K_{I,H-TCE}}} \quad (6)$$

Where $K_{I,H-cDC}$ is the Haldane inhibition coefficient for cDCE on its own dechlorination ($\mu\text{mol/L}$). Similar relationships can be expressed for TCE or VC Haldane type self-inhibition. Note that the Haldane inhibition is proportional to the square of the CAH concentration and is an inverse relation ship, meaning a large $K_{I,H}$ illustrates weak inhibition, and a small $K_{I,H}$ represents strong inhibition.

While Haldane inhibition refers to a compound inhibiting its own biotic conversion, we also consider the possibility of a Haldane-like inhibition of one compound on another. In this case, we examine the possibility of cDCE inhibiting TCE dechlorination as follows.

$$\frac{dC_{L,TCE}}{dt} = - \frac{k_{\max,TCE} X C_{L,TCE}}{K_{S,TCE} + C_{L,TCE} + \frac{C_{L,cDCE}^2}{K_{h-cDCE}}} \quad (7)$$

Where TCE dechlorination to cDCE is theoretically inhibited by the square of cDCE aqueous concentrations, and K_{h-cDCE} is the Haldane inhibition coefficient for cDCE on TCE ($\mu\text{mol/L}$). Other forms of inhibition explored in this study and commonly modeled are uncompetitive, non-competitive, and mixed inhibition. Because these models did not fit data in this study, they are not discussed in detail here.

Toxicity: Additionally, a concentration-based toxicity model has been explored based upon enhancing cellular decay with increasing concentrations of CAHs. The increased decay as function of increasing CAH concentrations can be modeled as follows.

$$k_d^* = k_d \left(1 + \frac{C_{cDCE}}{K_{t,cDCE}} + \frac{C_{TCE}}{K_{t,TCE}} \right) \quad (8)$$

Where k_d^* is the enhanced, concentration-dependent decay coefficient (day^{-1}), k_d is the endogenous decay coefficient used previously, $K_{t,cDCE}$ is the cDCE-specific toxicity coefficient ($\mu\text{mol/L}$), and $K_{t,TCE}$ is the TCE-specific toxicity coefficient ($\mu\text{mol/L}$). Note that when zero cDCE or TCE is present, the enhanced decay term, k_d^* , is equal to the endogenous decay coefficient, k_d . With inverse relationships for the toxicity coefficient, a high K_t indicates low impact on decay, while a small K_t indicates a strong impact on cellular decay. This concentration-dependent toxicity model is similar to an empirical toxicity model developed to describe observed effects of sodium on anaerobic sludge, where decay was described as follows (Kugelman and Chin, 1970).

$$b = 0.065 + 0.305([Na^+] - 0.15) \quad 0.15 \leq [Na] \leq 0.35 \quad (9)$$

Where b is the microbial decay, 0.065 is the endogenous decay rate, and the remaining term is the concentration effect of sodium over a bound concentration range.

CFSTR modeling: The above models can additionally be incorporated into continuous flow suspended growth systems by accounting for advection. CFSTR modeling for VC dechlorination, including competitive inhibition, would be as follows.

$$\begin{aligned} \frac{dC_{L,VC}}{dt} = & \frac{Q}{V} C_{L,VCin} - \frac{Q}{V} C_{L,VC} - \frac{k_{\max,VC} X C_{L,VC}}{K_{S,VC} \left(1 + \frac{C_{L,cDCE}}{K_{I,cDCE}} + \frac{C_{L,TCE}}{K_{I,TCE}} \right) + C_{L,VC}} \\ & + \frac{k_{\max,cDCE} X C_{L,cDCE}}{K_{S,cDCE} \left(1 + \frac{C_{L,TCE}}{K_{I,TCE}} \right) + C_{L,cDCE}} \end{aligned} \quad (10)$$

Where Q is the volumetric flow rate (mL/day), and V is the reactor volume (mL), and $C_{L,VCin}$ is the VC concentration in the influent. In this reactor, $C_{L,VCin}$ is zero, while $C_{L,TCEin}$ was approximately 7.4 mM. Similar expressions can be used for TCE and cDCE dechlorination.

CFSTR biomass change can be modeled by modifying Equation 2 as follows.

$$\frac{dX}{dt} = \frac{Q}{V} X_{in} - \frac{Q}{V} X + Y \sum_i \frac{dC_i}{dt} - k_d^* X \quad (11)$$

Where X_{in} would be biomass concentration introduced in the influent, which was zero for these experiments.

The above biomass CFSTR equation has been expanded to a simplified RPC model by the incorporation of a fraction of biomass suspended, to account for sloughing of cells, as follows.

$$\frac{dX}{dt} = \frac{Q}{V} X_{in} - \frac{Q}{V} X f_s + Y \sum_i \frac{dC_i}{dt} - k_d^* X \quad (12)$$

Where f_s represents the fraction of cells suspended, assumed to be 0.15, which means only 15% of cells in the reactor are subject to loss by advection from the system, while the remaining biomass is retained. Measured cell sloughing in a laminar tube reactor during steady operation has been reported in the range of approximately 10 to 25% (Telgmann et al., 2004). Note that this modeling approach does not treat the reactor specifically as a biofilm system, but more as a retentostat with a fraction of cell advection. Because this system was operated with high cDCE and TCE concentrations, it has been assumed that the biofilm would be fully penetrated, thus simplifying modeling significantly by omitting biofilm thickness and diffusion considerations. This

simplifying assumption also allows us to model the dechlorination kinetics for the RPC with the same equations used to describe the CFSTR.

A summary of kinetic modeling parameters and values for batch, CFSTR, and RPC models utilized in the study are supplied in Table 4.2. Simple adjustment of X biomass alone in simulations was insufficient in fitting data under lower concentrations where toxicity is not expected. Some k_{\max} parameters were therefore adjusted from original values reported by Yu and Semprini (2004) due to apparent shifts in culture performance, as can occur with multiple culture transfers over many years of maintenance. All models were constructed and solved using the STELLA® v.9.0 software (isee systems, inc.)

RESULTS AND DISCUSSION

Batch-fed Reactors: cDCE accumulation results from batch reactors fed repeated doses of TCE are presented in Figure 4.3. The two different cultures, EV-cDCE and PM exhibited different rates of cDCE accumulation and levels at which dechlorination of TCE to cDCE ceased. The PM culture produced cDCE to a greater extent early on, but was unable to dechlorinate TCE to as high of cDCE concentrations as the EV-cDCE culture before TCE dechlorination ceased. Error bars of the triplicate reactors, representing one standard deviation of CAH measurements indicate the two cultures had significant differences in their cDCE accumulation rates and tolerance to inhibition or toxicity. VC and ETH were not detected in the EV bottles, and VC and ETH in the PM bottles were never detected above 230 and 0.9 μM , respectively and have therefore not been plotted. TCE concentrations in all reactors, generally maintained between 100 and 600 μM , also have not been plotted due to extensive fluctuations associated with daily additions (up to 800 μM maximum) and removal by dechlorination activity.

cDCE accumulation data for each culture are plotted in Figures 4.4a and 4.4b with three possible models to account for observations. Data are plotted against standard Michaelis-Menten kinetics including competitive inhibition as depicted in Equation 3, Haldane-like inhibition by cDCE on TCE dechlorination as depicted in Equation 7, and enhanced decay toxicity as depicted in Equation 8 combined with the Michaelis-Menten kinetics of Equation 3. All three models were calibrated by adjusting the initial X and $k_{\max, \text{TCE}}$ to fit the early rate of cDCE accumulation observed between days 8 and 22 of operation, with the Haldane-type ($K_{\text{h-cDCE}}$) or toxicity ($K_{\text{t-cDCE}}$) terms being adjusted after fixing those variables. These and other parameter values used in the models are summarized in Table 4.2. Only the $k_{\max, \text{TCE}}$, $k_{\max, \text{cDCE}}$, and $k_{\max, \text{VC}}$ parameters were adjusted from Yu and Semprini's previously culture characterizations (2004). All other previously derived kinetic parameters (Yu and Semprini, 2004) were used for this study.

The standard Michaelis-Menten curves in Figures 4.4a and 4.4b were obtained with Equation 3, by modeling unlimited continuous TCE addition to illustrate the rate of cDCE production the reactors should have been capable of in the absence of any

inhibition by cDCE on TCE dechlorination. In reality, TCE was added on an “as needed” basis to prevent TCE buildup and avoid the need to determine if inhibition were due to cDCE or TCE increases. The standard Michaelis-Menten kinetics (Equations 3 through 5) fit to early dechlorination data indicates dechlorination kinetics, including energy yield-based growth and an endogenous decay rate of 0.024 day^{-1} (Yu and Semprini, 2004) could account for observed increases in dechlorination activity up to cDCE concentrations of 2 mM and 22 days for the EV culture (Figure 4.4a), and 3.6 mM for the PM culture (Figure 4.4b) for 14 days. However, continued growth without inhibition did not occur, since the rate of cDCE accumulation and TCE dechlorination theoretically should have accelerated to the extent illustrated in the simple Michaelis-Menten curves were this the case.

The Haldane-like inhibition curves were obtained by adjusting the $K_{h,\text{cDCE}}$ term to fit the slopes of cDCE formation observed between days 22 and 46 for the EV culture (Figure 4.4a), and days 15 and 35 in the PM culture (Figure 4.4b). Good fits were obtained for these time periods, but the Haldane-type inhibition model failed to capture the virtual cessation of dechlorination observed after day 50 in both cultures. One reason for this lack of fit in the later data is that, although the Haldane-like model could reduce the dechlorination rate as cDCE increased, much predicted biomass had accumulated during the 50 days of modeled dechlorination with this scenario, requiring much more time for cell numbers to decay low enough to reflect the stoppage of TCE dechlorination. It therefore would take hundreds of days to reduce modeled cell numbers to bring dechlorination of TCE to a virtual halt. Modifying the $K_{h,\text{cDCE}}$ coefficients to cause cessation of cDCE production at the levels observed (approximately 9 mM for PM and 12 mM for EV), resulted in much slower buildup of cDCE compared to the rate of accumulation observed between days 20 and 50. It should be noted that traditional competitive, uncompetitive, and non-competitive models for cDCE on TCE dechlorination were tested as well, but failed to provide fits to the data for similar reasons described for the Haldane-type inhibition models. The Haldane-type model, with

inhibition proportional to the square of cDCE concentration was the best fitting inhibition model tested and is therefore the only inhibition model presented.

The enhanced decay toxicity model fits the data from both cultures very closely with standard Michaelis-Menten kinetics and the incorporation of the extra decay term describe in Equation 8 (Figures 4.4a and 4.4b). Incorporation of Haldane terms for cDCE and TCE previously derived by Yu et al. (2004) had little impact in the model, indicating that the enhanced decay term was dominating the response. $K_{t,cDCE}$ values supplied in Table 4.2 for the batch experiments were based upon the assumption of no Haldane inhibition per Yu and Semprini (2004). Incorporation of the $K_{I,H-TCE}$ term did require increasing the $K_{t,cDCE}$ toxicity term by approximately 20% to fit cDCE accumulation data. Note that because there was essentially no dechlorination past cDCE, inclusion of Haldane coefficients $K_{I,H-cDCE}$ and $K_{I,H-VC}$ have no impact on the model outcome. The models fit to observed thresholds in cDCE produced was highly sensitive to the $K_{t,cDCE}$ term. Because TCE levels were maintained below 800 μM throughout the experiment, no $K_{t,TCE}$ term was added to these batch experiment models.

The $K_{t,cDCE}$ values used to fit observed cDCE accumulation rates were 800 μM for the EV culture and 710 μM for the PM culture (Table 4.2). These resulted in a k_d^* of 0.43 day^{-1} for the EV culture by day 50 when cDCE concentrations were approximately 12,000 μM , and a k_d^* of 0.31 day^{-1} by day 50 for the PM culture, when the cDCE concentration was approximately 8600 μM . The endogenous decay coefficient, k_d , for both of these cultures has previously been successfully modeled as 0.024 day^{-1} (Yu et al., 2004), indicating that decay was 13 to 18 times higher due to the presence of cDCE at 8 to 12 mM concentrations. Reported k_d values for reductively dechlorinating, and other anaerobic cultures have ranged from 0.024 day^{-1} to 0.05 day^{-1} for active cells, and 0.09 day^{-1} during non-growth conditions (Yu et al., 2004; Fennell and Gossett, 1998; Lee et al., 2004; Cupples et al., 2003; Sotemann et al., 2005; Lee et al., 2008). Elevated cellular decay coefficients similar to our modeled values have been reported previously, however. First order decay coefficients in the presence of approximately 8 mM cDCE were

estimated to be 0.1 to 0.14 day⁻¹ for two different reductively dechlorinating cultures (Chu, 2004).

CFSTR: The enhanced decay model that fit batch cDCE accumulation experiments was then utilized to fit the CFSTR CAH monitoring data (Figure 4.5). The Haldane inhibition model developed by Yu and Semprini (2004) is also provided in Figure 4.5, which did not fit the CFSTR data. Initial TCE concentrations correspond to inoculation with TCE in zero-flow mode, followed by a brief operation at an inflow rate of 28 mL/day leading to TCE buildup, after which time the flow was adjusted to 18mL/day starting on day 6. From days 8 to 31 of operation, with a 16.8-day retention time, the CFSTR maintained nearly complete dechlorination of TCE to cDCE, with no detectable VC or ETH, and only traces of TCE generally below 12 µM. TCE began to increase after day 31, and the reactor was operated in stop-flow mode from days 50 to 56 until TCE was reduced below 110 µM. Pumping was resumed for one day with the 16.8-day retention time, but increased TCE was observed in the effluent, and the rate was then reduced to produce a retention time of 25.3 days. TCE continued to increase in the effluent as pumping was maintained, and pumping was stopped after day 85 to determine if the reactor would recover performance as it had during stop-flow initiated on day 50. No observable dechlorination was measured from day 85 to 98, and the experiment was terminated.

Though the batch experiments maintained relatively low TCE concentrations as cDCE accumulated, TCE accumulated in the CFSTR. Other research has shown an increase in toxic effects to reductively dechlorinating cultures with high cDCE concentrations in the presence of as little as 39 µM PCE (Chu, 2004). Chu proposed that PCE, and possibly TCE are both toxic, and that the degree of toxicity is proportional to the solvents' octanol-water coefficients. We therefore added a second toxicity term, $K_{t,TCE}$, corresponding to TCE effects in the enhanced decay term, k_d^* , as described in Equation 8.

The CFSTR model, including transient operating conditions, was based upon expanded Michaelis-Menten kinetics (as shown in Equation 10), including the cDCE toxicity term, $K_{t,cDCE}$, plus the TCE toxicity term, $K_{t,TCE}$, as shown in Equation 8, but

excluding the TCE Haldane inhibition coefficient, $K_{I,H-TCE}$. The CFSTR model was calibrated by first matching the initial biomass (X) and $k_{max,TCE}$ to the observed dechlorination between days 0 and 3 during initial no-flow conditions. Flow changes were included in the model, and a constant TCE influent concentration of 8900 μM was assumed to maintain a mass balance consistent with effluent CAH measurements. The $K_{t,cDCE}$ term was then adjusted to fit the observed TCE accumulation and cDCE decline beginning after day 56.

The $K_{t,TCE}$ toxicity term was then heuristically adjusted to supply a good fit to the TCE increase and cDCE decrease observed after day 90, as well as the transient TCE increase observed between days 30 and 90. Exclusion of the $K_{t,TCE}$ term failed to predict the transient TCE peak from days 30 to 90. The simulation also resulted in reasonable fits with the transient TCE spikes observed starting on days 4 and 32 of reactor operation. It is interesting to note that the ratio of $K_{t,cDCE}:K_{t,TCE}$ in this model is 5.0, similar to the ratio of K_{ow} for TCE:cDCE (3.6). This is consistent with Chu's hypothesis that CAH effective concentrations at the cell wall impact toxicity (2004). In Chu's research, CAH concentrations at the cell membrane were estimated from aqueous cDCE, TCE, and PCE concentrations, and the K_{OW} values. Chu found dechlorination activity ceased under varying concentrations of predominantly cDCE and PCE, but under nearly identical estimate cell membrane CAH concentrations. Note the $K_{t,cDCE}:K_{t,TCE}$ ratio is reversed because the toxicity coefficients are expressed as inverse (μM^{-1}) values in the toxicity model.

The batch experiment models resulted in similar outcomes with or without the inclusion of Haldane inhibition coefficients determined by Yu and Semprini (2004). The CFSTR model could not fit the observations with incorporation of Yu and Semprini's TCE Haldane coefficient, in addition to the $K_{t,cDCE}$ and $K_{t,TCE}$ terms. Addition of TCE Haldane inhibition to the toxicity model could produce the ultimate reactor failure observed after day 55 and the initial transient TCE peak from days 2 to 8, but could not produce the large TCE transient peak observed between days 30 and 90 (Figure 4.5). Best fits with Yu and Semprini's Haldane coefficients plus either $K_{t,cDCE}$ alone or both

$K_{t,cDCE}$ and $K_{t,TCE}$ are supplied in supplemental Figure C2. As with the batch experiments, because there was essentially no dechlorination past cDCE, inclusion of Haldane coefficients $K_{I,H-cDCE}$ and $K_{I,H-VC}$ had no impact on the model outcome.

RPC: The RPC CAH monitoring data and the enhanced decay model are displayed together in Figure 4.6. Dechlorination of TCE to cDCE with no detectable VC or ETH, and only traces of TCE below 41 μM was maintained from days 9 to 78. A spike of TCE to 1280 μM was observed on day 79, associated with a minor pumping problem, which was removed to below 18 μM by day 82 under resumed normal operation. At day 101, the influent pump rate was increased to 12 mL/day to shift operation from an 11.8-day hydraulic residence time to a 5.9-day residence time. TCE began to increase in the effluent, remained relatively constant between 894 and 1350 μM from day 103 to 127, but then sharply increased as cDCE concentrations rapidly decreased from days 127 to 155, when the experiment was terminated.

Parameters used for the RPC model are summarized in Table 4.2. The RPC model was first calibrated by establishing the $k_{\max,TCE}$ and X that fit initial TCE dechlorination observed between days 5.7 and 9.6. Due to mass balance complications with early data, these parameters were used as starting values of the model run from days 16 to 160. The $K_{t,cDCE}$ term was then adjusted until the rate of increase in simulated TCE between days 97 and 105 matched the experimental observations. No adjustments of $K_{t,cDCE}$ alone in the model was able to predict the observed plateau of TCE concentrations observed from days 103 to 127 or the ultimate buildup of TCE and flushing of cDCE, beginning on day 128. Adjusting the $K_{t,cDCE}$ parameter alone either resulted in a transient spike of TCE that returned to negligible concentrations by day 110, or predicted premature reactor failure (beginning at day 99) compared to the data. The $K_{t,TCE}$ term was therefore included and adjusted to best fit the observed plateau and subsequent buildup of TCE, accompanied by flushing of cDCE from the RPC (Figure 4.6). Note the ratio of $K_{t,cDCE}:K_{t,TCE}$ for the RPC model (values supplied in Table 4.2) is 3.7, nearly identical to the K_{ow} ratios, suggesting good agreement with the hypothesis that degree of toxicity is proportional to concentrations at the cell wall (Chu, 2004).

To confirm failure of the RPC, which was shortly after increasing flows from 6 mL/day to 12 mL/day, was due to CAH toxicity and not possible increased advection of cells, the fraction of cells suspended (f_s of Equation 12) was modified in the model up to 0.5. This produced little effect on modeled performance when included simultaneously with $K_{t,cDCE}$ and $K_{t,TCE}$ terms, and did not result in failure of the simulated RPC in the absence of the toxicity terms until adjusted above 0.85.

The RPC model did not fit the data well when including the TCE Haldane inhibition coefficient, $K_{I,H-TCE}$, derived by Yu and Semprini (2004). $K_{t,cDCE}$ and $K_{t,TCE}$ values of 4250 and 1590 μM , respectively could produce RPC failure after day 100 with the simultaneous inclusion of the $K_{I,H-TCE}$ term, but no values for $K_{t,cDCE}$ and $K_{t,TCE}$ were found that could produce the observed plateau of TCE concentrations between days 103 and 131 in the RPC monitoring data. Increasing the $K_{I,H-TCE}$ (or decreasing the sensitivity to Haldane inhibition) in model simulations did have the effect of broadening the TCE plateau observed in the simulation between days 103 and 127, indicating that reducing TCE dechlorination rates via Haldane inhibition quickly causes TCE to buildup, further exacerbating the loss of activity, but decreasing the Haldane effect (or increasing the Haldane coefficient) reduces the rapid shutting down of TCE dechlorination as TCE increase. The toxicity model, however, allows for continued maximum TCE dechlorination rates with the sudden initial TCE increase, but results in increased decay of active cell mass to produce the transitory TCE plateau as cells are both growing from dechlorination energy but decaying from TCE and cDCE combined exposure.

CONCLUSIONS

That model fits could not be found with inclusion of $K_{I,H-TCE}$ for the RPC or CFSTR may be an indication that the proposed toxicity model more accurately reflects the effects of high CAH concentrations long term than a Haldane inhibition model. It is possible that a combination of inhibition and toxicity were experienced by the cultures tested, though the assumption of Haldane inhibition combined with the proposed toxicity model did not produce better model fits to the experimental data. Model fits in the batch-fed systems also excluded TCE Haldane inhibition, but TCE was maintained at fairly low concentrations to negate possible TCE impacts in the batch studies. The proposed toxicity model produced K_t values in the different systems, from low to high: batch-fed < CFSTR < RPC (attached growth). This suggests batch-fed cells were the most sensitive, followed by the CFSTR grown cells, with attached cells in the RPC being the least sensitive. This compares well with other observations of increased resistance often found in chemostat cells compared to batch-fed cells (Chang and Alvarez-Cohen, 1996; Qu, and Bhattacharya, 1997; Piringer and Bhattacharya, 1999), and in attached growth cells compared to suspended cells (Harrison et al., 2007; Stewart and Costerton, 2001; Walters et al., 2003).

The inhibition and toxicity of high CAH concentrations is still not fully understood. Inhibition models could not account for observed loss of dechlorination activity in the systems studied. Inclusion of the enhanced decay toxicity model was able to reflect batch, CFSTR, and RPC data, however. Future work is required to more directly test the conceptual toxicity model proposed in this study.

ACKNOWLEDGEMENTS

Funding for this research was provided by NSF Integrative Graduate Education and Research Traineeship Program (IGERT), U.S. EPA Western Region Hazardous Substance Center (Grant # R-828772), and National Institute of Environmental Health Sciences (Graduate Training Grant #1P42 ES10338). This article has not been reviewed by the above agencies and no endorsement should be inferred.

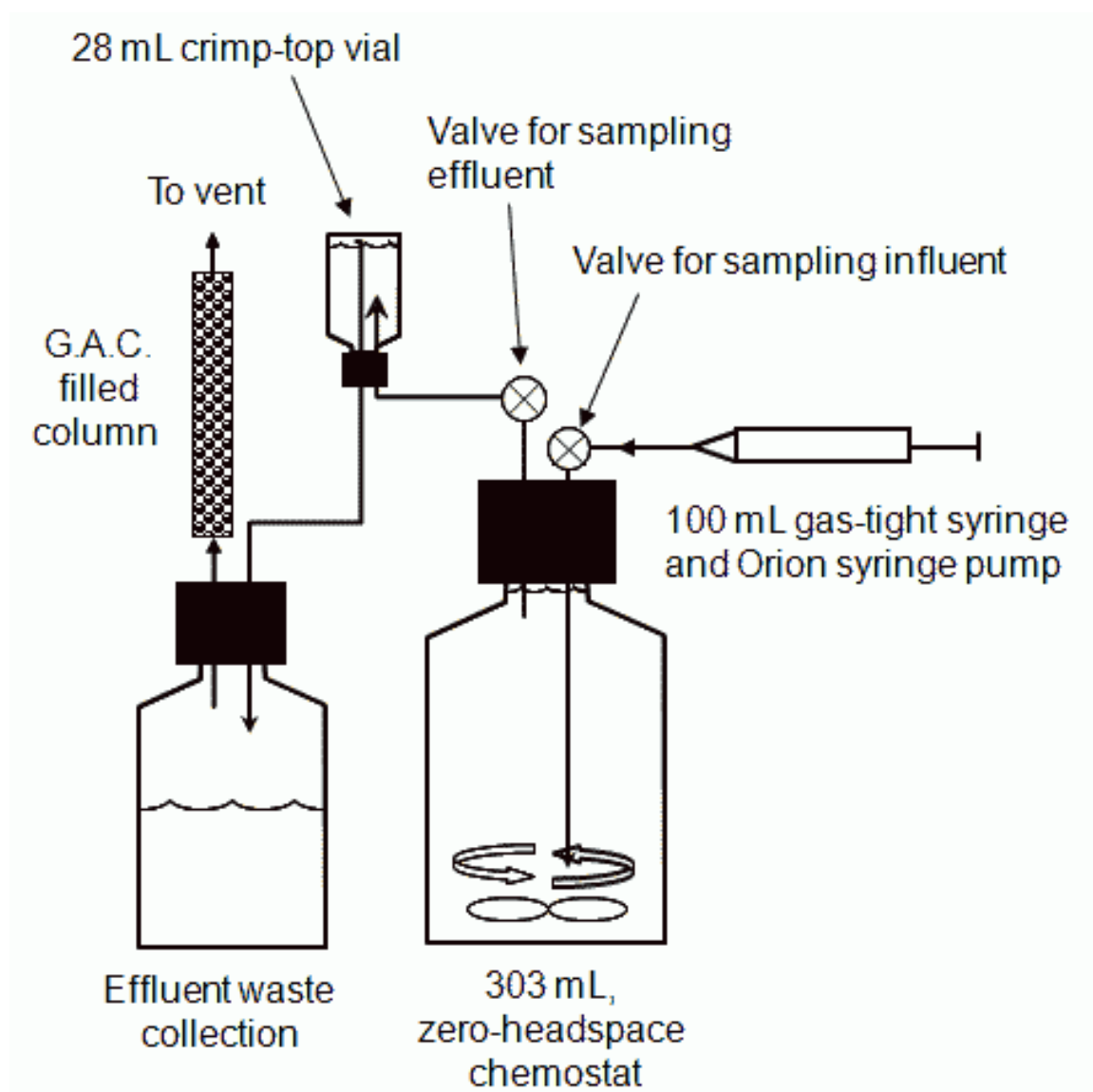


Figure 4.1. CFSTR schematic diagram. Not to scale.

Table 4.1. CFSTR pumping conditions.

Days of operation	Pumping rate (mL/day)	Residence time (days)
0-3	0	--
4-5	28	10.8
6-49	18	16.8
50-55	0	--
56	18	16.8
57-84	12	25.3
85-99	0	--

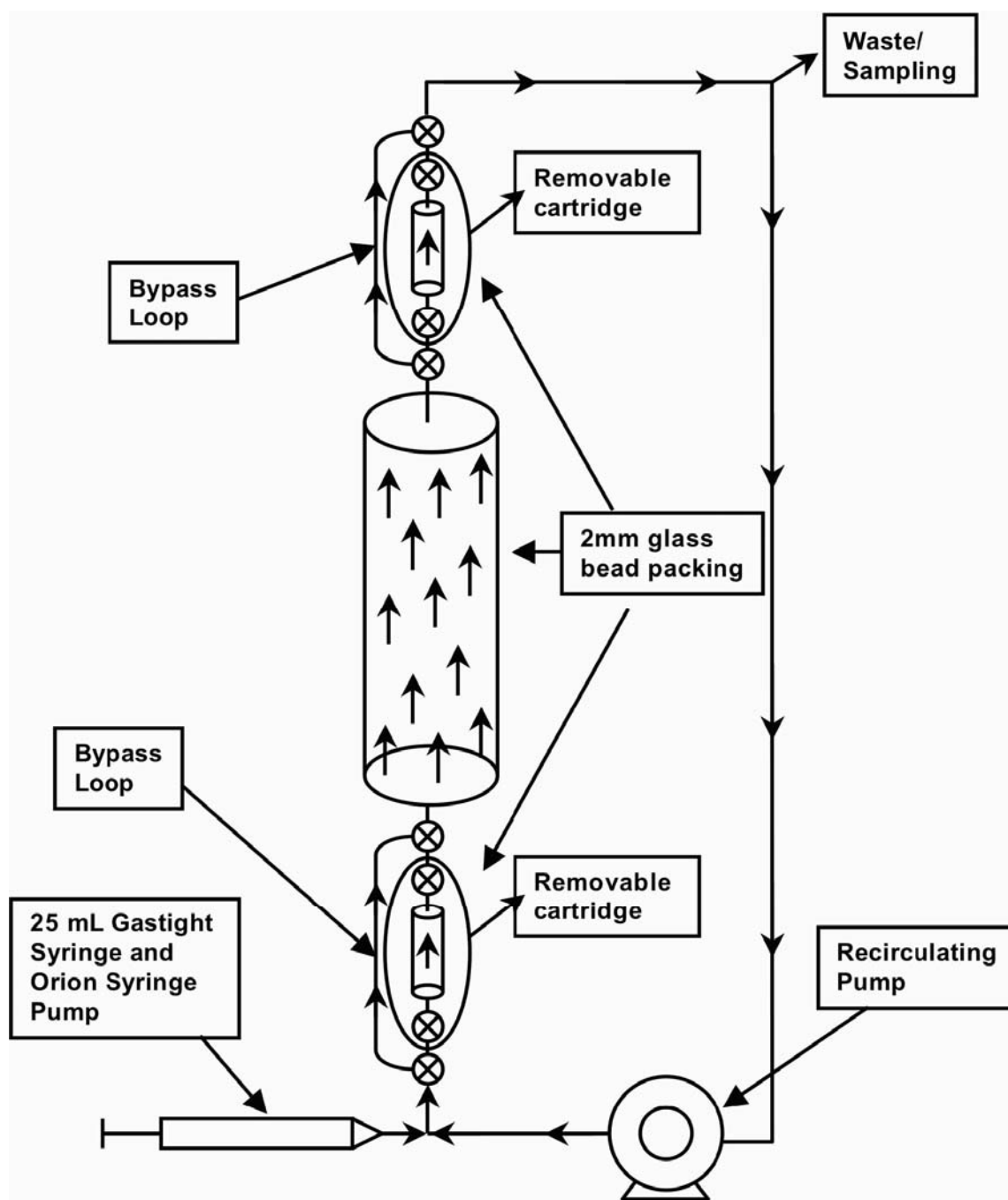


Figure 4.2. RPC schematic diagram. Not to scale.

Table 4.2. Model kinetic parameters for batch, CFSTR, and RPC simulations.^a

Parameter	PM-batch	EV-batch	EV-CFSTR	EV-RPC
$k_{\max, \text{TCE}}$ ($\mu\text{mol}/\text{mg protein}/\text{day}$)	23	28	28	28
$k_{\max, \text{cDCE}}$ ($\mu\text{mol}/\text{mg protein}/\text{day}$) ^b	2	0.0000001	0.0000001	0.0000001
$k_{\max, \text{VC}}$ ($\mu\text{mol}/\text{mg protein}/\text{day}$)	2.4	8.1 ^b	8.1 ^b	8.1 ^b
$K_{\text{s}, \text{TCE}}$ (μM) ^c	2.8	1.8	1.8	1.8
$K_{\text{s}, \text{cDCE}}$ (μM) ^c	1.9	1.8	1.8	1.8
$K_{\text{s}, \text{VC}}$ (μM) ^c	602	62.6	62.6	62.6
$K_{\text{I}, \text{H-TCE}}$ (μM) ^b	9999999	9999999	9999999	9999999
$K_{\text{I}, \text{H-cDCE}}$ (μM) ^c	6000	750	750	750
$K_{\text{I}, \text{H-VC}}$ (μM) ^c	7000	750	750	750
$K_{\text{h-cDCE}}$ (μM) ^d	400	3500	N/A	N/A
$K_{\text{t}, \text{TCE}}$ (μM)	N/A	N/A	400	770
$K_{\text{t}, \text{cDCE}}$ (μM)	710	800	2020	2600
X_0 (mg protein/L)	2.4	0.8	22.5	20

^aAny culture parameters not supplied, including competitive inhibition and yield coefficients, are as reported previously for PM and EV cultures (Yu and Semprini, 2004). ^bValue of 0.0000001 or 9999999 indicates parameter excluded from model fit to data. ^cSame values as reported by Yu and Semprini (2004). ^dParameters only evaluated in batch experiments. N/A indicates a parameter not incorporated in the model.

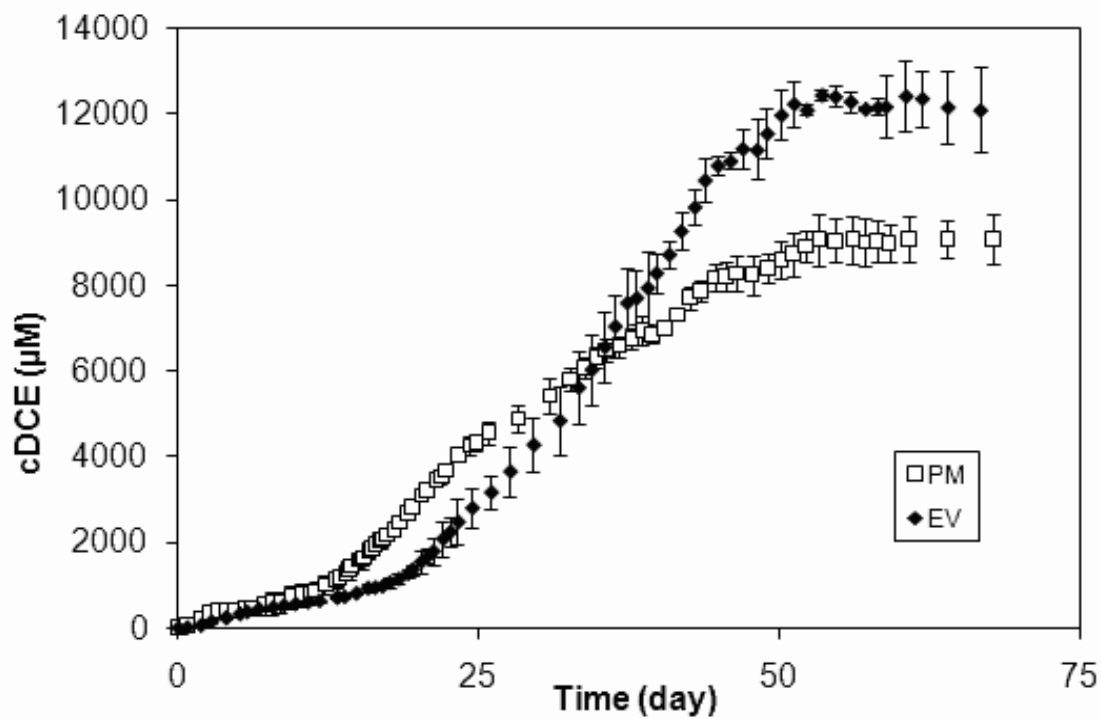


Figure 4.3. Difference in cDCE accumulation in TCE batch-fed reactors for the PM and EV cultures. Symbols are for monitoring data as indicated in the legend. Error bars represent one standard deviation of triplicate analyses.

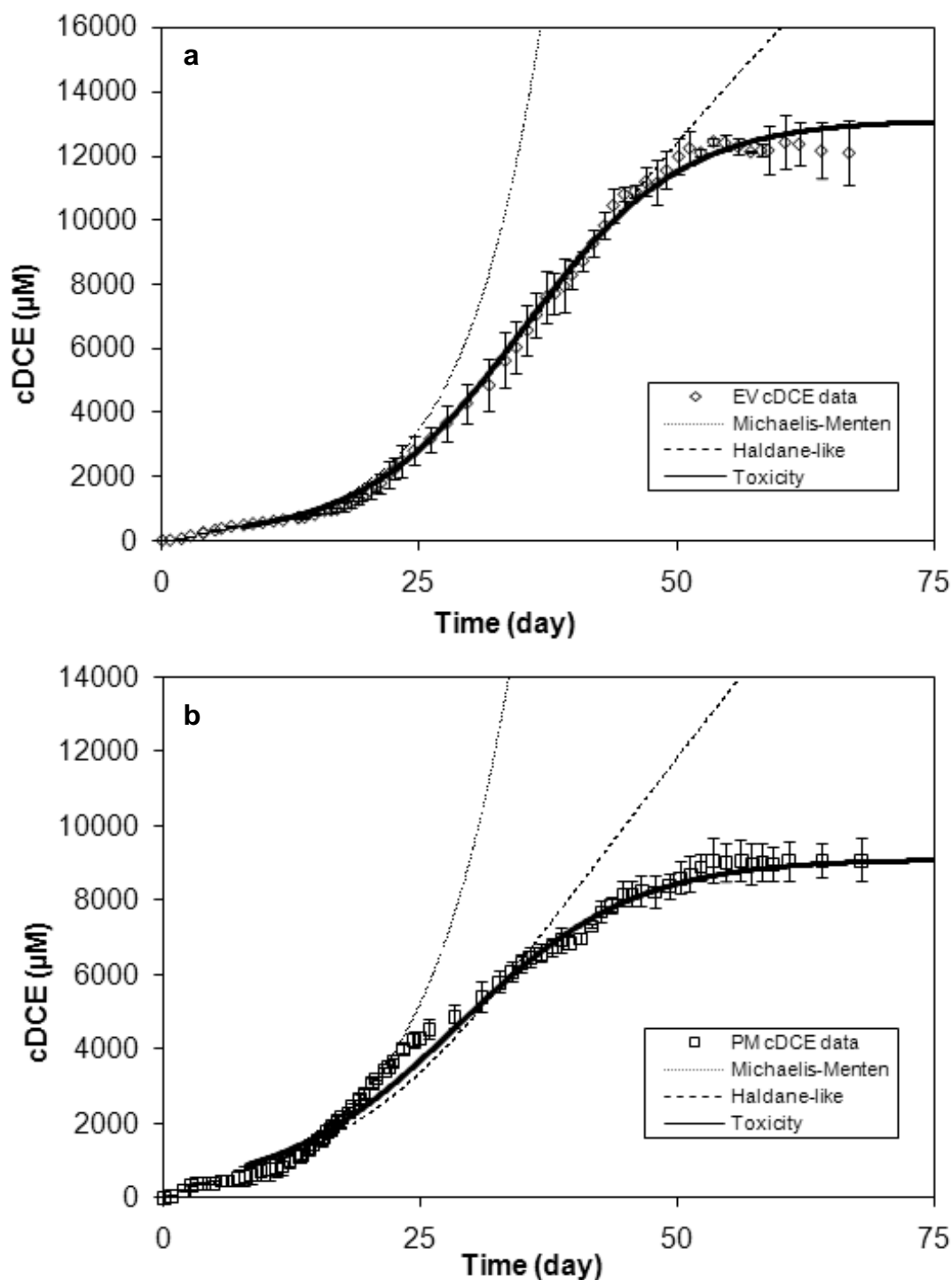


Figure 4.4. Modeled cDCE accumulation in batch-fed reactors. a) the EV-cDCE subculture, and b) the PM culture. Symbols are data and lines are from models as indicated in legends.

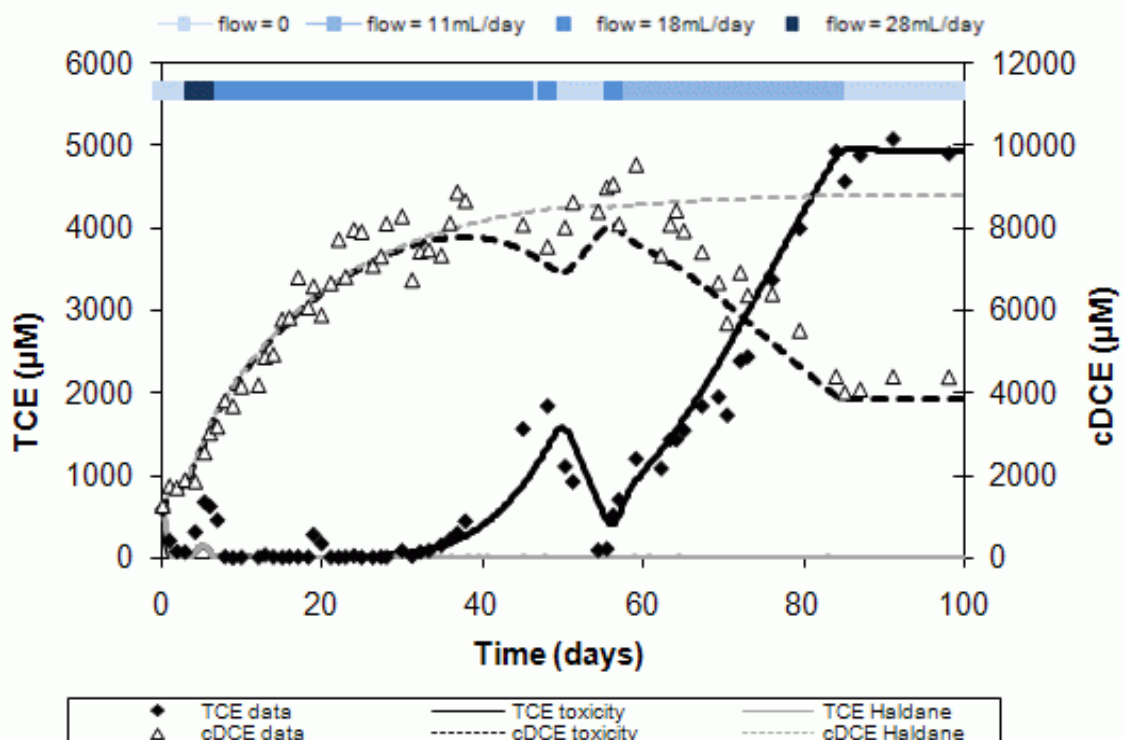


Figure 4.5. CAH monitoring data for the CFSTR with fitted cDCE and TCE concentration-dependent toxicity model and previously proposed Haldane inhibition model. Black lines are produced by the toxicity model, and gray lines are produced by the Haldane model. Both models of TCE concentrations overlap at the transient peak between days 2 and 8, with the Haldane model showing complete removal of TCE after day 8. Note the different scales for TCE and cDCE concentrations.

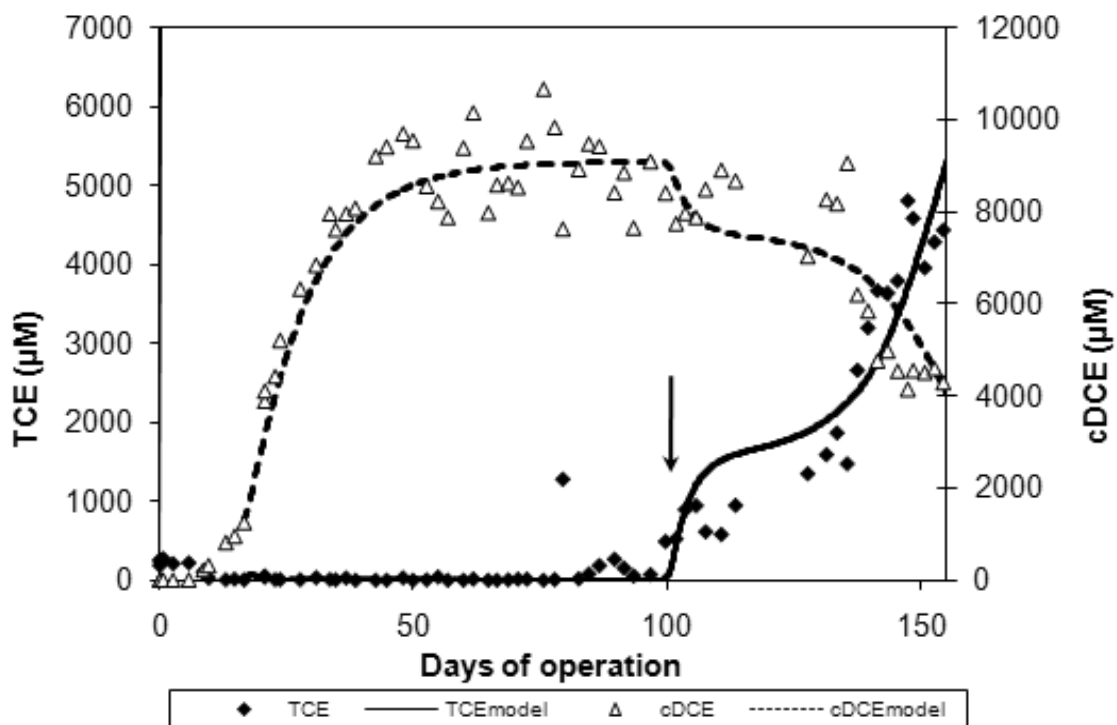


Figure 4.6. CAH monitoring data for the RPC with fitted cDCE and TCE concentration-dependent toxicity model. Arrow indicates pumping increased from 6 mL/day to 12 mL/day on day 101. Note the different scales for TCE and cDCE concentrations.

Chapter 5

Summary and Engineering Significance

Summary

Little is known about how dehalogenating community composition and capabilities shift in time, especially within continuously fed suspended growth systems. Different electron donor supplies have been utilized in field remediation practices (Rahm et al., 2006a; Lee et al., 2008; Major et al., 2002; Lowe et al., 2002), and batch comparisons of culture capabilities using different electron donors have been made, but little is known about how community capabilities shift temporally as a result of continuous steady enrichment on different electron donors. Though a few studies have evaluated shifts in reductase gene quantity profiles after enrichment with different CAHs (Holmes et al., 2006; Ritalahti et al., 2006; Sung et al., 2006b), there appears to be no continuous tracking of reductase quantity profiles to assess how communities shift as a result of conditions created by different electron donor or CAH continuous enrichments. Additionally, there is the need to better understand culture responses to the long-observed problem of high CAH inhibition or toxicity (Yang and McCarty, 2000; Duhamel et al., 2002; Chu, 2004; Adamson et al., 2004).

Results from this work have increased our understanding of the relationships between conditions applied, community composition, community performance, and the ways such parameters can be measured. Regarding effects of electron donors, it was shown that: 1) formate supplied longer and more complete dechlorination of TCE than lactate in the CFSTRs, 2) formate better maintained proportions of *Dehalococcoides* in the community than lactate, and 3) formate better supported growth of a population containing the *vcrA* gene, associated with cDCE and VC dechlorination, while lactate better supported a *tceA*-containing population. One likely reason for the differences in formate- and lactate-fed reactors treating TCE was unavailability of H₂ due to propionate accumulation. Regarding CAH enrichment effects in CFSTRs, it was shown that: 1)

TCE supported a greater amount of *Dehalococcoides* and *Bacteria* than VC, 2) VC did not maintain a substantial *Dehalococcoides* population with the 12.5-day retention time applied, and 3) within the *Dehalococcoides* population of the VC-fed reactor, formate and VC did promote *vcrA* dominance, and switching to TCE ultimately increased *tceA* presence. qPCR analyses of reductases in the CFSTRs also showed the likelihood of two different *Dehalococcoides* populations: one containing only the *tceA* gene, and one likely containing both the *vcrA* and *pceA* genes, though not the *tceA* gene. Such a distinction in culture composition could not be made with single time-point analysis. Additionally, modeling and experimental results from this work have supplied several tools for potential use in remediation design and implementation. Specifically, it was shown that: 1) temporally distributed short-term batch kinetic tests closely reflected transient performance in the continuous systems from which the cells were harvested, 2) qPCR analysis of *Dehalococcoides* 16S rRNA genes can correlate to and predict cDCE and VC dechlorination rate potential, and 3) modeling high cDCE and TCE effects as concentration-dependent toxicity can simulate observed declines in dechlorination activity.

Engineering Significance

This work has shown that two electron donors which both rapidly produce hydrogen produce quite different results in continuously fed suspended growth systems. In the CFSTRs tested, formate supplied greater longevity and degree of completeness for dechlorination activity. Formate also maintained proportions of *Dehalococcoides* better throughout operation. The likely reason for the differences in performance and community composition was the incomplete fermentation, with the slow-fermenting propionate accumulating that represents a large amount of hydrogen formation potential (3 moles of H₂ per mole of propionate fermented to acetate). The buildup of propionate in the lactate-fed CFSTR is important to consider, and highlights the importance of both maintaining relevant fermentation populations, and contact time for reaction. Different microbial communities may be adapted to propionate utilization, and attachment to aquifer materials can avoid complications associated with CFSTR cell washout.

However, propionate formation from lactate fermentation in the presence of incomplete dechlorination (CAH daughter products) has been observed in laboratory attached growth systems, as well as field operations (Adamson et al., 2003; Azizian et al., 2008; Rahm et al., 2006a). Because propionate ferments slowly and can be a significant product of lactate fermentation (Heimann et al., 2007; Fennell et al., 1997; Aulenta et al., 2006), contact time for propionate fermentation can therefore be an important issue in field remediation, and dechlorination to lower degrees than anticipated can result as propionate migrates with groundwater flow while fermentation rates are insufficient to release H_2 in the CAH contamination zone.

Formate dehydrogenation is a rapid process by which hydrogen is formed with no hydrogen-rich intermediate products, and formate dehydrogenase enzymes are ubiquitous (e.g. as summarized in Popov and Lamzin, 1994). Formate therefore represents a potentially valuable electron donor source for field operations. Possible disadvantages of formate utilization are fostering growth of homoacetogens, and further acidification resulting from acetogenesis. However, the use of formate in this CFSTR study not only maintained *Dehalococcoides* populations in greater proportions and for longer duration, but also resulted in domination by the *vcrA* gene within the *Dehalococcoides* community. This is an important result because it is one of only two genes presently known to be associated with production of an enzyme capable of reductive dechlorination of cDCE or VC (as summarized in Daprato et al., 2007).

Additionally, batch-measured maximum dechlorination rates were shown to closely reflect continuous reactor performance. As CFSTR dechlorination performance declined, with increases in effluent CAH concentrations, batch-measured rates of harvested cells also declined. Conversely, as CFSTR performance improved, with reduced effluent CAH concentrations, batch-measured rates increased. Such comparability in continuous culture performance and batch-measured assessments demonstrates the utility and accuracy of simple batch measurements. The implications of the comparability are that differences in short-term batch measured rates from different sampling locations at a contaminated site, for instance, are likely representative of real

differences in dechlorination capabilities, as opposed to experimental noise (Lendvay, et al., 2003; Azizian et al., 2002). Such information can be important when trying to optimize field remediation strategies.

Batch measured cDCE and VC dechlorination rates from this study correlated very well with the *Dehalococcoides* 16S rRNA gene quantities, regardless of which reductase gene dominated the systems. Different *Dehalococcoides* strains contain different sets of dehalogenases, as demonstrated by Behrens et al. (2008). It is therefore important, to determine that a relevant reductase gene for cDCE and VC dechlorination is present, such as the *vcrA* gene quantified in all CFSTRs, if one is to make predictions with only the *Dehalococcoides* 16S rRNA gene. Because reductase gene expression levels can vary by up to four orders of magnitude (Johnson et al., 2005; Lee et al., 2006), it is possible that the mere presence of relevant dehalogenase genes is sufficient to overwhelm differences in multiple *Dehalococcoides* populations, thereby allowing dechlorination rate predictions with simple *Dehalococcoides* 16S rRNA gene quantification.

The ability to predict dechlorination rate potential is important in estimating the time of treatment, as well as in determining rate limiting factors, such as insufficient organisms, insufficient electron donors, or insufficient contact. In this study, qPCR DNA quantification was more sensitive than batch-measured rates. DNA quantification therefore can potentially demonstrate remediation potential at a site exists, in the absence of appreciable observed rates on site or in site-derived microcosms, as has been shown previously (Lu et al., 2006). Such information can be important in deciding between biostimulation or bioaugmentation, which can substantially impact remediation costs. If observable rates and confirmed relevant organism quantities can be confirmed, no further action may be required in a natural attenuation scenario.

While the ability to predict dechlorination rates is important, understanding and predicting lack of activity can be equally important. Reduced activity due to high CAH concentrations has been previously observed in numerous studies (Yang and McCarty, 2000; Duhamel et al., 2002; Chu, 2004; Adamson et al., 2004). Our work has

demonstrated reduced TCE dechlorination in the presence of high CAH (cDCE and/or TCE) concentrations, in three different modes of growth: batch-fed suspended, continuously fed suspended, and continuously fed attached growth. Performances in these systems could not be adequately described by traditional inhibition models. However, temporal observations in all three systems could be successfully simulated using a single model that incorporated cDCE and TCE concentration-dependent toxicity terms that directly increased the cell decay coefficient. It is possible that other forms of inhibition also occur, or other unknown factors contribute to reduced activity. However, the single model to describe decreased activity, even if perhaps mechanistically inaccurate, had the ability to simulate the observed responses where CAHs accumulated simultaneously with decreases and eventual cessation of dehalogenation activity. Being able to determine how dechlorination rates decline with increasing CAH concentrations is of great value in designing remediation strategies, especially since remediating CAHs near the source zone, where the majority of the contaminant mass resides and where concentrations are highest, can potentially reduce remediation time and cost.

Bibliography

- Adamson, D. T., J. M. McDade, and J. B. Hughes. 2003. Inoculation of a DNAPL Source Zone To Initiate Reductive Dechlorination of PCE. *Environmental Science and Technology*, **37**:2525-2533.
- Adamson, D. T., D. Y. Lyon, and J. B. Hughes. 2004. Flux and Product Distribution during Biological Treatment of Tetrachloroethene Dense Non-Aqueous-Phase Liquid.. *Environmental Science and Technology*, **38**:2021-2028.
- Adrian, L., U. Szewzyk, J. Wecke, and H. Görisch. 2000. Bacterial dehalorespiration with chlorinated benzenes. *Nature*, **408**:580-583.
- Aulenta, F., M. Majone, and V. Tandoi. 2006. Review: Enhanced anaerobic bioremediation of chlorinated solvents: environmental factors influencing microbial activity and their relevance under field conditions. *Journal of Chemical Technology and Biotechnology*, **81**:1463–1474.
- Aulenta, F., A. Pera, S. Rossetti, M.P. Papini, and M. Majone. 2007. Relevance of side reactions in anaerobic reductive dechlorination microcosms amended with different electron donors. *Water Research*, **41**:27-38.
- Azizian, M. F., J. D. Istok, and L. Semprini. 2002. Push-pull test evaluation of the in situ aerobic cometabolism of chlorinated ethenes by toluene-utilizing microorganisms. *Water Science and Technology*, **52**:35-40.
- Azizian, M. F., S. Behrens, A. Sabalowsky, M. E. Dolan, A. M. Spormann, and L. Semprini. 2008. Continuous-flow column study of reductive dehalogenation of PCE upon bioaugmentation with the Evanite enrichment culture. *Journal of Contaminant Hydrology*, **100**:11:21.
- Behrens, S., M. F. Azizian, P. J. McMurdie, A. Sabalowsky, M. E. Dolan, L. Semprini, and A. M. Spormann. 2008. Monitoring Abundance and Expression of *Dehalococcoides* sp. Chloroethene Reductive Dehalogenases in a PCE-Dechlorinating Continuous Flow Column. *Applied and Environmental Microbiology*, **74**:5695-5703.
- Carr, C.S., S. Garg, and J.B. Hughes. 2000. Effect of Dechlorinating Bacteria on the Longevity and Composition of PCE-Containing Nonaqueous Phase Liquids under Equilibrium Dissolution Conditions. *Environmental Science and Technology*, **34**:1088-1094.
- Chang, H-L and L. Alvarez-Cohen. 1996. Biodegradation of individual and multiple chlorinated aliphatic hydrocarbons by methane-oxidizing cultures. *Applied and Environmental Microbiology*, **62**:3371-3377.
- Chapelle, F. H., P. M. Bradley, C. C. Casey. 2005. Behavior of a chlorinated ethene plume following source-area treatment with Fenton's reagent. *Ground Water Monitoring & Remediation*, **25**:131-141.

- Chu, M-Y. 2004. Factors controlling the efficiency of bio-enhanced PCE NAPL dissolution. *Ph.D. dissertation*, Department of Civil and Environmental Engineering, Stanford University, Stanford, CA.
- Cope, N. and J. B. Hughes. 2001. Biologically-Enhanced Removal of PCE from NAPL Source Zones. *Environmental Science and Technology*, **35**:2014-2021.
- Cupples, A.M., A.M. Spormann, and P.L. McCarty. 2003. Growth of a *Dehalococcoides*-Like Microorganism on Vinyl Chloride and *cis*-Dichloroethene as Electron Acceptors as Determined by Competitive PCR. *Applied and Environmental Microbiology*, **69**:953-959.
- Cupples, A. M., A. M. Spormann, and P. L. McCarty. 2004. Vinyl Chloride and *cis*-Dichloroethene Dechlorination Kinetics and Microorganism Growth under Substrate Limiting Conditions. . *Environmental Science and Technology*, **38**:1102-1107.
- Cupples, A.M. 2008. Real-time PCR quantification of *Dehalococcoides* populations: Methods and applications. *Journal of Microbiological Methods*, **72**:1-11
- Daprato, R.C., F.E. Löffler, and J.B. Hughes. 2007. Comparative Analysis of Three Tetrachloroethene to Ethene Halorespiring Consortia Suggests Functional Redundancy. *Environmental Science and Technology*, **41**:2261-2269.
- Deborde , C. and P. Boyaval. 2000. Interactions between Pyruvate and Lactate Metabolism in *Propionibacterium freudenreichii* subsp. *shermanii*: In Vivo ¹³C Nuclear Magnetic Resonance Studies. *Applied and Environmental Microbiology*, **66**:2012-2020.
- Dolfing, J. and D.B. Janssen. 1994. Estimates of Gibbs Free Energies of Formation of Chlorinated Aliphatic Compounds. *Biodegradation*, **5**:21-28.
- Drzyzga, O., J. Gerritse, J. A. Dijk, H. Elissen, and J. C. Gottschal. 2001. Coexistence of a sulphate-reducing *Desulfovibrio* species and the dehalorespiring *Desulfotobacterium frappieri* TCE1 in defined chemostat cultures grown with various combinations of sulphate and tetrachloroethene. *Environmental Microbiology*, **3**:92-99.
- Duhamel, M., S. D. Wehr, L. Yu, H. Rizvi, D. Seepersad, S. Dworatzek, E. E. Cox, E. A. Edwards. 2002. Comparison of anaerobic dechlorinating enrichment cultures maintained on tetrachloroethene, trichloroethene, *cis*-dichloroethene and vinyl chloride. *Water Research*, **36**:4193-4202.
- Duhamel, M., K. Mo, and E. A. Edwards. 2004. Characterization of a Highly Enriched *Dehalococcoides*-Containing Culture That Grows on Vinyl Chloride and Trichloroethene. *Applied and Environmental Microbiology*, **70**:5538-5545.
- Ellis, D. E., E. J. Lutz, J. M. Odom, R. J. Buchanan, Jr., C. L. Bartlett, M. D. Lee, M. R. Harkness, K. A. DeWeerd. 2000. Bioaugmentation for Accelerated In Situ Anaerobic Bioremediation. *Environmental Science and Technology*, **34**:2254-2260.

- Ensley, B.D. 1991. Biochemical diversity of trichloroethylene metabolism. *Ann. Rev. Microbiol.* **45**:283-399.
- Fennell, D.E., J.M. Gossett, and S.H. Zinder. 1997. Comparison of butyric acid, ethanol, lactic acid, and propionic acid as hydrogen donors for the reductive dechlorination of tetrachloroethene. *Environmental Science and Technology*, **31**:918-926.
- Fennell, D. E. and J. M. Gossett. 1998. Modeling the Production of and Competition for Hydrogen in a Dechlorinating Culture. *Environmental Science and Technology*, **32**:2450-2460.
- Freeborn, R. A., K. A. West, V. K. Bhupathiraju, S. Chauhan, B. G. Rahm, R. E. Richardson, and L. Alvarez-Cohen. 2005. Phylogenetic Analysis of TCE-Dechlorinating Consortia Enriched on a Variety of Electron Donors. *Environmental Science and Technology*, **39**:8358-8368.
- Fukuzaki, S., N. Nishio, M. Shobayashi, and S. Nagai. 1990. Inhibition of the Fermentation of Propionate to Methane by Hydrogen, Acetate, and Propionate. *Applied and Environmental Microbiology*, **56**:719-723.
- Fung, J. M., R. M. Morris, L. Adrian, and S. H. Zinder. 2007. Expression of Reductive Dehalogenase Genes in *Dehalococcoides ethenogenes* Strain 195 Growing on Tetrachloroethene, Trichloroethene, or 2,3-Dichlorophenol. *Applied and Environmental Microbiology*, **73**:4439-4445.
- Gerritse, J., V. Renard, J. C. Gottschal and J. Visser. 1995. Complete degradation of tetrachloroethene by combining anaerobic dechlorinating and aerobic methanotrophic enrichment cultures. *Applied Microbiology and Biotechnology*, **43**:920-928.
- Gerritse, J., O. Drzyzga, G. Kloetstra, M. Keijmel, L. P. Wiersum, R. Hutson, M. D. Collins, and J. C. Gottschal. 1999. Influence of Different Electron Donors and Acceptors on Dehalorespiration of Tetrachloroethene by *Desulfitobacterium frappieri* TCE1. *Applied and Environmental Microbiology*, **65**:5212-5221.
- Gossett, J. M. 1987. Measurement of Henry's law constants for C1 and C2 chlorinated hydrocarbons. *Environmental Science and Technology*, **21**:202-208.
- Harrison, J. J., H. Ceri, and R. J. Turner. 2007. Multimetal resistance and tolerance in microbial biofilms. *Nature Reviews. Microbiology*, **5**:928-938.
- Haston, Z. and P. L. McCarty. 1999. Chlorinated Ethene Half-Velocity Coefficients (K_S) for Reductive Dehalogenation. *Environmental Science and Technology*, **33**:223-226.
- He, J., Y. Sung, M.E. Dollhopf, B.Z. Fathepure, J.M. Tiedje, and F.E. Löffler. 2002. Acetate versus Hydrogen as Direct Electron Donors To Stimulate the Microbial Reductive Dechlorination Process at Chloroethene-Contaminated Sites. *Environmental Science and Technology*, **36**:3945-3952.

- He, J., K. M. Ritalahti, K.L. Yang, S. S. Koenigsberg, and F. E. Löffler. 2003. Detoxification of vinyl chloride to ethene coupled to growth of an anaerobic bacterium. *Nature*, **424**:62-65
- He, J., Y. Sung, R. Krajmalnik-Brown, K. M. Ritalahti, and F. E. Löffler. 2005. Isolation and characterization of *Dehalococcoides* sp. strain FL2, a trichloroethene (TCE)- and 1,2- dichloroethene-respiring anaerobe. *Environmental Microbiology*, **7**:1442-1450.
- Heimann, A.C., A.K. Friis, C. Scheutz, and R. Jakobsen. 2007. Dynamics of reductive TCE dechlorination in two distinct H₂ supply scenarios and at various temperatures. *Biodegradation*, **18**:167-179.
- Holliger, C., G. Wohlfarth, and G. Diekert. 1999. Review: Reductive dechlorination in the energy metabolism of anaerobic bacteria. *FEMS Microbiology Reviews*, **22**:383-398.
- Holmes, V.F., J. He, P.K.H. Lee, and L. Alvarez-Cohen. 2006. Discrimination of Multiple *Dehalococcoides* Strains in a Trichloroethene Enrichment by Quantification of Their Reductive Dehalogenase Genes. *Applied and Environmental Microbiology*, **72**:5877-5883.
- Johnson, D.R., P.K.H. Lee, V.F. Holmes, A.C. Fortin, and L. Alvarez-Cohen. 2005. Transcriptional Expression of the *tceA* Gene in a *Dehalococcoides*-Containing Microbial Enrichment. *Applied and Environmental Microbiology*, **71**:7145-7151.
- Kielhorn, J., C. Melber, U. Wahnschaffe, A. Aitio, and I. Mangelsdorf. 2000. Vinyl chloride: still a cause for concern. *Environ. Health Perspec.* **7**:579-588.
- Klappenbach, J. A., P. R. Saxman, J. R. Cole, and T. M. Schmidt. 2001. rrndb: the Ribosomal RNA Operon Copy Number Database. *Nucleic Acids Research*, **29**:181-184.
- Krajmalnik-Brown, R., T. Hölscher, I. N. Thomson, F. M. Saunders, K. M. Ritalahti, and F. E. Löffler. 2004. Genetic Identification of a Putative Vinyl Chloride Reductase in *Dehalococcoides* sp. Strain BAV1. *Applied and Environmental Microbiology*, **70**:6347-6351.
- Kube, M., A. Beck, S. H Zinder, H. Kuhl, R. Reinhardt, and L. Adrian. 2005. Genome sequence of the chlorinated compound-respiring bacterium *Dehalococcoides* species strain CBDB1. *Nature Biotechnology*, **23**:1269-1273.
- Kugelman, I. J. and Chin, K. K. 1970. Toxicity, Synergism, and Antagonism in Anaerobic Waste Treatment Processes. In: Gould, R. F. (ed.), *Anaerobic biological treatment processes*, Advances in Chemistry Series 105, American Chemical Society, Washington, D. C., pp. 55-90.
- Lee, I-S, J-H Bae, Y. Yang, and P.L. McCarty. 2004. Simulated and experimental evaluation of factors affecting the rate and extent of reductive dehalogenation of chloroethenes with glucose. *Journal of Contaminant Hydrology*, **74**:313-331.

- Lee, I-S, J-H Bae, and P.L. McCarty. 2007. Comparison between acetate and hydrogen as electron donors and implications for the reductive dehalogenation of PCE and TCE. *Journal of Contaminant Hydrology*, **94**:76-85.
- Lee, P.K.H., D.R. Johnson, V.F. Holmes, J. He, and L. Alvarez-Cohen. 2006. Reductive Dehalogenase Gene Expression as a Biomarker for Physiological Activity of *Dehalococcoides* spp. *Applied and Environmental Microbiology*, **72**:6161-6168.
- Lee, P.K.H., T.W. Macbeth, K.S. Sorenson, Jr., R.A. Deeb, and L. Alvarez-Cohen. 2008. Quantifying Genes and Transcripts to Assess the In Situ Physiology of “*Dehalococcoides*” spp. in a Trichloroethene-Contaminated Groundwater Site. *Applied and Environmental Microbiology*, **74**:2728-2739.
- Lee, S, J. Kim, S. G. Shin, S. Hwang. 2008. Biokinetic parameters and behavior of *Aeromonas hydrophila* during anaerobic growth. *Biotechnology Letters*, **30**:1011-1016.
- Lendvay, J. M., F. E. Löffler, M. Dollhopf, M. R. Aiello, G. Daniels, B. Z. Fathepure, M. Gebhard, R. Heine, R. Helton, J. Shi, R. Krajmalnik-Brown, C. L. Major, Jr., M. J. Barcelona, E. Petrovskis, R. Hickey, J. M. Tiedje, and P. Adriaens. 2003. Bioreactive Barriers: A Comparison of Bioaugmentation and Biostimulation for Chlorinated Solvent Remediation. *Environmental Science and Technology*, **37**: 1422-1431.
- Ling, M. and H. S. Rifai. 2007. Modeling Natural Attenuation with Source Control at a Chlorinated Solvents Dry Cleaner Site. *Ground Water Monitoring & Remediation*, **27**:108-121.
- Löffler, F. E. J. M. Tiedje, and R. A. Sanford. 1999. Fraction of Electrons Consumed in Electron Acceptor Reduction and Hydrogen Thresholds as Indicators of Halorespiratory Physiology. *Applied and Environmental Microbiology*, **65**:4049-4056.
- Lovely, D.R. 2003. Cleaning up with genomics: applying molecular biology to bioremediation. *Nature Reviews Microbiology*, **1**:35-44.
- Lowe, M., E. L. Madsen, K. Schindler, C. Smith, S. Emrich, F. Robb, R. U. Halden. 2002. Geochemistry and microbial diversity of a trichloroethene-contaminated Superfund site undergoing intrinsic in situ reductive dechlorination. *FEMS Microbiology Ecology*, **40**:123-134.
- Lu, X-X., S. Tao, T. Bosma, and J. Gerritse. 2001. Characteristic Hydrogen Concentrations for Various Redox Processes in Batch Study. *Journal of Environmental Science & Health, Part A: Toxic/Hazardous Substances & Environmental Engineering*, **36**:1725-1734.
- Lu, X., J. T. Wilson, and D. H. Kampbell. 2006. Relationship between *Dehalococcoides* DNA in groundwater and rates of reductive dechlorination at field scale. *Water Research*, **40**:3131-3140.

- Luijten, M.L.G.C., J. deWeert, H. Smidt, H.T.S. Boschker, W.M. deVos, G. Schraa, and A.J.M. Stams. 2003. Description of *Sulfurospirillum halorespirans* sp. nov., an anaerobic, tetrachloroethene-respiring bacterium, and transfer of *Dehalospirillum multivorans* to the genus *Sulfurospirillum* as *Sulfurospirillum multivorans* comb. nov. *International Journal of Systematic and Evolutionary Microbiology* **53**:787–793.
- Luijten, M.L.G.C., W. Roelofsen, A.A.M. Langenhoff, G. Schraa, and A.J.M. Stams. 2004. Brief Report: Hydrogen threshold concentrations in pure cultures of halorespiring bacteria and at a site polluted with chlorinated ethenes. *Environmental Microbiology* **6**:646–650.
- Magnuson, J. K., R. V. Stern, J. M. Gossett, S. H. Zinder, and D. R. Burris. 1998. Reductive Dechlorination of Tetrachloroethene to Ethene by a Two-Component Enzyme Pathway. *Applied and Environmental Microbiology*, **64**:1270–1275.
- Magnuson, J. K., M. F. Romine, D. R. Burris, and M. T. Kingsley. 2000. Trichloroethene Reductive Dehalogenase from *Dehalococcoides ethenogenes*: Sequence of *tceA* and Substrate Range Characterization. *Applied and Environmental Microbiology*, **66**:5141-5147.
- Major, D. W., M. L. McMaster, E. E. Cox, E. A. Edwards, S. M. Dworatzek, E. R. Hendrickson, M. G. Starr, J. A. Payne, and L. W. Buonamici. 2002. Field Demonstration of Successful Bioaugmentation To Achieve Dechlorination of Tetrachloroethene To Ethene. *Environmental Science and Technology*, **36**:5106-5116.
- Maymó-Gatell, X., Y. T. Chien, J. M. Gossett, and S. H. Zinder. 1997. Isolation of a Bacterium That Reductively Dechlorinates Tetrachloroethene to Ethene. *Science*, **276**:1568-1571.
- McCarty, P.L. 1997. Breathing with Chlorinated Solvents. *Science*, **276**: 1521-1522.
- Moran, M. J., J. S. Zogorski, and P. J. Squillace. 2007. Chlorinated Solvents in Groundwater of the United States. *Environmental Science and Technology*, **41**:74-81.
- Müller, J. A., B. M. Rosner, G. von Abendroth, G. Meshulam-Simon, P. L. McCarty, and A. M. Spormann. 2004. Molecular Identification of the Catabolic Vinyl Chloride Reductase from *Dehalococcoides* sp. Strain VS and Its Environmental Distribution. *Applied and Environmental Microbiology*, **70**:4880-4888.
- Muyzer, G., E. C. de Waal, and A. G. Uitterlinden. 1993. Profiling of complex microbial populations by denaturing gradient gel electrophoresis analysis of polymerase chain reaction-amplified genes coding for 16S rRNA. *Applied and Environmental Microbiology*, **59**:695–700.
- Panagiotakis, I., D. Mamais, M. Pantazidou, M. Marneri, M. Parapouli, E. Hatziloukas, and V. Tandoi. 2007. Dechlorinating ability of TCE-fed microcosms with different electron donors. *Journal of Hazardous Materials*, **149**:582-589.

- Perry, R. H., D. W. Green, and J. O. Maloney. 1997. *Perry's Chemical Engineers Handbook*, 7th ed. McGraw Hill, New York.
- Piringer, G. and S. K. Bhattacharya. 1999. Toxicity and fate of pentachlorophenol in anaerobic acidogenic systems. *Water Research*, **33**:2674-2682.
- Pon, G., M.R. Hymann, and L. Semprini. 2003. Acetylene Inhibition of Trichloroethene and Vinyl Chloride Reductive Dechlorination. *Environmental Science and Technology*, **37**: 3181 -3188.
- Popov, V. O. and V. S. Lamzin. 1994. Review Article: NAD⁺-dependent formate dehydrogenase. *Biochemical Journal*, **301**:625-643.
- Qu, M. and S. K. Bhattacharya. 1997. Toxicity and biodegradation of formaldehyde in anaerobic methanogenic culture. *Biotechnology and Bioengineering*, **55**:727-736.
- Rahm, B. G., S. Chauhan, V. F. Holmes, T. W. Macbeth, K. S. Jr. Sorenson, and L. Alvarez-Cohen. 2006a. Molecular characterization of microbial populations at two sites with differing reductive dechlorination abilities. *Biodegradation*, **17**:523-534.
- Rahm, B. G., R. M. Morris, and R. E. Richardson. 2006b. Temporal Expression of Respiratory Genes in an Enrichment Culture Containing *Dehalococcoides ethenogenes*. *Applied and Environmental Microbiology*, **72**:5486-5491.
- Rahm, B. G. and R. E. Richardson. 2008a. Correlation of Respiratory Gene Expression Levels and Pseudo-Steady-State PCE Respiration Rates in *Dehalococcoides ethenogenes*. *Environmental Science and Technology*, **42**:416-421.
- Rahm, B. G. and R. E. Richardson. 2008b. *Dehalococcoides*' Gene Transcripts As Quantitative Bioindicators of Tetrachloroethene, Trichloroethene, and *cis*-1,2-Dichloroethene Dehalorespiration Rates. *Environmental Science and Technology*, **42**:5099-5105.
- Regeard, C., J. Maillard, C. Dufraigne, P. Deschavanne, and C. Holliger. 2005. Indications for Acquisition of Reductive Dehalogenase Genes through Horizontal Gene Transfer by *Dehalococcoides ethenogenes* Strain 195. *Applied and Environmental Microbiology*, **71**:2955-2961.
- Ritalahti, K. M., B. K. Amos, Y. Sung, Q. Wu, S. S. Koenigsberg, and F. E. Löffler. 2006. Quantitative PCR Targeting 16S rRNA and Reductive Dehalogenase Genes Simultaneously Monitors Multiple *Dehalococcoides* Strains. *Applied and Environmental Microbiology*, **72**:2765-2774.
- Schulman, M. D. and D. Valentino. 1975. Factors Influencing Rumen Fermentation: Effect of Hydrogen on Formation of Propionate. *Journal of Dairy Science*, **59**:1444-1451.
- Seshadri, R., L. Adrian, D. E. Fouts, J. A. Eisen, A. M. Phillippy, B. A. Methe, N. L. Ward, W. C. Nelson, R. T. Deboy, H. M. Khouri, J. F. Kolonay, R. J. Dodson, S. C. Daugherty, L. M. Brinkac, S. A. Sullivan, R. Madupu, K. E. Nelson, K. H. Kang, M. Impraim, K. Tran, J. M. Robinson, H. A. Forberger, C. M. Fraser, S. H. Zinder, and J.

- F. Heidelberg. 2005. Genome Sequence of the PCE-Dechlorinating Bacterium *Dehalococcoides ethenogenes*. *Science*, **307**: 105-108.
- Shellenberger, K. and B. E. Logan. 2002. Effect of Molecular Scale Roughness of Glass Beads on Colloidal and Bacterial Deposition. *Environmental Science and Technology*, **36**:184-189.
- Sotemann, S. W., Ristow, N. E., Wentzel, M. C., and G. A. Ekama. 2005. A steady state model for anaerobic digestion of sewage sludges. *Water SA*, **31**:511-527.
- Stewart, P. S. and J. W. Costerton. 2001. Antibiotic resistance of bacteria in biofilms. *Lancet*, **358**:135-138.
- Sung, Y., K.E. Fletcher, K.M. Ritalahti, R.P. Apkarian, N. Ramos-Hernandez, R.A. Sanford, N.M. Mesbah, and F.E. Löffler. 2006a. *Geobacter lovleyi* sp. nov. Strain SZ, a Novel Metal-Reducing and Tetrachloroethene-Dechlorinating Bacterium. *Applied and Environmental Microbiology*, **72**:2775-2782.
- Sung, Y., K. M. Ritalahti, R. P. Apkarian, and F. E. Löffler. 2006b. Quantitative PCR Confirms Purity of Strain GT, a Novel Trichloroethene-to-Ethene-Respiring *Dehalococcoides* Isolate. *Applied and Environmental Microbiology*, **72**:1980-1987.
- Telgmann, U., H. Horn, and E. Morgenroth. 2004. Influence of growth history on sloughing and erosion from biofilms. *Water Research*, **38**:3671-3684.
- Thauer, R.K., K. Jungermann, and K. Decker. 1977. Energy conservation in chemotrophic anaerobic bacteria. *Bacteriological Reviews*, **41**:100-180.
- van Eekert, M.H.A. and G. Schraa. The potential of anaerobic bacteria to degrade chlorinated compounds. *Water Science and Technology*, **44**:49-56.
- Waller, A. S., R. Krajmalnik-Brown, F. E. Löffler, and E. A. Edwards. 2005. Multiple Reductive-Dehalogenase-Homologous Genes Are Simultaneously Transcribed during Dechlorination by *Dehalococcoides*-Containing Cultures. *Applied and Environmental Microbiology*, **71**:8257-8264.
- Walters, III, M. C., F. Roe, A. Bugnicourt, M. J. Franklin, and P. S. Stewart. 2003. Contributions of Antibiotic Penetration, Oxygen Limitation, and Low Metabolic Activity to Tolerance of *Pseudomonas aeruginosa* Biofilms to Ciprofloxacin and Tobramycin. *Antimicrobial Agents and Chemotherapy*, **47**:317-323.
- Weast, R.C. and M.J. Astle. 1980. CRC Handbook of Chemistry and Physics (61 ed.). CRC Press, Inc., Boca Raton, FL.
- West, K. A., D. R. Johnson, P. Hu, T. Z. DeSantis, E. L. Brodie, P. K. H. Lee, H. Feil, G. L. Andersen, S. H. Zinder, and L. Alvarez-Cohen. 2008. Comparative Genomics of "Dehalococcoides ethenogenes" 195 and an Enrichment Culture Containing Unsequenced "Dehalococcoides" Strains. *Applied and Environmental Microbiology*, **74**:3533-3540.

- Yang, Y. and P.L. McCarty. 1998. Competition for Hydrogen within a Chlorinated Solvent Dehalogenating Anaerobic Mixed Culture. *Environmental Science and Technology*, **32**:3591-3597.
- Yang, Y. and P. L. McCarty. 2000. Biologically Enhanced Dissolution of Tetrachloroethene DNAPL. *Environmental Science and Technology*, **34**:2979-2984.
- Yim, Y.-J., J. Seo, S.-I. Kang, J.-H. Ahn and H.-G. Hur. 2008. Reductive Dechlorination of Methoxychlor and DDT by Human Intestinal Bacterium *Eubacterium limosum* Under Anaerobic Conditions. *Archives of Environmental Contamination and Toxicology*, **54**:406-411.
- Young, C. F. (ed.). 1981. Hydrogen and Deuterium. Pergamon Press, Elmsford, NY.
- Yu, S. and L. Semprini. 2002. Comparison of trichloroethylene reductive dehalogenation by microbial communities stimulated on silicon-based organic compounds as slow-release anaerobic substrates. *Water Research*, **36**:4985-4996.
- Yu, S. and L. Semprini. 2004. Kinetics and modeling of reductive dechlorination at high PCE and TCE concentrations. *Biotechnology and Bioengineering*, **88**:451-464.
- Yu, S., M.E. Dolan, and L. Semprini. 2005. Kinetics and Inhibition of Reductive Dechlorination of Chlorinated Ethylenes by Two Different Mixed Cultures. *Environmental Science and Technology*, **39**:195-205.
- Zheng, D., C. S. Carr, and J. B. Hughes. 2001. Influence of Hydraulic Retention Time on Extent of PCE Dechlorination and Preliminary Characterization of the Enrichment Culture. *Bioremediation Journal*, **5**:159-168.

Appendix A

Supporting information for Chapter 2

Table A1. Tabulated pH values for all three CFSTRs reported in this study.

Day of Operation	Reactor 1	Reactor 2	Reactor 3
5	6.50	6.73	7.04
10	6.34	6.66	7.21
14	6.47	6.97	7.45
19	6.30	6.78	7.47
27	6.27	6.82	7.68
36	6.72	7.42	8.37
45	6.43	7.01	8.38
53	6.69	7.26	8.45
63	6.59	6.84	8.14
69	6.69	7.01	8.28
75	6.72	7.07	8.36
82	7.16	7.47	8.81
103	7.09	7.23	8.38
114	8.02	7.56	8.30
162		6.90	7.52
171		7.11	7.66
179		7.12	7.70
201		7.21	7.84
212		7.20	7.60
228		7.67	7.50
247		7.27	7.26
260		7.29	7.37
269		7.27	7.41
298		7.37	7.57
317			7.48
336			7.78
354			7.04
Average	6.71	7.13	7.78
Std Dev	0.46	0.26	0.48

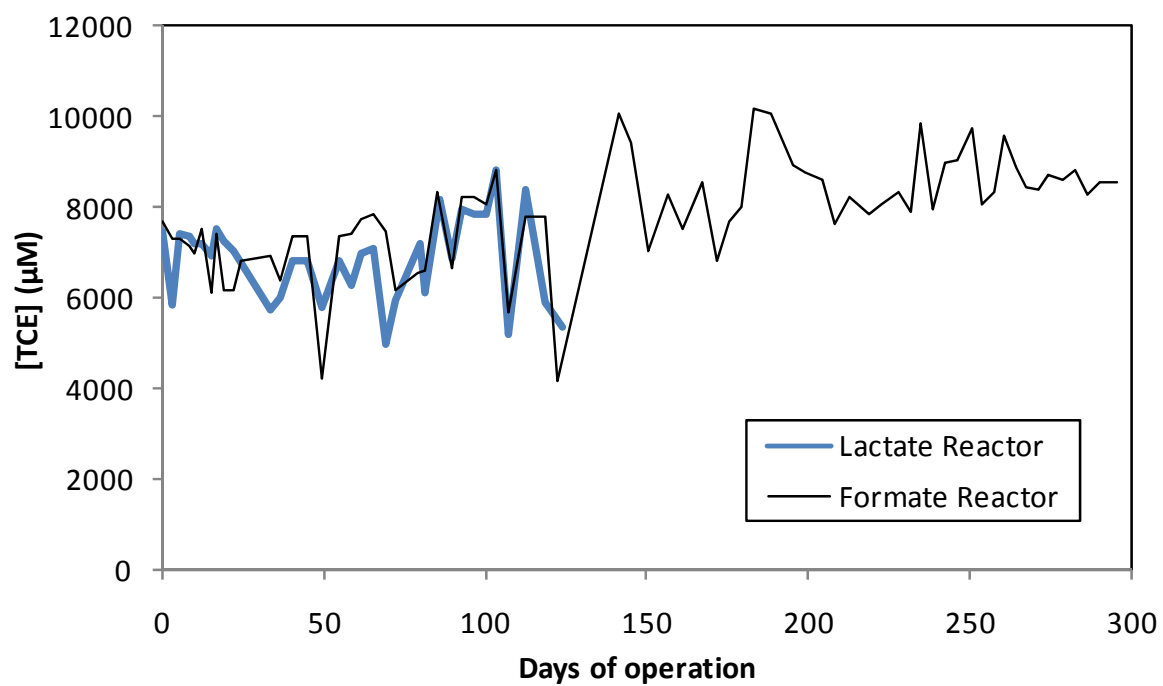


Figure A1. Influent TCE concentrations for both continuously fed suspended growth reactors.

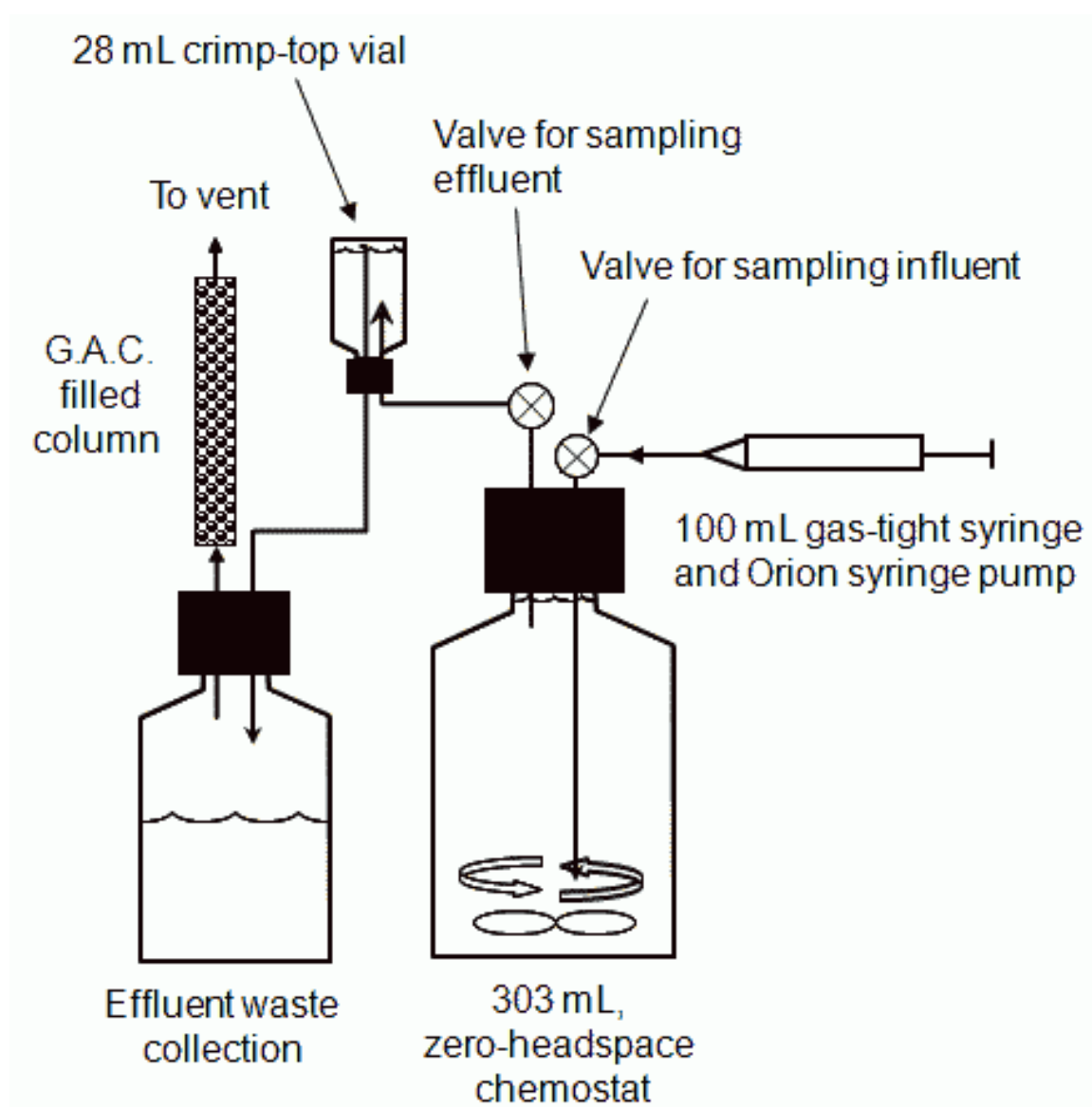


Figure A2. Schematic diagram of continuous culture reactors. Not to scale.

Batch Kinetic Test Detailed Procedure

Batch kinetic assays were conducted on 24-hr composite effluent samples as follows. An autoclaved 28 mL N₂-sparge crimp-top vial was clamped inverted next to the chemostat 24 hrs prior to commencement of the batch kinetic test (as shown in Figure S1). The effluent tubing was fitted with a 22 gauge needle, and inserted into the vial. A 3" 20 gauge exhaust needle connected to the anaerobic waste collection bottle was inserted to completely fill the inverted vial with effluent sample. After 24 hours, the vial was taken off-line, sparged for 15 min with anaerobic gas (10%CO₂/90%N₂), and imported into the anaerobic glove-box.

11.5 mL of the sample was added to each of duplicate 28 mL crimp-top vials using a new 5 mL disposable syringe fitted with a 20 gauge needle. The vials were then capped, removed from the glovebox, and sparged for 10 minutes with anaerobic gas comprised of 10% H₂, 90%{10%CO₂/90%N₂}. The sparged vials were then reimported into the glove box and augmented with the anaerobically equilibrated CAH of interest; either 1.2 µL of neat TCE, 0.22 mL of cDCE saturated autoclaved ultra-pure water, or 0.75 mL of gaseous VC. These vials were incubated at room temperature (25.2°C ± 1.3°C std dev) within the glove box on a 200 rpm shaker table for 10 hours, reaugmented with more CAH if necessary to ensure aqueous concentrations were maintained at levels sufficient to saturate enzyme activity.

After the initial 10-hour incubation, batch reactor headspace samples were collected for CAHs, ETH, and H₂ analyses to determine total CAH transformation and H₂ consumption under non-limiting H₂ conditions. All sampling was performed inside the anaerobic glove box to insure anaerobic conditions were maintained.

Quantitative rate measurements were then performed as follows. Each batch reactor vial was sparged for 10 minutes with the anaerobic gas mixture of 10% H₂, 90%{10%CO₂/90%N₂} and reaugmented with the CAH of interest to achieve aqueous concentrations of 500 µM, 700 µM, and 1000 µM for TCE, cDCE and VC, respectively. These concentrations were sufficiently above respective half-saturation coefficients, but below potentially inhibitory levels to ensure maximum dechlorination rates were achieved (Yu and Semprini, 2004). Five headspace samples were collected over a period of one to three hours to determine CAH-specific maximum dechlorination rates, as calculated from the slope of a linear regression line through the five product formation data points, and normalized to protein concentrations.

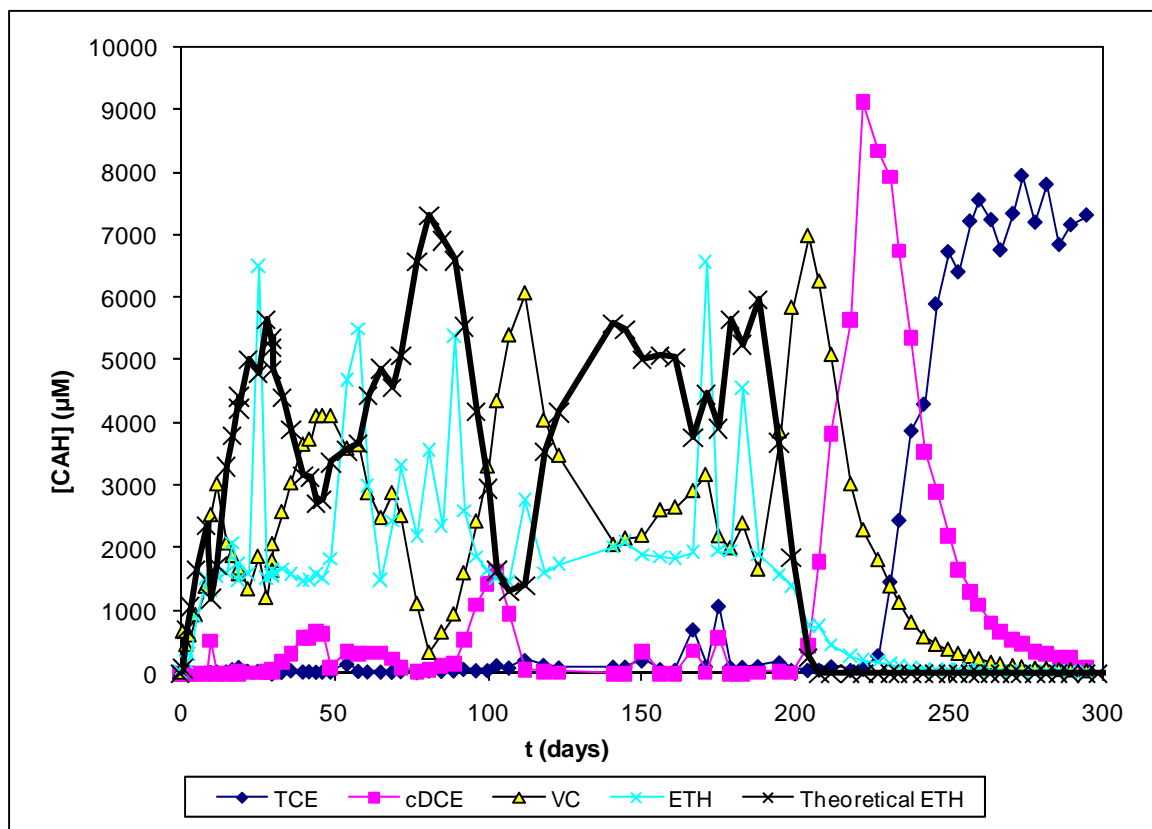
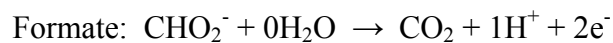
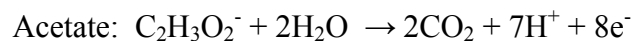
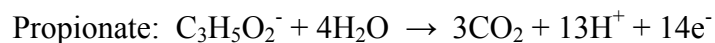
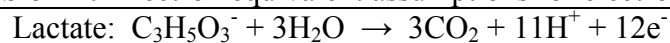
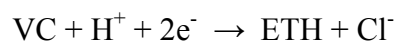
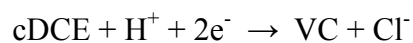
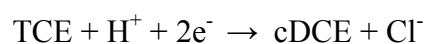


Figure A3. Formate-fed effluent CAH monitoring with theoretical ETH concentrations. Theoretical ETH concentrations are calculated as the average influent TCE concentration minus the sum of effluent TCE + cDCE + VC measured.

Table A2. Electron equivalent assumptions for electron balance.



Biomass: 1 mg protein = 2 mg cell. Cell formula = $\text{C}_5\text{H}_7\text{O}_2\text{N}$, MW = 113, 10 meq./mole of cell for 354 uequiv/mg protein



NOTE: effluent H_2 is ignored because concentrations were several orders of magnitude lower than above electron sources and sinks

Appendix B

Supporting information for Chapter 3

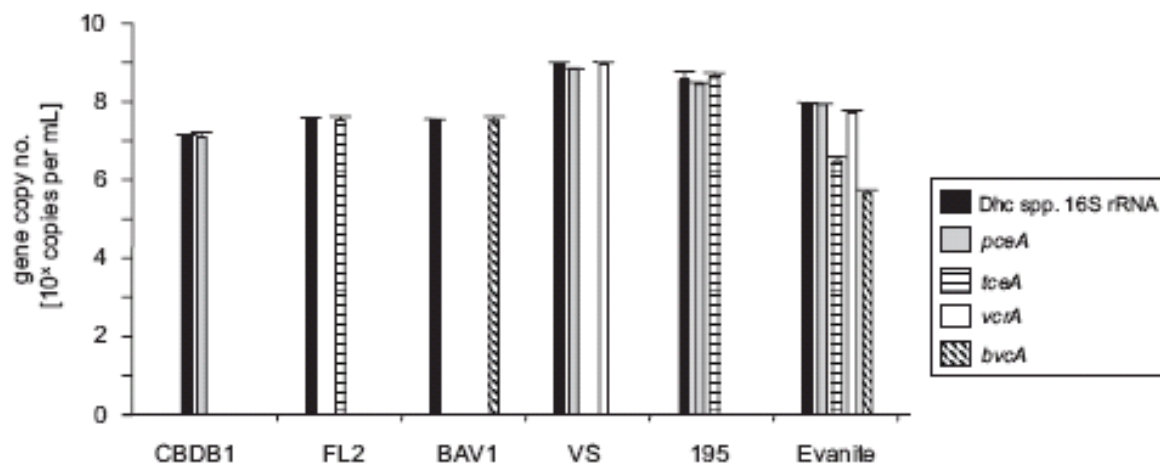
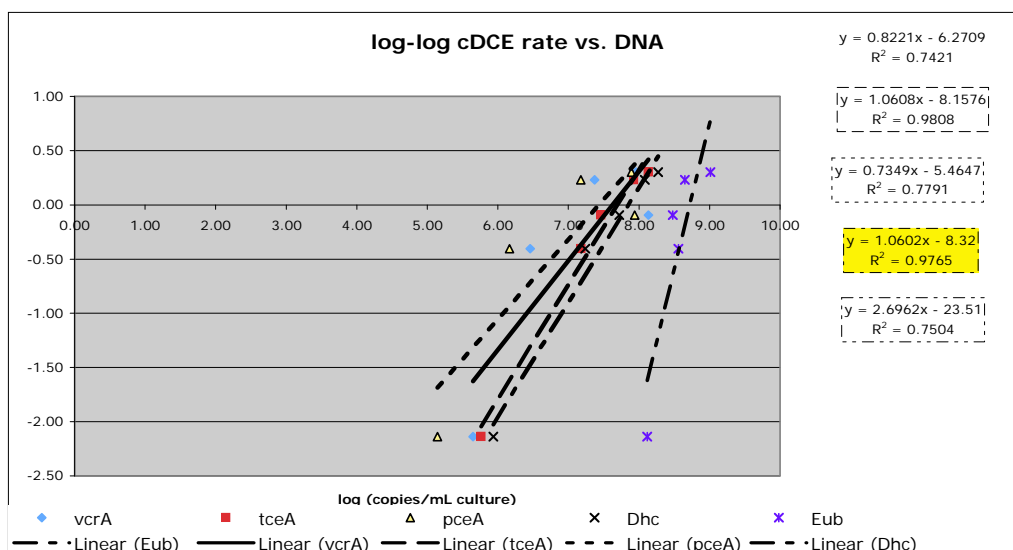


Figure B1. Reductase gene profiles of the Evanite culture and pure *Dehalococcoides* strains. Originally published in: Behrens, et al. 2008. Monitoring Abundance and Expression of "*Dehalococcoides*" Species Chloroethene-Reductive Dehalogenases in a Tetrachloroethene-Dechlorinating Flow Column. Applied and Environmental Microbiology, **74**: 5695-5703.

Regression-based dechlorination rate predictions

The log of each dechlorination rate measurement is plotted against the log of each qPCR DNA quantity associated with that same sample. Each gene is considered separately from the other genes analyzed. I.e. Only *pceA* log quantities are plotted together against the log of cDCE dechlorination rates from corresponding samples, only *tceA* log quantities are plotted together against corresponding log of cDCE dechlorination rates, etc. A linear regression is then performed on each set of data for each separate gene, as illustrated below.



The regression fit curve generated from the *Dehalococcoides* 16S rRNA gene quantification data associated with Reactor 1 cDCE dechlorination rates has been highlighted for an example calculation. The regression curve of the log data can be converted to a rate prediction based upon *Dehalococcoides* 16S rRNA gene quantities as follows:

$$\log(\text{rate}) = 1.0602 \times \log(\#Dhc16S) - 8.32$$

$$\therefore \text{rate} = 10^{-8.32} \times \left((10^{\#Dhc16S})^{1.0602} \right)$$

Quantified *Dehalococcoides* 16S rRNA genes (as copies per mL of culture) from any reactor can be inserted into the above equation to predict rates on a $\mu\text{moles/day/mL}$ of culture basis.

Appendix C

Supporting information for Chapter 4

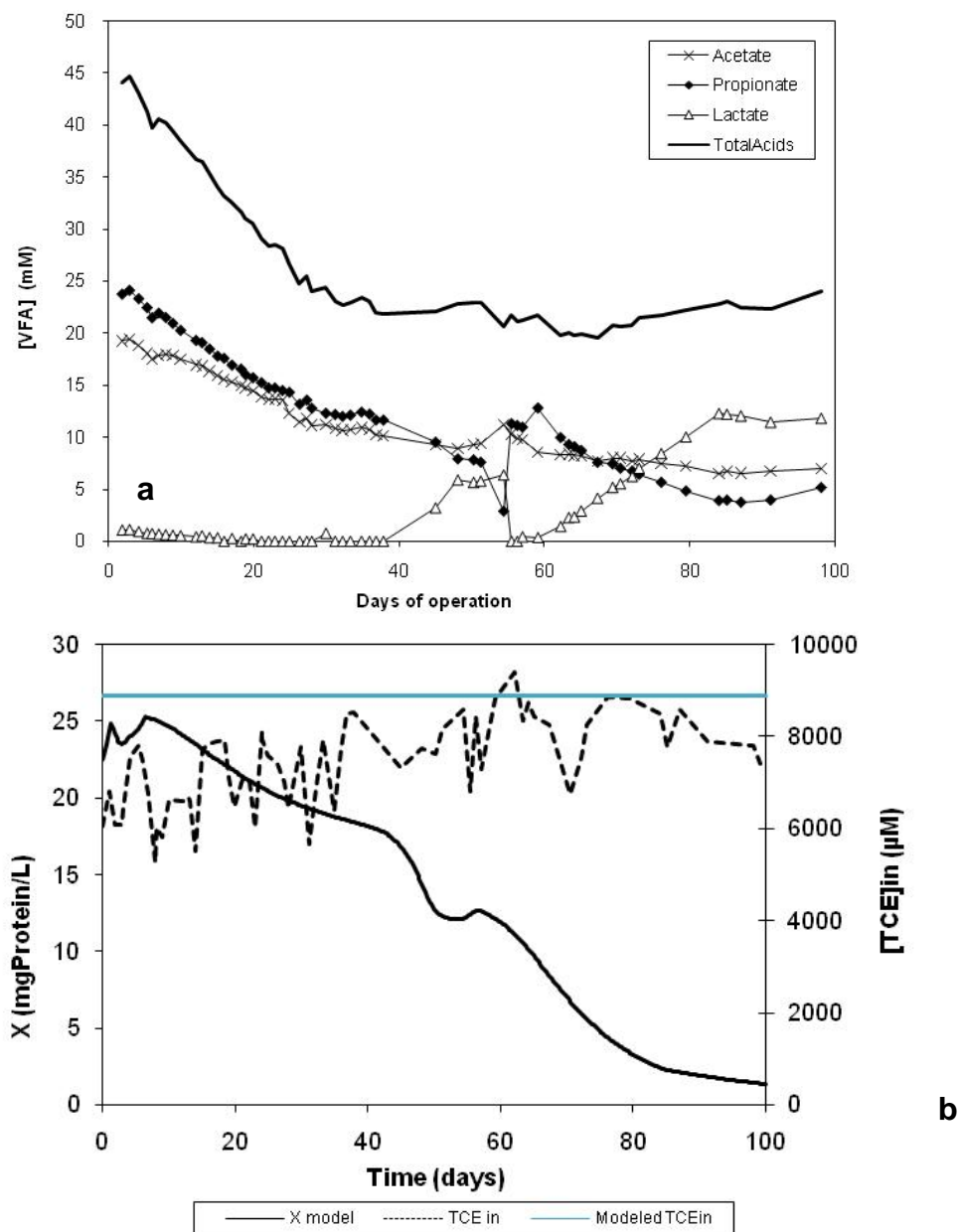


Figure C1. CFSTR acids monitoring data (a), and (b) measured influent TCE, modeled influent TCE concentrations, and modeled biomass (X).

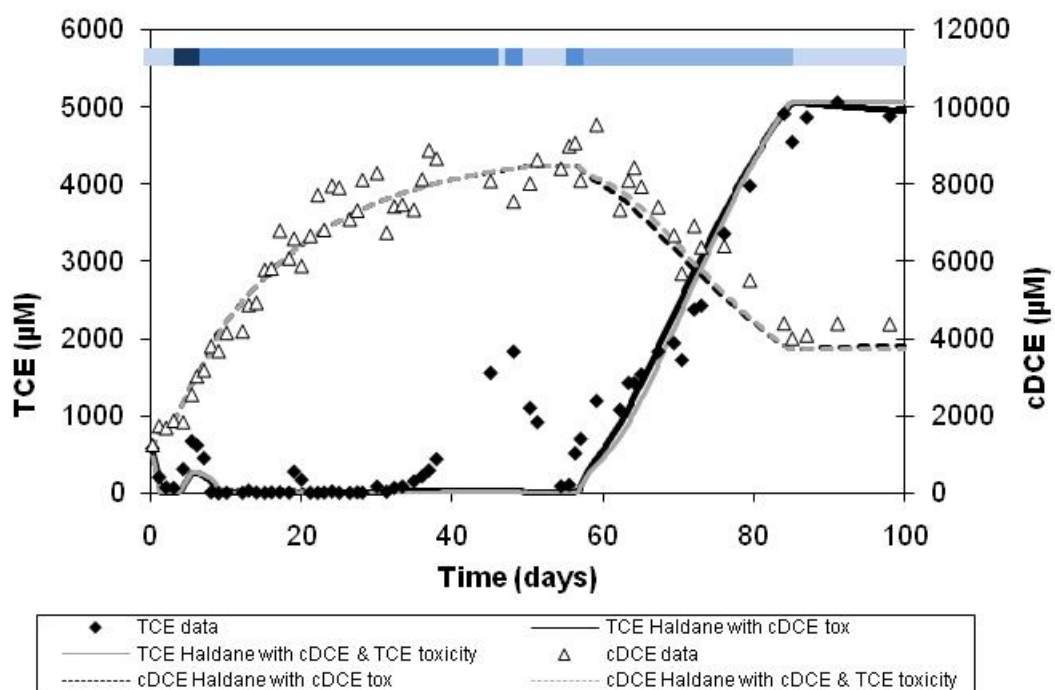


Figure C2. Best fit models for CFSTR data with TCE Haldane inhibition plus either cDCE toxicity alone (black lines), or both cDCE and TCE toxicity (gray lines).

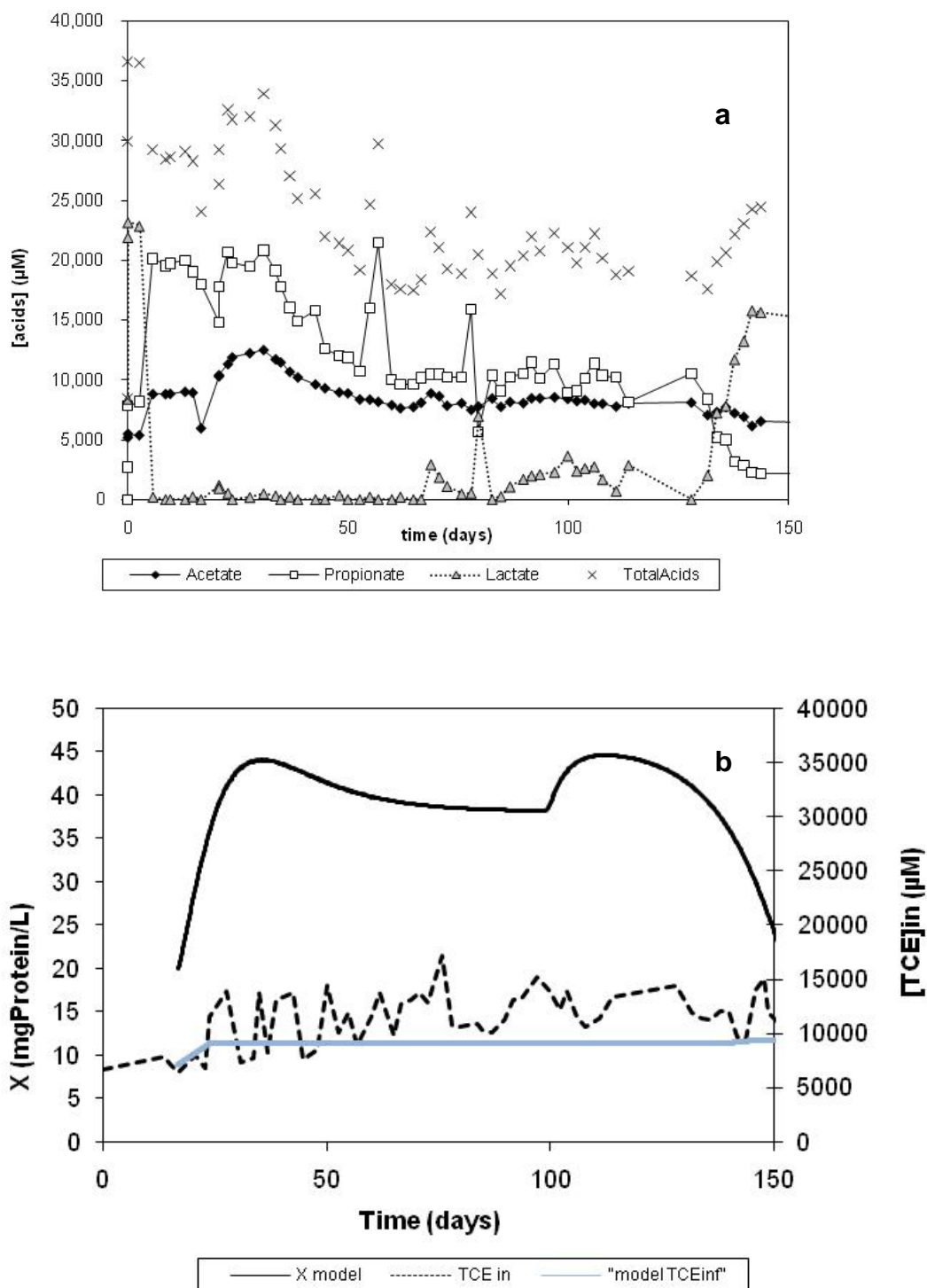


Figure C3. RPC acids monitoring data (a), and (b) measured influent TCE, modeled influent TCE concentrations, and modeled biomass (X).